

We get technical

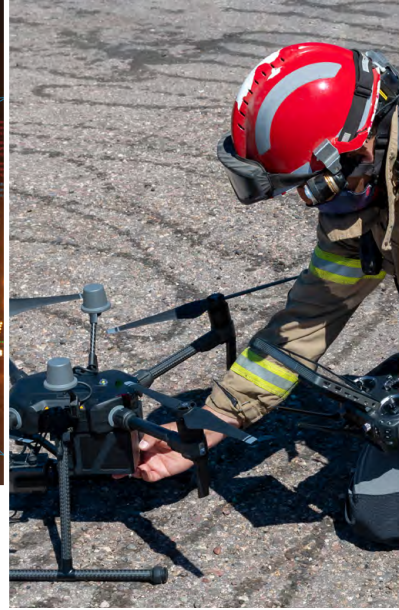
How to use smart air quality sensors for environmental monitoring

The basics of applying ultrasonic transducers for sensing objects or fluid flow

How to choose and use angle sensors for power steering, motors and robotics

Use IMUs for precise location data when GPS won't suffice





contents

- 4** Get started quickly with 3D time-of-flight applications
- 14** How to use smart air quality sensors for environmental monitoring
- 20** Understand drone design trade-offs before piling on the sensors
- 28** An introduction to pressure sensors
- 32** **Special feature: retroelectro**
The rise of designators: from deforest to western electric
- 40** The basics of applying ultrasonic transducers for sensing objects or fluid flow
- 50** How to choose and use angle sensors for power steering, motors and robotics
- 58** Using a MEMS sensor for vibration monitoring
- 66** Use IMUs for precise location data when GPS won't suffice
- 74** Use a PCR module to rapidly develop accurate, low-power radar-based sensors

Editor's note

Recent advancements in sensor hardware and algorithms are driving significant transformations across industrial and consumer applications, particularly in automated systems, robotics, and digitalization efforts within industrial environments.

The widespread adoption of key sensor technologies across different industries has been instrumental in fostering innovation. These advancements have enabled the miniaturization, ruggedization, and enhanced connectivity of transducers and processing elements. Moreover, there's a growing trend towards integrated sensing solutions that combine multiple modalities such as angle, speed, and temperature. This integration not only reduces design complexity and footprint but also lowers costs.

3D time-of-flight (ToF) imaging exemplifies this trend by integrating optical design, precision timing circuits, and advanced signal processing capabilities. It's tailored for applications in industrial safety, robotic navigation, and gesture-based controls.

Advancements in sensors now incorporate wireless communication capabilities, real-time data collection, and sophisticated calibration techniques to achieve higher levels of accuracy. These technologies, complemented by machine-learning algorithms, support predictive maintenance in industrial settings and enable adaptive functionalities in drones and other mobile platforms.

There is a notable shift towards energy-efficient and energy-harvesting sensors, which are increasingly integrated into new applications and upgraded legacy systems.

In this magazine, we delve into 10 specific sensor technologies, exploring how they enable scalability, enhance design performance, and facilitate the smart engineering functions crucial for today's evolving needs.



Get started quickly with 3D time-of-flight applications

By Stephen Evanczuk

Contributed By DigiKey's North American Editors

3D time-of-flight (ToF) imaging offers an efficient alternative to video imaging for a broad range of applications including industrial safety, robotic navigation, gesture control interfaces, and much more. This approach does, however, require a careful blend of optical design, precision timing circuits, and signal processing capabilities that can often leave developers struggling to implement an effective 3D ToF platform.

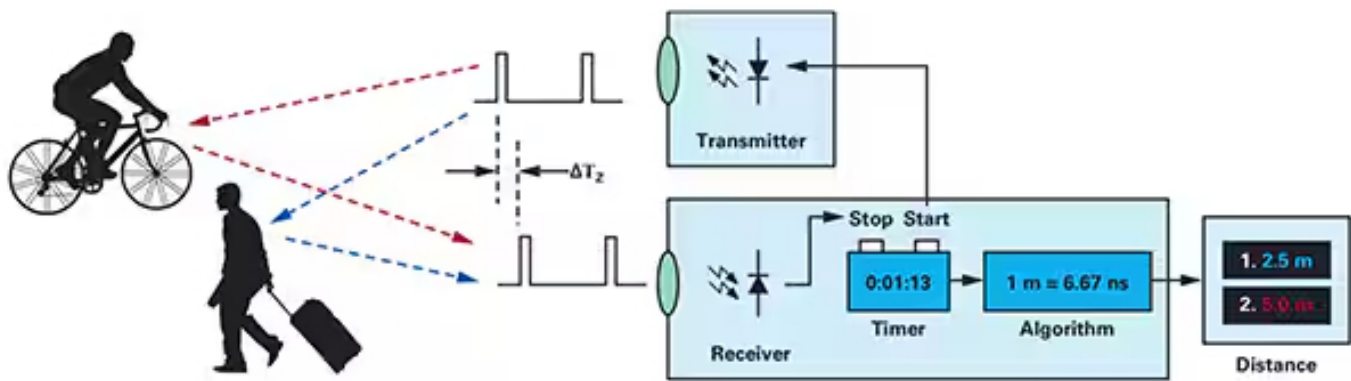


Figure 1: Human and robot collaboration includes a broad range of possible levels of interaction. (Image source: [SICK](#))

This article will describe the nuances of ToF technology before showing how two off-the-shelf 3D ToF kits—Analog Devices’ [AD-96TOF1-EBZ](#) development platform and [ESPROS Photonics’ EPC660 evaluation kit](#)—can help developers quickly prototype 3D ToF applications and gain needed experience to implement 3D ToF designs to meet their unique requirements.

What is ToF technology?

ToF technology relies on the familiar principle that the distance between an object and some source point can be found by measuring the difference between the time that energy is transmitted by the source and the time that its reflection is received by the source (Figure 1).

Although the basic principle remains the same, ToF solutions vary widely and bear the capabilities and limitations inherent in their underlying

technologies including ultrasound, light detection and ranging (LiDAR), cameras, and millimeter wave (mmWave) RF signals:

- Ultrasonic ToF solutions offer a low-cost solution but with limited range and spatial resolution of objects
- Optical ToF solutions can achieve greater range and spatial resolution than ultrasonic systems but are compromised by heavy fog or smoke
- Solutions based on mmWave technology are typically more complex and expensive, but they can operate at significant range while providing information about the target object's velocity and heading despite smoke, fog, or rain

Manufacturers take advantage of the capabilities of each technology as needed to meet specific requirements. For example, ultrasonic sensors are well suited for detecting obstructions as

robots move across a path or as drivers park their vehicles. In contrast, mmWave technology provides vehicles with the kind of long-distance sensing capability needed to detect approaching road hazards even when other sensors are unable to penetrate heavy weather conditions.

ToF designs can be built around a single transmitter/receiver pair. For example, a simple optical ToF design conceptually requires only an LED to illuminate some region of interest and a photodiode to detect reflections from objects within that region of interest. This seemingly simple design nevertheless requires precise timing and synchronization circuits to measure the delay. In addition, modulation and demodulation circuits may be needed to differentiate the illumination signal from background sources or support more complex continuous wave methods.

Design complexity rises quickly as developers work to enhance the signal to noise ratio (SNR) and eliminate artifacts in ToF systems. Further compounding complexity, more advanced detection solutions will employ multiple transmitters and receivers to track multiple objects or support more sophisticated motion tracking algorithms. For example, mmWave systems will often employ multiple receivers to track the heading and velocity of multiple independent objects. (See, "[Use Millimeter Wave Radar Kits for Fast Development of Precision Object Detection Designs](#)".)

3D optical ToF systems

3D optical ToF systems extend the idea of using more receivers by using imaging sensors typically based on an array of charge-coupled devices (CCDs). When a set of lenses focuses some region of interest onto the CCD array, each charge storage device in the CCD array is charged by the return illumination reflected from a corresponding point in that region of interest. Synchronized with pulsed or continuous wave illumination, reflected light reaching the CCD array is essentially captured in a sequence of windows or phases, respectively. This data is further processed to create a 3D depth map comprising voxels (VOLUME

piXELs) whose value represents the distance to the corresponding point in the region of interest.

Like frames in a video, individual depth maps can be captured in sequence to provide measurements with temporal resolution limited only by the frame rate of the image capture system and with spatial resolution limited only by the CCD array and optical system. With the availability of larger 320 x 240 CCD imagers, higher resolution 3D optical ToF systems find applications in broadly diverse segments including industrial automation, unmanned aerial vehicles (UAVs), and even gesture interfaces (Figure 2).

Unlike most camera-based methods, 3D ToF systems can provide accurate results despite shading or changing lighting conditions. These systems provide their own illumination, typically using lasers or high-power infrared LEDs such as [Lumileds' Luxeon](#) IR LEDs able to operate at the megahertz (MHz) switching rates used in these systems. Unlike methods such as stereoscopic cameras, 3D ToF systems provide a compact solution for generating detailed distance information.

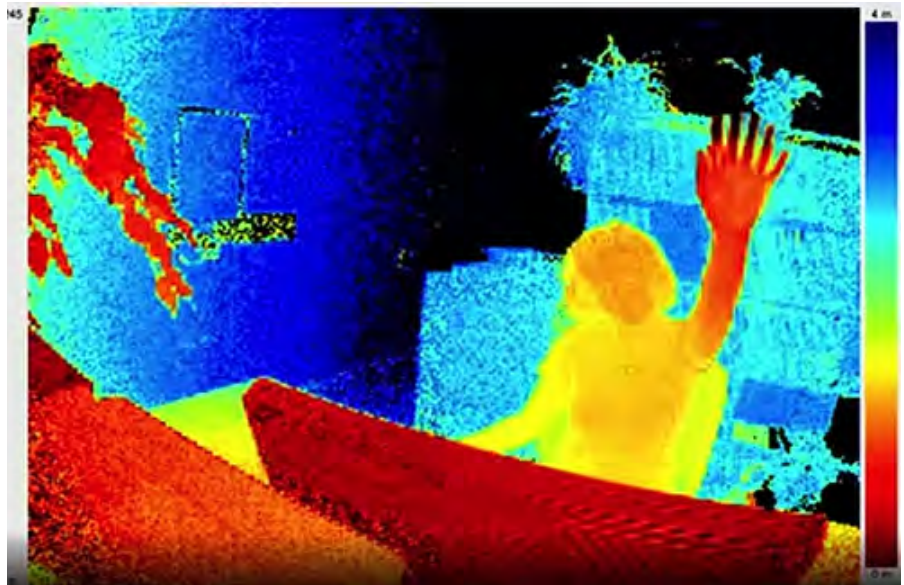


Figure 2: With their high frame rate and spatial resolution, 3D optical ToF can provide gesture interface systems with detailed data such as a person's hand being raised toward the ToF camera as shown here. (Image source: ESPROS Photonics)

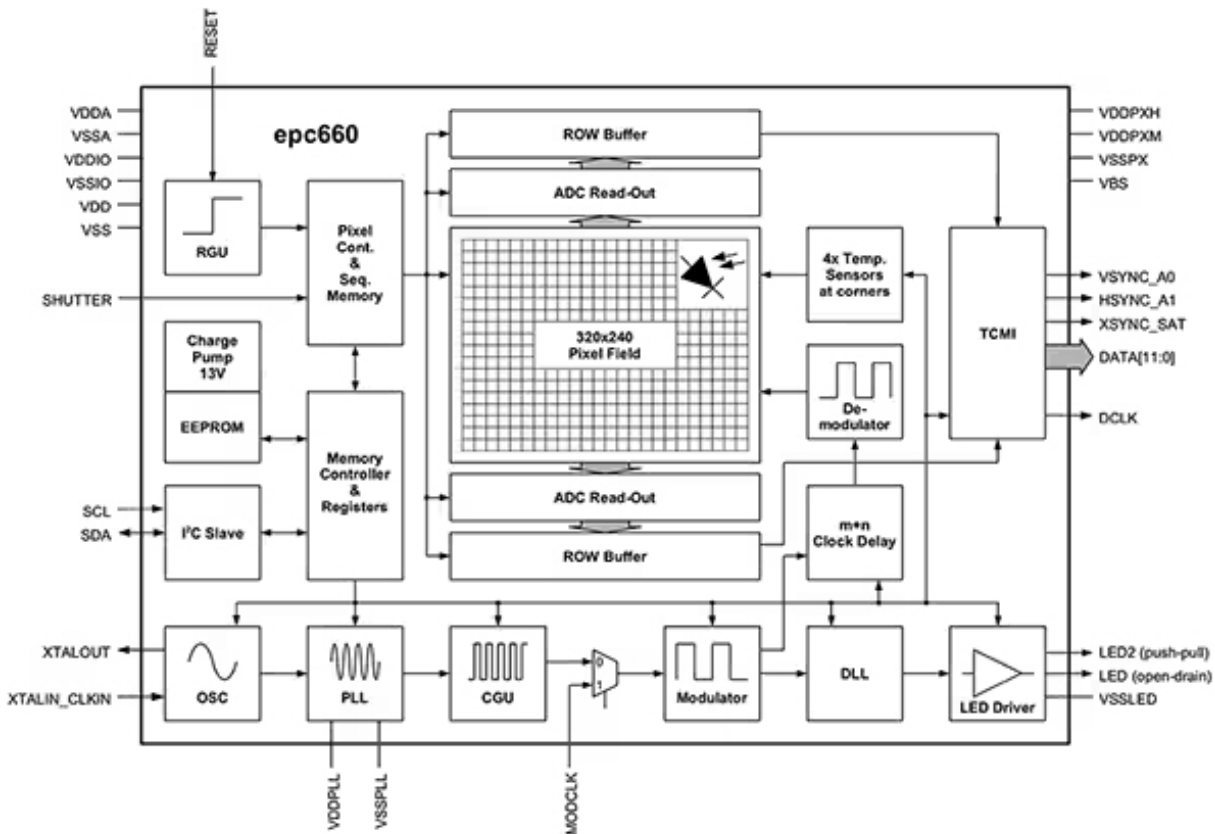


Figure 3: The ESPROS Photonics epc660 integrates a 320 x 240 pixel imager with a full complement of timing circuits and controllers required to convert raw imager data into depth maps. (Image source: ESPROS Photonics)

Pre-built solutions

To implement 3D ToF systems, however, developers face multiple design challenges. Besides the timing circuits mentioned earlier, these systems depend on a carefully designed signal processing pipeline optimized to rapidly read results from the CCD array for each window or phase measurement, and then complete the processing required to turn that raw data into depth maps. Advanced 3D ToF imagers such as ESPROS Photonics'

[EPC660-CSP68-007](#) ToF imager combine a 320 x 240 CCD array with the full complement of timing and signal processing capabilities required to perform 3D ToF measurements and provide 12-bit distance data per pixel (Figure 3).

ESPROS Photonics' EPC660-007 card-edge connector chip carrier mounts the epc650 imager on a 37.25 x 36.00 millimeter (mm) printed circuit board (pc board) complete with decoupling capacitors and card edge

connector. Although this chip carrier addresses the basic hardware interface in a 3D ToF system design, developers are left with the tasks of completing the appropriate optical design on the front end and providing processing resources on the backend. ESPROS Photonics' epc660 evaluation kit eliminates these tasks by providing a full 3D ToF application development environment that includes a pre-built 3D ToF imaging system and associated software (Figure 4).

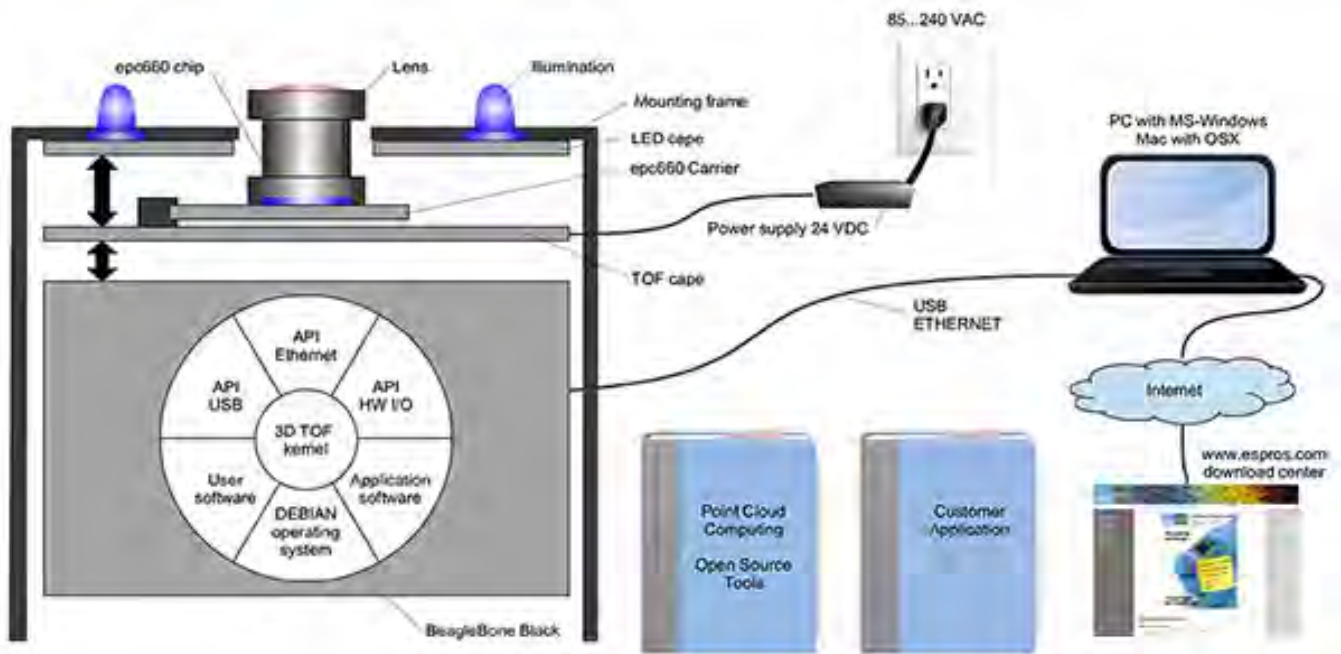


Figure 4: The ESPROS Photonics' epc660 evaluation kit provides a pre-built 3D ToF camera system and associated software for using depth information in applications. (Image source: ESPROS Photonics)

Designed for evaluation and rapid prototyping, the ESPROS kit provides a pre-assembled camera system that combines the epc660 CC chip carrier, optical lens assembly, and a set of eight LEDs. Along with the camera system, a **BeagleBone Black** processor board with 512 megabytes (Mbytes) of RAM and 4 gigabytes (Gbytes) of flash serves as the host controller and application processing resource.

ESPROS also provides [epc660 eval kit support software](#) that can be downloaded from its website and opened with a password

that can be requested from the company's local sales office. After gaining access to the software, developers simply run a graphical user interface (GUI) application with one of several provided configuration files to begin operating the camera system. The GUI application also provides control and display windows for setting additional parameters including spatial and temporal filter settings and finally for viewing the results. With minimal effort developers can use the kit to begin capturing depth maps in real time and use them as input to their own applications software.

Enhanced resolution 3D ToF systems

A 320 x 240 imager such as the ESPROS epc660 can serve many applications but may lack the resolution required to detect small movements in gesture interfaces or to distinguish small objects without severely restricting the range of interest. For these applications, the availability of ready-made development kits based on 640 x 480 ToF sensors enables developers to quickly prototype high resolution applications.

[Seeed Technology's DepthEye Turbo](#) depth camera integrates a 640 x 480 ToF sensor, four 850 nanometer (nm) vertical-cavity surface-emitting laser (VCSEL) diodes, illumination and sensing operating circuitry, power, and USB interface support in a self-contained cube measuring 57 x 57 x 51 mm. Software support is provided through an open-source [libPointCloud SDK github repository](#) with support for Linux, Windows, Mac OS, and Android platforms.

Along with C++ drivers, libraries and sample code, the libPointCloud SDK distribution includes a Python API for rapid prototyping as well as a visualization tool. After installing the distribution package on their host development platform, developers can connect the camera via USB to their computer and immediately begin using the visualization tool to display phase, amplitude, or point cloud maps, which are essentially enhanced depth maps rendered with texture surfaces to provide a smoother 3D image (Figure 5).

Analog Devices' AD-96TOF1-EBZ 3D ToF evaluation kit provides a more open hardware design built with a pair of boards and designed to use [Raspberry Pi's Raspberry Pi 3 Model B+](#) or [Raspberry Pi 4](#) as the host controller and local processing resource (Figure 6).

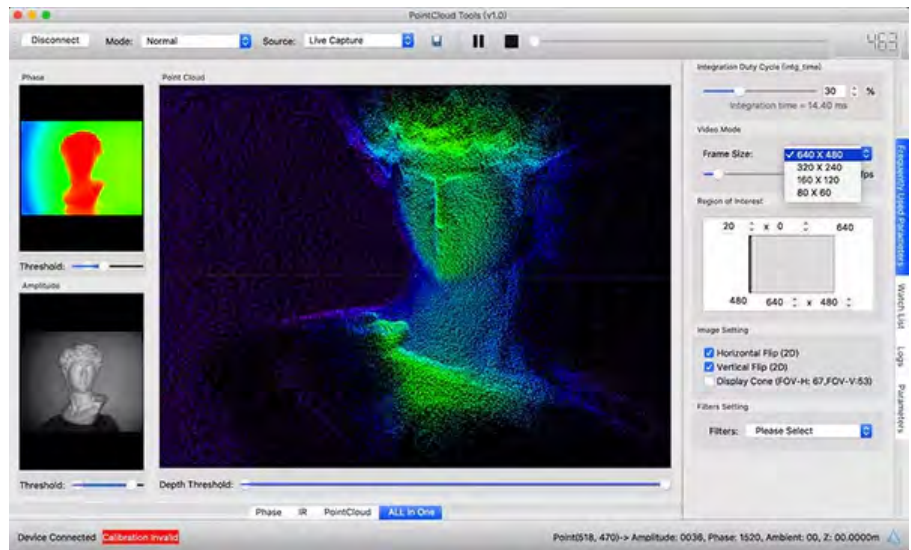


Figure 5: Used in combination with the Seeed Technology DepthEye Turbo depth camera, the associated software package enables developers to easily visualize 3D ToF data in a variety of renderings including point clouds as shown here in the main window pane. (Image source: Seeed Technology/PointCloud.AI)

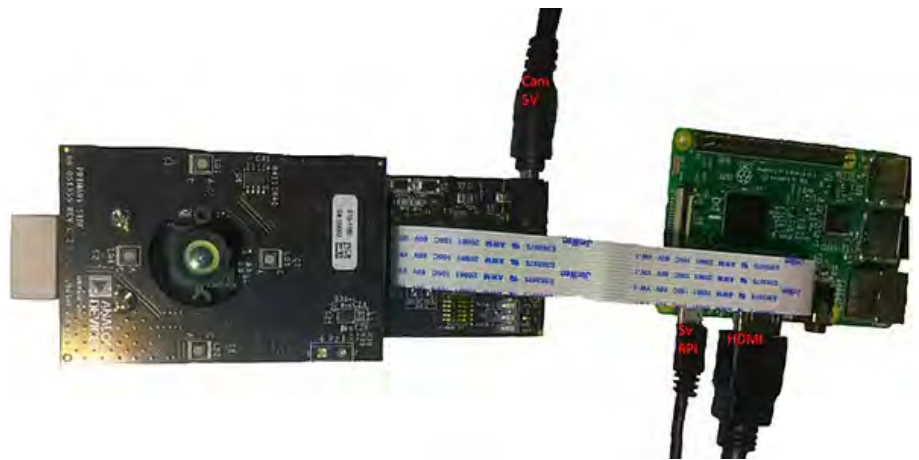


Figure 6: The Analog Devices AD-96TOF1-EBZ 3D ToF evaluation kit combines a two-board assembly for illumination and data acquisition with a Raspberry Pi board for local processing. (Image source: Analog Devices)

The kit's analog front-end (AFE) board holds the optical assembly, CCD array and buffers, firmware storage, and a processor that manages overall camera operation including illumination timing, sensor synchronization, and depth map generation. The second board holds four 850 nm VCSEL laser diodes and drivers and is designed to connect to the AFE board so that the laser diodes surround the optical assembly as shown in the figure above.

Analog Devices supports the AD-96TOF1-EBZ kit with its open-source [3D ToF software suite](#) featuring the 3D ToF SDK along with sample code and wrappers for C/C++, Python, and Matlab. To support both host applications and low-level hardware interactions in a networked environment, Analog Devices splits the SDK into a host partition optimized for USB and network connectivity, and a low-level partition running on Embedded Linux and built on top of a Video4Linux2 (V4L2) driver (Figure 7).

This network-enabled SDK allows applications running on network connected hosts to work remotely with a ToF hardware system to access the camera and capture depth data. User programs can also run in the Embedded Linux partition and take full advantage of advanced options available at that level.

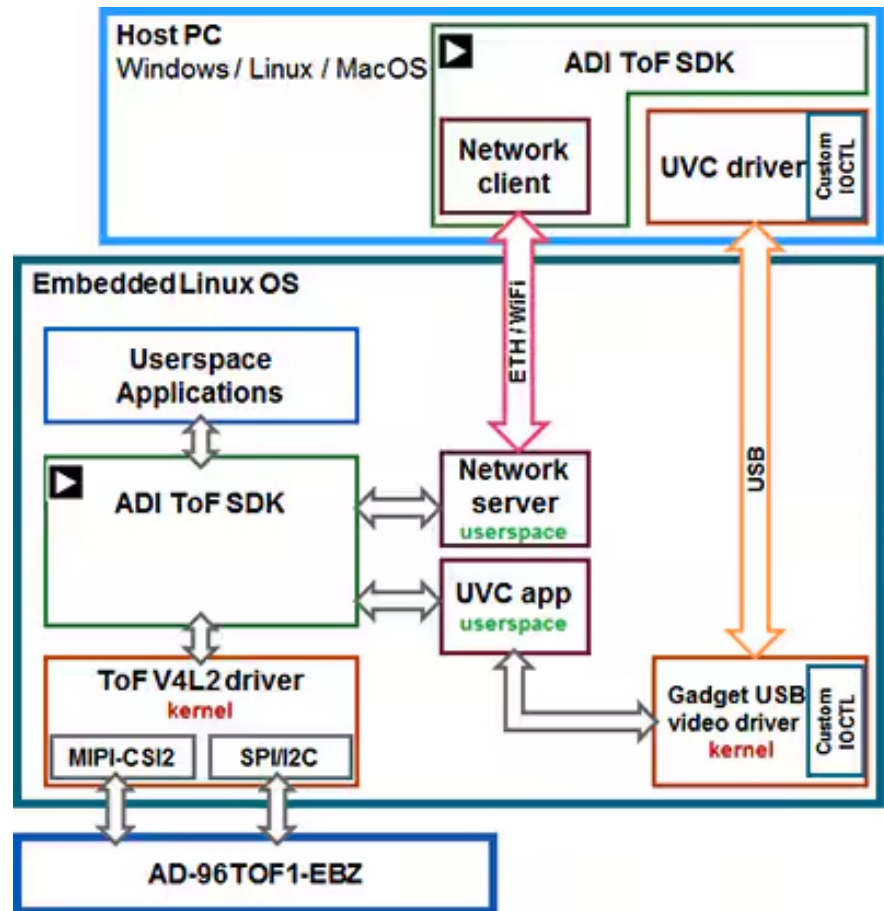


Figure 7: The Analog Devices 3D ToF SDK API supports applications running on the local Embedded Linux host and applications running remotely on networked hosts. (Image source: Analog Devices)

As part of the software distribution, Analog Devices provides sample code demonstrating key low-level operational capabilities such as camera initialization, basic frame capture, remote access, and cross-platform capture on a host computer and locally with Embedded Linux. Additional sample applications build on these

basic operations to illustrate the use of captured data in higher level applications such as point cloud generation. In fact, a sample application demonstrates how a deep neural network (DNN) inference model can be used to classify data generated by the camera system. Written in Python, this DNN sample application

(dnn.py) shows each step of the process required to acquire data and prepare its classification by the inference model (Listing 1).

Here, the process begins by using OpenCV's DNN methods (cv.dnn.readNetFromCaffe) to read the network and associated weights for an existing inference model. In this case, the model is a Caffe implementation of the Google MobileNet Single Shot Detector (SSD) detection network known for achieving high accuracy with relatively small model sizes. After loading the class names with the supported class identifiers and class labels, the sample application identifies the available cameras and executes a series of initialization routines (not shown in Listing 1).

The bulk of the sample code deals with preparing the depth map (depth_map) and IR map (ir_map) before combining them (cv.addWeighted) into a single array to enhance accuracy. Finally, the code calls another OpenCV DNN method (cv.dnn.blobFromImage) which converts the combined image into the four-dimensional blob data type required for inference. The next line of code sets the resulting blob as the input to the inference model (net.setInput(blob)). The call to net.forward() invokes the inference model which returns the classification results.

```
import aditofpython as tof
import numpy as np
import cv2 as cv
...
try:
    net = cv.dnn.readNetFromCaffe(args.prototxt, args.weights)
except:
    print("Error: Please give the correct location of the prototxt and caffemodel")
    sys.exit(1)
swapRB = False
classNames = {0: 'background',
              1: 'aeroplane', 2: 'bicycle', 3: 'bird', 4: 'boat',
              5: 'bottle', 6: 'bus', 7: 'car', 8: 'cat', 9: 'chair',
              10: 'cow', 11: 'diningtable', 12: 'dog', 13: 'horse',
              14: 'motorbike', 15: 'person', 16: 'pottedplant',
              17: 'sheep', 18: 'sofa', 19: 'train', 20: 'tvmonitor'}

system = tof.System()
status = system.initialize()
if not status:
    print("system.initialize() failed with status: ", status)

cameras = []
status = system.getCameraList(cameras)
...
while True:
    # Capture frame-by-frame
    status = cameras[0].requestFrame(frame)
    if not status:
        print("cameras[0].requestFrame() failed with status: ", status)

    depth_map = np.array(frame.getData(tof.FrameDataType.Depth), dtype="uint16", copy=False)
    ir_map = np.array(frame.getData(tof.FrameDataType.IR), dtype="uint16", copy=False)

    # Creation of the IR image
    ir_map = ir_map[0: int(ir_map.shape[0] / 2), :]
    ir_map = np.float32(ir_map)
    distance_scale_ir = 255.0 / camera_range
    ir_map = distance_scale_ir * ir_map
    ir_map = np.uint8(ir_map)
    ir_map = cv.cvtColor(ir_map, cv.COLOR_GRAY2RGB)

    # Creation of the Depth image
    new_shape = (int(depth_map.shape[0] / 2), depth_map.shape[1])
    depth_map = np.resize(depth_map, new_shape)
    distance_map = depth_map
    depth_map = np.float32(depth_map)
    distance_scale = 255.0 / camera_range
    depth_map = distance_scale * depth_map
    depth_map = np.uint8(depth_map)
    depth_map = cv.applyColorMap(depth_map, cv.COLORMAP_RAINBOW)

    # Combine depth and IR for more accurate results
    result = cv.addWeighted(ir_map, 0.4, depth_map, 0.6, 0)

    # Start the computations for object detection using DNN
    blob = cv.dnn.blobFromImage(result, inScaleFactor, (inWidth, inHeight), (meanVal, meanVal,
    net.setInput(blob)
    detections = net.forward()
    ...
    for i in range(detections.shape[2]):
        confidence = detections[0, 0, i, 2]
        if confidence > thr:
            class_id = int(detections[0, 0, i, 1])
            ...
            if class_id in classNames:
                value_x = int(center[0])
                value_y = int(center[1])
                label = classNames[class_id] + ": " + \
                    "{0:.3f}".format(distance_map[value_x, value_y] / 1000.0 * 0.3) + " "
            ...
    # Show image with object detection
    cv.namedWindow(WINDOW_NAME, cv.WINDOW_AUTOSIZE)
    cv.imshow(WINDOW_NAME, result)

    # Show Depth map
    cv.namedWindow(WINDOW_NAME_DEPTH, cv.WINDOW_AUTOSIZE)
    cv.imshow(WINDOW_NAME_DEPTH, depth_map)
```

Listing 1: This snippet from a sample application in the Analog Devices 3D ToF SDK distribution demonstrates the few steps required to acquire depth and IR images and classify them with an inference model. (Code source: Analog Devices)

Get started quickly with 3D Time-of-light applications

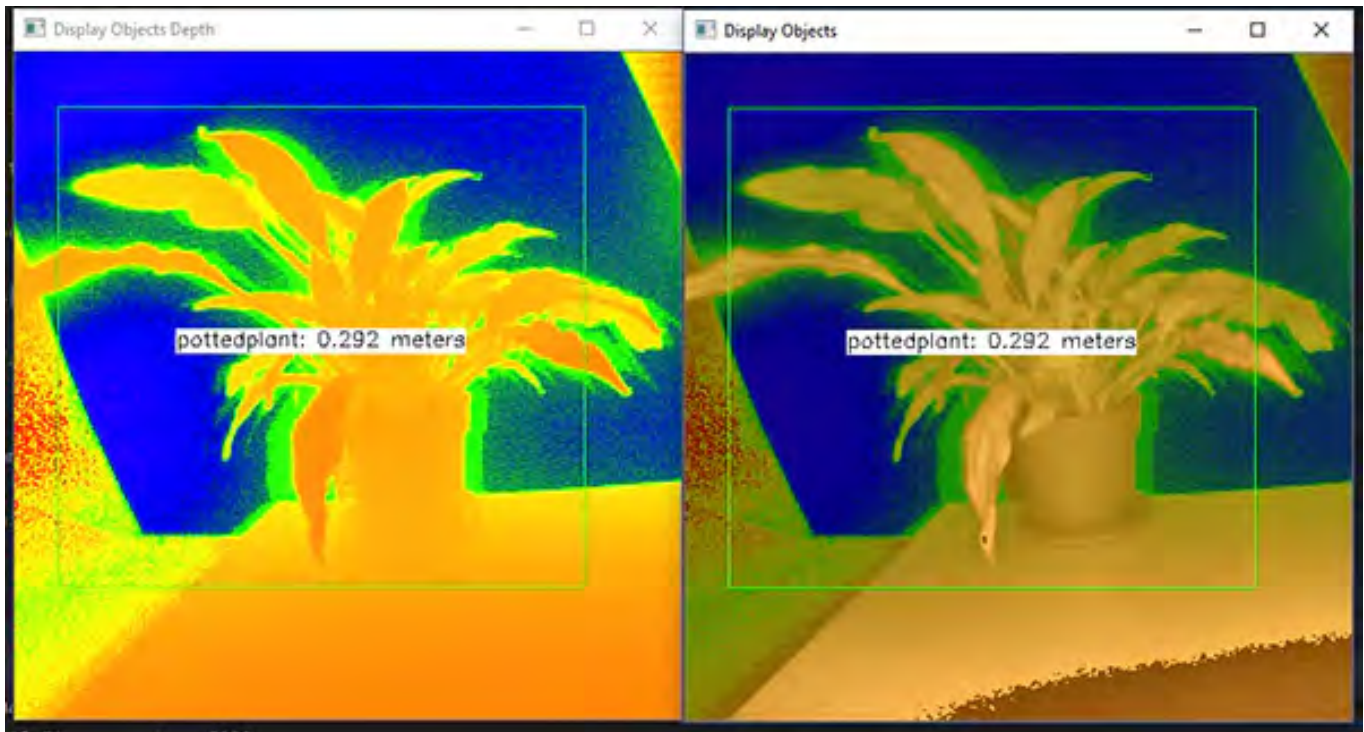
The remainder of the sample application identifies classification results that exceed a preset threshold and generates for those a label and bounding box displaying the captured image data, the label identified by the inference model, and its distance from the camera (Figure 8).

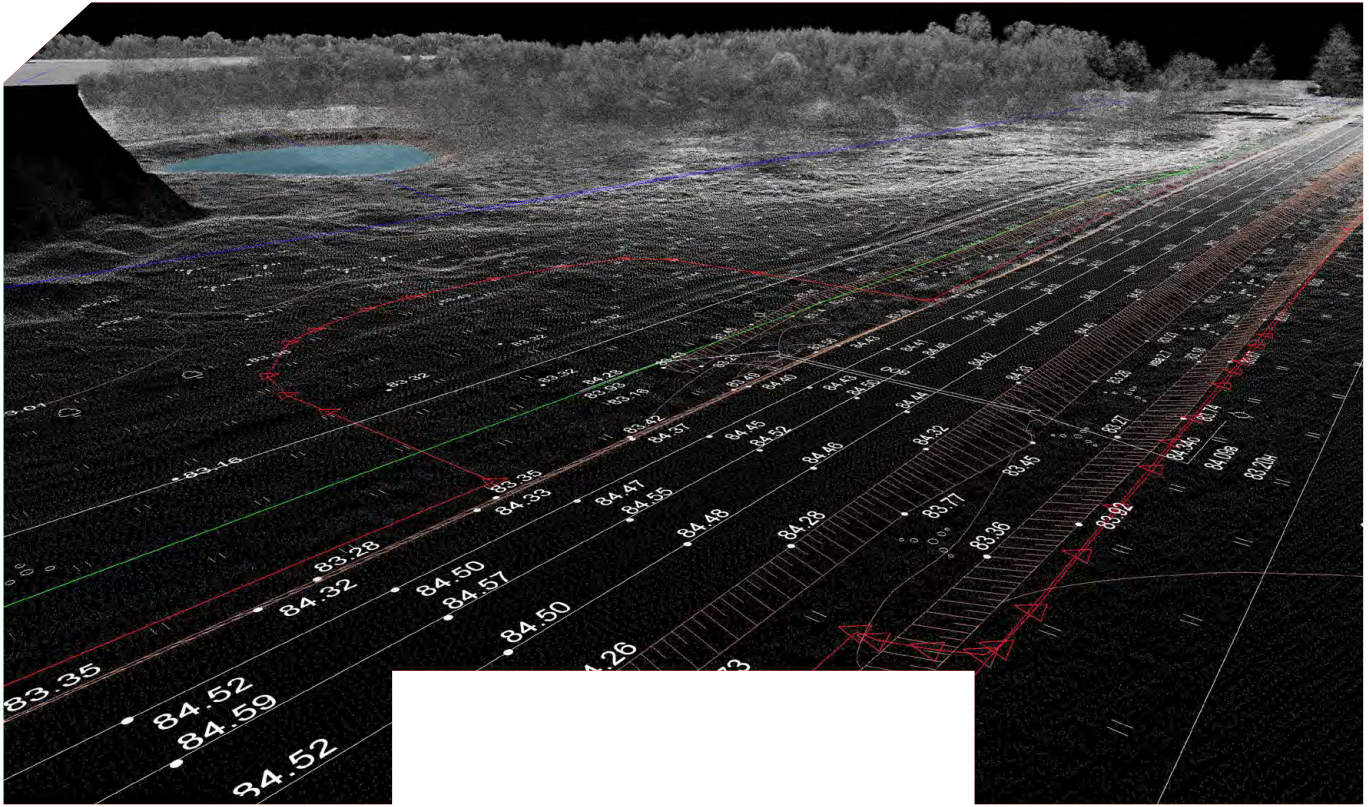
Figure 8: Using a few lines of Python code and the OpenCV library, the DNN sample application in Analog Devices' 3D ToF SDK distribution captures depth images, classifies them, and displays the identified object's label and distance. (Image source: Analog Devices)

As Analog Devices' DNN sample application demonstrates, developers can use 3D ToF depth maps in combination with machine learning methods to create more sophisticated application features. Although applications that require low latency responses will more likely build these features with C/C++, the basic steps remain the same.

Using 3D ToF data and high performance inference models, industrial robotic systems can more safely synchronize their movements with other equipment

or even with humans in "cobot" environments where humans and robots work cooperatively in close proximity. With different inference models, another application can use a high-resolution 3D ToF camera to classify fine movements for a gesture interface. In automotive applications, this same approach can help improve the accuracy of advanced driver-assistance systems (ADAS), taking full advantage of the high temporal and spatial resolution available with 3D ToF systems.





Conclusion

ToF technologies play a key role in nearly any system that depends critically on accurate measurement of distance between the system and other objects. Among ToF technologies, optical 3D ToF can provide both high spatial resolution and high temporal resolution, enabling

finer distinction between smaller objects and more precise monitoring of their relative distance.

To take advantage of this technology, however, developers have needed to deal with multiple challenges associated with optical design, precision timing, and synchronized signal acquisition

of these systems. As shown, the availability of pre-built 3D ToF systems, such as Analog Devices' AD-96TOF1-EBZ development platform and ESPROS Photonics' EPC660 evaluation kit, removes these barriers to application of this technology in industrial systems, gesture interfaces, automotive safety systems, and more.

How to use smart air quality sensors for environmental monitoring

By Jeff Shepard
Contributed By DigiKey's North American Editors



Environmental monitoring using smart air quality sensors is expanding across various applications from smart homes, buildings, and cities, to conventional and electric vehicles (EVs) and battery energy storage systems (BESS). In smart homes, buildings, and cities, air quality sensors can help ensure health and safety by monitoring airborne particles and gases associated with poor air quality, as well as smoke detection for early fire warnings. In vehicle passenger compartments, these sensors can identify volatile organic compounds (VOCs) and high levels of CO₂ that can raise health concerns. In EVs and BESS, they can be used to detect an increase in pressure and high levels of hydrogen in a battery enclosure following the first venting phase of a cell, enabling the battery management system (BMS) to react and prevent a second venting event or thermal runaway of the whole battery system.

The sensors used in these applications need to be compact, low power, and able to support secure boot and secure firmware updates. They often need to include multiple sensors, covering a broad spectrum of air quality monitoring. Integrating this range of functionality in a compact and low-power unit can be a daunting process, prone to restarts, resulting in a high-cost solution and delaying time to market.

To speed time to market and control costs, designers can turn to sensor modules that are factory calibrated, support secure boot and firmware updates, and provide connectivity options, including sending data to the cloud or using a CAN or other bus for local connections.

This article begins by comparing optical particulate counters, screen-printed electrochemical, and multi-parameter sensor technologies. It presents air quality sensor solutions and development platforms from [Sensirion](#), Metis Engineering, and [Spec Sensors](#), along with companion devices from [Infineon Technologies](#), and includes suggestions to speed the development process.

Particulate matter (PM) sensors provide counts for specific particle sizes such as PM_{2.5} and PM₁₀, which correspond to particles with diameters of 2.5 microns and 10 microns, respectively, as well as other particle sizes as needed by the specific application. Optical particle counters (OPCs) are a specific PM technology that moves the air to be measured through a measurement cell that contains a laser and a photodetector (Figure 1). Particles in the air scatter the light from the laser, and the detector measures the scattered light. The measurement is converted into mass concentration in micrograms per cubic meter ($\mu\text{g}/\text{m}^3$) and counts the number of particles per cubic centimeter (cm^3). Counting particles using an OPC is straightforward but converting that information into

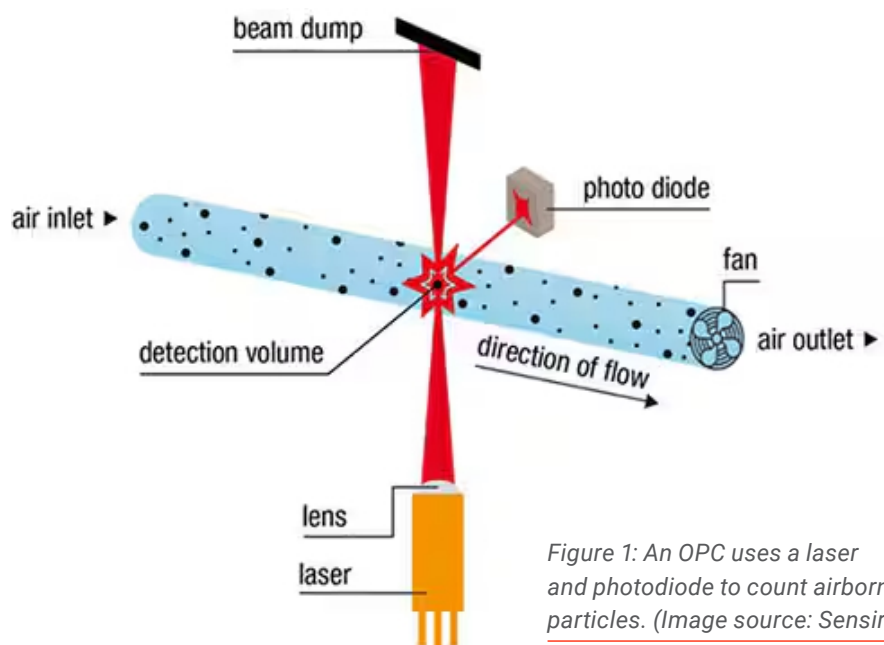


Figure 1: An OPC uses a laser and photodiode to count airborne particles. (Image source: Sensirion)

a mass concentration number is more complex. The software used for the conversion needs to consider the particles' optical parameters like shape and refractive index. As a result, OPCs can suffer from greater inaccuracy compared with other PM sensing methods such as direct, weight-based, gravimetric technologies.

Not all OPCs are the same. Highly accurate and expensive, laboratory-grade OPCs can count every particle in the measurement cell. Lower-cost commercial-grade OPCs are available that sample only about 5% of the aerosol particles and use software-based estimation techniques to arrive at an overall 'measurement.' In particular, the density of large particles like PM10 is typically very low, and they can't be measured directly by low-cost OPCs.

As particle size increases, the number of particles in a given particle mass drops dramatically. Compared with an aerosol of PM1.0 particles, an aerosol with PM8 particles has about 500 times fewer particles for a given mass. To measure larger particles with the same accuracy as small particles, a low-cost OPC has to integrate data over several hours to arrive at an estimate. Fortunately, aerosols have fairly consistent distributions of small and large particles in real-

world environments. With properly designed algorithms, it's possible to accurately estimate the number of larger particles, such as PM4.0 and PM10, using measurements of PM0.5, PM1.0, and PM2.5 particles.

Amperometric gas sensors

Instead of measuring particle counts, amperometric sensors measure gas concentrations. They are electrochemical devices that produce a current linearly proportional to the volumetric fraction of the gas being measured. A basic amperometric sensor consists of two electrodes and an

electrolyte. Gas concentration is measured at the sensing electrode, which consists of a catalytic metal that optimizes the reaction of the gas to be measured. The gas reacts with the sensing electrode after entering the sensor through a capillary diffusion barrier. The counter electrode acts as a half-cell and completes the circuit (Figure 2). An external circuit measures the current flow and determines the gas concentration. In some designs, a third 'reference' electrode is included to improve the stability, signal-to-noise ratio, and speed the response time of the basic amperometric sensor.

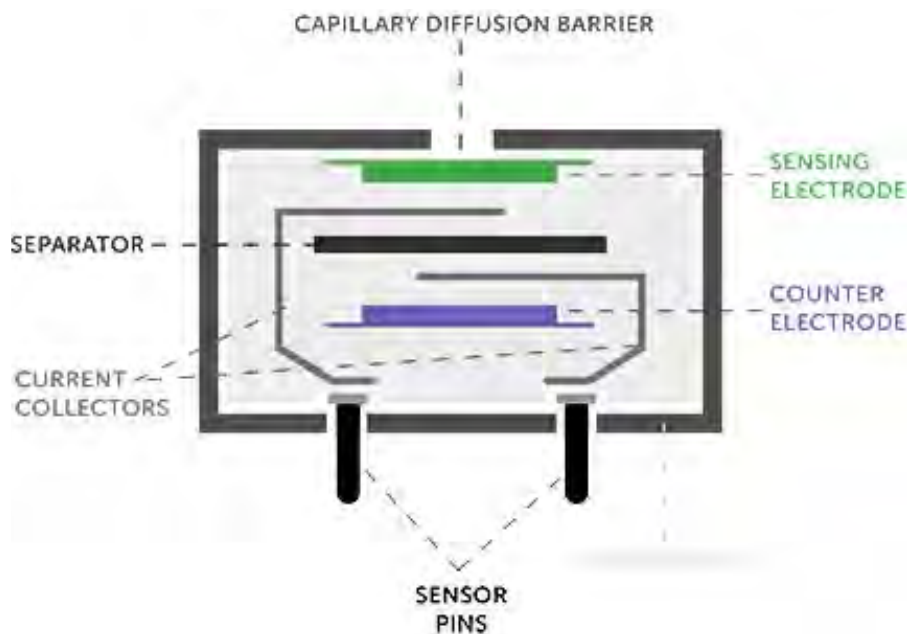


Figure 2: Amperometric sensors use two electrodes separated by an electrolyte to measure the concentrations of gases. (Image source: Spec Sensor)

Multi-parameter sensor for battery packs

Monitoring air quality is just the start for sensors designed to protect battery packs in EVs and BESS installations. These sensors monitor pressure, air temperature, humidity, dew point, and absolute water content, in addition to volatile organic compounds (VOCs) such as methane (CH₄), ethylene (C₂H₄), hydrogen (H₂), carbon monoxide (CO) and carbon dioxide (CO₂). During the first phase of battery venting, the gaseous product of a

common lithium-ion battery with a nickel manganese and cobalt cathode has a known chemical composition (Figure 3). The hydrogen concentration is critical; if it approaches 4%, hydrogen's lower explosive limit, there is a possibility of an explosion or fire. Actions should be taken to prevent the cell from going into thermal runaway. The pressure sensor can detect small increases in pressure inside a battery pack caused by venting. False positives can be avoided by cross-checking any increase in pressure with the other sensor measurements.

This multi-parameter sensor also monitors for too cool of an operating condition. Large battery packs in EVs and BESS often include active cooling to keep the packs from overheating when they are charged or discharged. If they are cooled too much, the internal temperature can drop below the dew point, resulting in condensation inside the pack, potentially shorting the cells and causing thermal runaway. The dew point sensor alerts the BMS before condensation can collect on the battery terminals.

Laser AQ sensor

Designers of heating, ventilation, and air conditioning (HVAC) systems, air purifiers, and similar applications can use Sensirion's [SPS30](#) PM sensor to monitor air quality indoors or outdoors. [SPS sensors](#) measure mass concentrations of PM1.0, PM2.5, PM4, and PM10, as well as PM0.5, PM1.0, PM2.5, PM4, and PM10 particle counts. It has a mass concentration precision of ±10%, a mass concentration range of 0 to 1000 µg/m³, and an operational life of over ten years. The SPS30 includes an I2C interface for short connections and a UART7 for cables longer than 20 centimeters (cm).

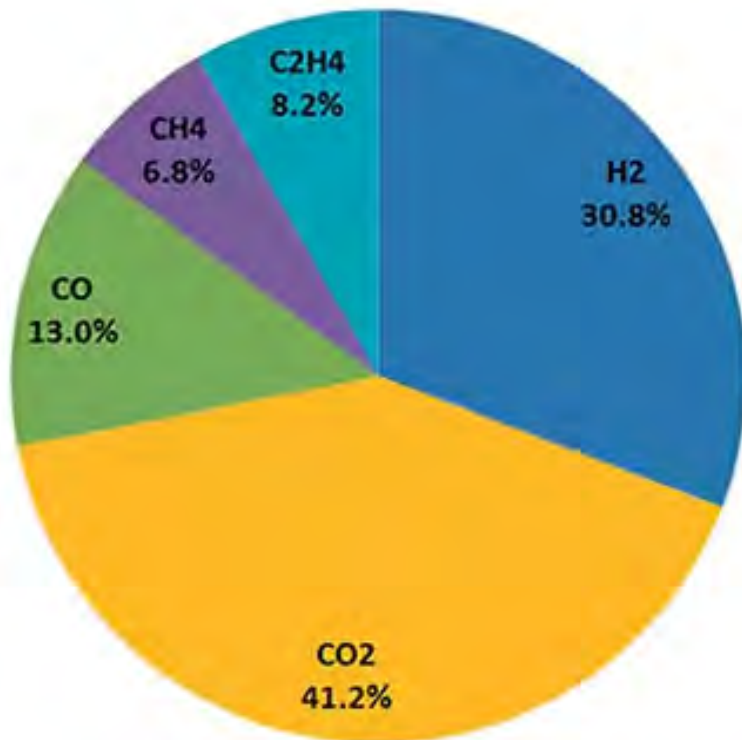


Figure 3: A specific mixture of gases is characteristic of the first phase of battery venting (Image source: Metis Engineering)

An automatic fan cleaning mode can be triggered at a preset interval to ensure consistent measurements. Fan cleaning accelerates the fan to maximum speed for 10 seconds and blows out accumulated dust. The PM measurement function is offline during fan cleaning. The default cleaning interval is weekly, but other intervals can be set to meet specific application requirements.

Dev kits and secure boot

The [SEK-SPS30](#) air quality monitor sensor evaluation board can be used to connect the SPS30 to a PC to start exploring the capabilities of this PM sensor. In addition, DigiKey offers a [platform](#) to combine Sensirion's air quality sensors with Infineon's PSoC 6 MCUs to develop next-generation intelligent air quality monitoring systems. For smart building systems where privacy is a concern, PSoC 6 supports secure boot and secure firmware updates (Figure 4).

Battery pack sensor

EV and BESS battery pack designers can use the CANBSSGEN1 from Metis Engineering for battery safety monitoring. It's designed to detect early failures due to cell venting. This CAN bus-based sensor includes a replaceable air filter and is especially useful in EVs (Figure 5). An optional accelerometer can



Figure 4: This dev kit from Sensirion and Infineon can implement secure boot and secure firmware updates. (Image source: DigiKey)

monitor for shocks up to 24G and impact duration, enabling the system to identify when the battery pack has been exposed to shocks above safe levels. It can measure:

- 0.2 to 5.5 Bar absolute pressure
- -30°C to +120°C air temperatures
- VOCs, equivalent CO₂ (eCO₂), and H₂ in parts per billion (ppb)
- Absolute humidity in milligrams of water vapor per cubic meter (mg/m³)
- Dew point temperature

CAN sensor dev kit

The DEVKGEN1V1 development kit helps to shorten the system integration time when using Metis CAN sensors. The sensors include a configurable CAN bus speed and address along with a DBC CAN database that supports integration into almost any vehicle with a CAN bus. The basic dev kit can be expanded, enabling developers to add more sensors to the CAN network.



Figure 5: This battery safety monitor sensor includes a replaceable air filter (center white circle). (Image source: Metis Engineering)

Indoor air quality sensor

Designers of indoor and vehicle in-cabin air quality monitoring systems can use the [110-801](#) from SPEC Sensors. The 110-801 is a screen-printed amperometric gas sensor that can detect a broad array of gases associated with poor air quality, including alcohols, ammonia, carbon monoxide, various odorous gases, and sulfides. The response of these sensors is linearly proportional to the volumetric fraction of the gas being measured, which simplifies system integration (Figure 6). Other features of this 20 x 20 x 3 mm sensor include:

- Parts per million (ppm) sensitivity
- Less than ten microwatts (μW) sensor power
- -10°C to $+40^{\circ}\text{C}$ operating temperature range (0°C to $+40^{\circ}\text{C}$ continuous operation)
- Robust and stable operation in the presence of a wide range of contaminants



Figure 6: This screen-printed amperometric gas sensor can measure the presence of a variety of gases. (Image Source: Spec Sensors)

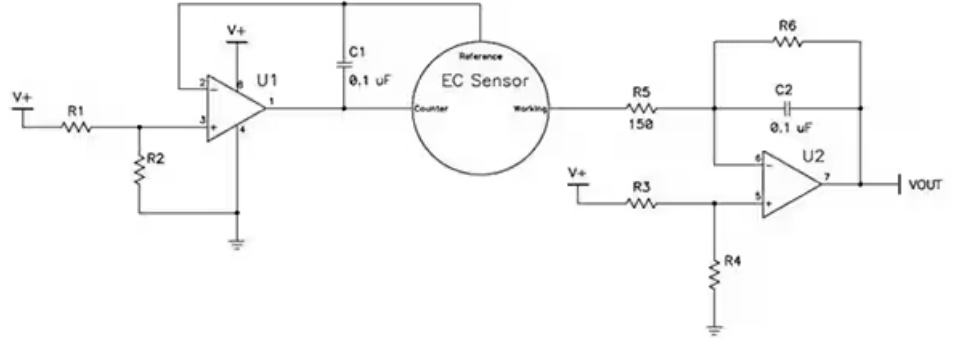


Figure 7: Simplified potentiostat circuit used to implement gas detection using an amperometric sensor. (Image source: Spec Sensors)

Amperometric gas sensor integration

A potentiostat circuit controls the working electrode's potential in an amperometric gas sensor and converts the electrode current to an output voltage (Figure 7). The voltage at pin 2 of the operational amplifier (op amp) U1 sets the reference electrode voltage, and the working electrode's potential is set by pin 6 of op amp U2. Op amp U2 also converts the current

output from the sensor to a voltage signal. At the same time, op amp U1 supplies current to the counter electrode that is equal to the working electrode current.

Summary

As shown, designers have a range of air quality sensor technologies to choose from when designing environmental monitoring systems. OPCs can be used to monitor for potentially dangerous particulate levels indoors and outdoors. CAN-based, multi-sensor systems can monitor for first stage venting in EV and BESS battery packs and help to prevent thermal runaway and possible fires or explosions. Low-power, screen-printed amperometric gas sensors can be used to detect a broad array of gases that cause poor air quality.



Understand drone design trade-offs before piling on the sensors

By Steve Taranovich
Contributed By DigiKey's North American Editors



[BME680](#) Drones are increasingly finding use in many applications, including as part of a first responder's tool kit at the scene of an emergency or disaster. For example, during the fire at the Notre-Dame Cathedral in Paris they were used to initially report the size, heat, and extent of the active fire. They were also outfitted with thermal imaging capability to search for people still inside. Later, they were used to assess the damage. Clearly this kind of application presents challenges in trying to see through complex conditions such as smoke and flames with adequate resolution.

As enticing as it may be to add more sensors to a drone to address these challenges, designers need to remain aware that drones are battery powered, and in many cases, cost sensitive. As a result, designers need to perform a delicate balancing act between functionality, cost, size, weight, and power consumption (SWaP). Finding this balance is the primary objective when considering the addition of sensors and imaging equipment to a drone design.

This article discusses the architectural trade-offs designers need to consider when adding sensors to a drone. In doing so, particular attention is paid to the power supply, which will likely have magnetics that can add excess weight and take up precious space. In addition, suitable power supply and sensor solutions

are introduced from vendors that include [Texas Instruments](#), [Efficient Power Conversion](#), Analog Devices, [Bosch Sensortec](#), [STMicroelectronics](#), and [SparkFun Electronics](#).

Drone architectural design considerations

The power supply: Once the designer knows the key areas on which to focus for optimum drone performance, they can then look at ways to minimize its physical size and weight, beginning with creating the most efficient power supply possible. This will lead to the minimization of the overall power supply size and weight, and so to a smaller, lighter drone.

Being battery operated, a drone with greater power supply efficiency can operate with a smaller battery size and weight. A typical choice for a drone battery would be a rechargeable lithium battery—Li-Ion or Li-Po type—especially if the designer plans to recharge the battery when landing or hovering over a wireless charger, or just upon landing with an external charger. Designers can also use a standard non-rechargeable battery as the power source and replace it once it is discharged.

When choosing a DC/DC converter, designers will need to use a wide input device due to the high voltage pulse of back EMF

(BEMF) from the rotor motors. Under motor deceleration, this BEMF will appear at the DC/DC converter's input as it comes after the separate DC/DC conversion powering the rotor motors.

The Texas Instruments [LM5161](#) DC/DC power converter IC is a good choice for a drone power supply because when programmed for discontinuous conduction mode (DCM) operation, it provides a tightly regulated buck output without any additional external feedback ripple injection circuit. It also has integrated high-side and low-side MOSFETs which save on board space. For added reliability, the LM5161 has peak and valley current limit circuits which protect against overload conditions. As an added precautionary feature, an undervoltage lockout (UVLO) circuit provides independently adjustable input undervoltage threshold and hysteresis.

There most likely will be many sensors aboard a drone, along with an associated sensor fusion IC, the main processor, and propeller motors. These require a good battery control system.

Designers may opt for gallium nitride (GaN) power transistors in the power supply architecture they choose that normally uses a power transistor. GaN will help with optimum performance efficiency with minimum size/footprint.

Wireless power - Re-charging while hovering [theoretical discussion]:^{1, 2, 3} This is desirable because when a drone lands and powers down to re-charge and takes off again, the start-up and liftoff of the rotor motors takes a great deal of power from the battery. Efficient Power Conversion is one of many companies researching wireless charging while hovering. An option for the power supply could be a wireless charging architecture based on a GaN FET, such as Efficient Power Conversion's [EPC2019](#).

GaN-based FETs allow switching at 13.56 megahertz (MHz)—a switching frequency difficult to reach with ordinary silicon FETs. This high switching frequency will also minimize the size and weight of power supply magnetics. In addition, GaN transistors are five to ten times smaller than silicon devices yet can handle the same power levels. With this type of power supply, drones do not have to land; they can instead hover over a wireless charging base.

Designers will find that there are a great many evaluation/development boards to speed time to market with wireless power. In the case of the EPC2019 GaN FET, Efficient Power Conversion supports it with the [EPC9513](#) wireless power receiver development board, to be used inside the drone. This development board is important to designers because it is based on the AirFuel standard, which ensures a certified wireless design that is interoperable with other wireless charging products, globally. Designers can request the Gerber files from the supplier for the demo board to recreate the board's optimized layout.



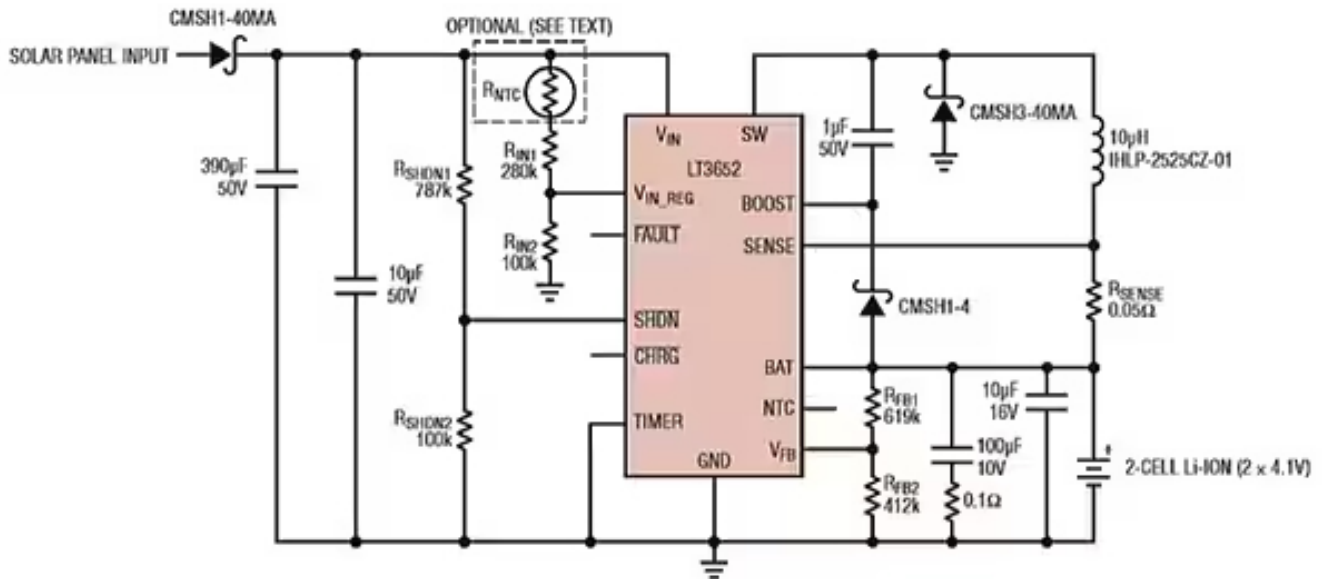


Figure 1: Designers can create reliable, efficient drone power with the addition of this 2 A solar-powered battery charger where thermistor RNTC has been added to compensate for a solar cell (like the PT15-75) temperature coefficient at maximum power levels. (Image source: Analog Devices)

Solar power: Another power option is to use solar energy to charge a drone battery. For this purpose, the [PT15-75](#) solar cell from [PowerFilm Inc.](#) is a good option.

The PT15-75 can be used in conjunction with an Analog Devices [LT3652](#) battery charger IC to implement a clever, compact battery charger design (Figure 1). Remember, there really is no situation in which open-circuit voltage (Voc) is output when the panel is attached to a load and providing current.

The LT3652 input regulation loop also has the capability to find the maximum power operating point

of the solar panel, which optimizes the efficiency of conversion from the sun's power to supply maximum output power to the battery.

Sensors: Sensors will both increase the controllability of drones, as well as their usefulness. With regard to controlling the drone, a sensor can enable an auto level mode, a constant altitude mode, or an orbit mode for circling around a specific object or point of interest. All of these added features rely on higher performance inertial measurement units (IMUs) and barometric pressure sensors to achieve an optimal user experience, as well as improved reliability for special purpose or commercial drones.

Designers may need to increase drone performance, which may require a gyroscope with extremely low output signal drift to ensure drone orientation, position, and balance, especially under changing temperature conditions. This can be achieved using a Bosch Sensortec [BMI160](#) accelerometer and gyroscope combination that comes as a small, low-power IMU with nine-axis sensor data fusion. It measures 2.5 x 3.0 millimeters (mm) with a height of 0.83 mm and consumes only 925 microamps (µA), even when the gyroscope and accelerometer are in full operating mode. It operates from a 1.71 volt to 3.6 volt supply.

To complement the BMI160, a digital barometric pressure sensor with temperature sensor will help to measure vertical velocity, enhance GPS navigation, and determine a drone's altitude. It is recommended that barometers be occasionally calibrated at sea level pressures to stay accurate. Bosch Sensortec's [BMP388](#) barometric pressure and temperature sensor is a good example of an IC that designers can integrate into their architecture. With a small footprint of 2 x 2 mm² at 0.88 mm high, and a low power consumption of just 3.4 μ A at 1 hertz (Hz), this sensor module is well suited for battery operation. The device has a typical relative accuracy of +/-8 Pa with a typical absolute accuracy of +/-50 Pa that will improve drone hovering and obstacle avoidance capabilities.

To detect motion along multiple axes, the STMicroelectronics' [ISM330DLCTR](#) iNEMO IMU system-in-package (SiP) module combines an accelerometer and gyroscope along with a magnetometer in a monolithic six-axis IC. This kind of configuration enables a drone to maintain horizontal, vertical, and rotational stability while hovering. For applications like professional-grade drone photography and 3D imagery, six-axis gyro stabilization is necessary and is provided by the ISM330DLCTR.

The gyroscope measures and maintains drone orientation. When integrating three accelerometers, each of which are oriented along a different axis, the degree of motion of a drone along any axis can be determined. This will better enable the collection of information regarding the drone's roll, pitch, and yaw, and then feed this information back to the drone's proportional-integral-derivative (PID) controller.

The magnetometer will measure the strength and direction of the Earth's magnetic north field in order to correct its trajectory. Be sure the magnetometer is calibrated frequently; power lines, motors, and any other strong fields emitted from electrical devices can affect it.

Drone movement caused by external forces, like a strong gust of wind, will be detected by the accelerometer and relayed to the PID controller, which in turn adjusts the motors to compensate.

Rangefinders: Landing, hovering, and distance from an object

Drones need to have good sensors to land safely, hover when wirelessly charging, and sense objects to avoid collisions when in motion. This ranging can be performed using sound or light.

Ultrasonic rangefinder sensing: Drone landing, hovering, and ground tracking capabilities can be provided using ultrasonic sensors. When a drone is in the process of landing, it needs to detect the distance from the bottom of the drone to the area in which it is landing. Although GPS and a barometer are part of this control function, accurate distance sensing is the key to a safe landing.

Ultrasonic sensors can also assist in safe hovering and ground tracking, which may need the drone to fly at a fixed height. One such distance ranging sensor for landing assistance, hovering, and ceiling detection is [MaxBotix's MB1010-000](#) ultrasonic time-of flight (ToF) ranging sensor board.

Understanding ToF

All of these cases need to use the ToF method, which is the time taken for an emitted ultrasonic wave to reach a target, plus the time for the reflected signal to travel back to the drone's sensor (Figures 2 and 3).

To calculate the distance from the drone to any object, use the equation:

$$\text{Distance}(d) = \text{ToF}(t) \times \text{Speed of sound } (v) / 2$$



Figure 2: Designers will need to understand the concepts of ToF during a drone landing, hovering, or wireless charging. (Image source: Texas Instruments)

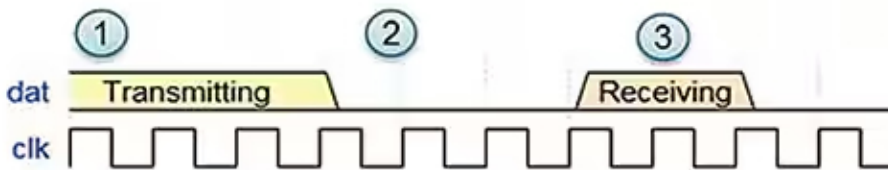


Figure 3: The three phases of ultrasonic ToF. Initial transmitted sound (1), silence (2), and received echo (3) for accurate range finding in their drone designs. An understanding of this graphic, coupled with the evaluation board and sensors discussed in this article, can help designers meet the goals of flight stability, collision avoidance, and optimum wireless charging when implementing the hardware suggestions in this section. (Image source: Texas Instruments)

Texas Instruments offers the [PGA460PSM-EVM](#) ultrasonic proximity sensing evaluation module that will shorten design time.

LiDAR range sensing: Another means of distance sensing is with the use of light detection and ranging (LiDAR) with pulsed lasers. The information gained from ToF LiDAR systems may be used to create a three-dimensional image. LiDAR technology allows for high accuracy and resolution, and a large coverage area.

Designers can select an optical laser distance ranging sensor such as the SparkFun Electronics [SEN-14032](#), a laser-based optical ranging sensor with a range of 40 m. An external microcontroller will be needed to interface with the sensor via I2C.

There are two primary kinds of architectures used for this kind of LiDAR: a solid-state LiDAR and a motorized 360° field of view rotating LiDAR. These both use the same principle, with a laser sending out a beam of light. In the solid-state case a mirror is used to scan, while the scanning rotating disk architecture uses a spinning disk, driven by a motor.

A third type of LiDAR known as flash LiDAR, flashes many short pulses at the same time, uses a camera chip to receive the pulse reflections, and subsequently measures the ToF. Flash LiDAR has very high resolution but is limited to about 30 meters (m).

Sensing the environment

Thermal imaging camera: A thermal imaging camera on a drone will detect heat signatures/temperature from objects and materials and display them as still images or videos. The Notre-Dame fire in Paris was observed and tracked using thermal image cameras. These cameras can detect small differences in heat, sometimes as small as 0.01°C .

Another important area for drone thermal imaging use is in disaster recovery, such as after an earthquake or severe hurricane, which can leave behind damaged or collapsed structures with people trapped inside (Figures 4 and 5).

A good way for designers to start using thermal imaging in a drone is to use something like the [500-0771-01](#), a micro thermal camera from [FLIR Lepton](#). The camera has a spectral range of 800 nanometers (nm) to 1400 nm, a scene dynamic range of 0° to 120°C , and a nominal power consumption of 150 milliwatts (mW) (operating), 650 mW (during shutter event), and 5 mW (standby).



Figure 4: A drone's-eye view of a collapsed building is an important first step a drone would take with a conventional camera. Then, with the use of a thermal imaging camera, it could sense the body heat of those trapped in the rubble. (Image source: IEEE⁴)



Figure 5: Designers now have the tools to locate and save lives in disaster situations. This image of a trapped person was taken using a DJI drone during a fire fighter drill. (Image source: Industrial Equipment News/Menlo Fire UAS/Drone program, via AP)

Humidity, pressure, and temperature sensing: To help determine atmospheric conditions, designers can use Bosch Sensortec's [BME280](#), a digital humidity, pressure, and temperature sensor with an SPI interface. It's highly integrated, measuring 2.5 mm x 2.5 mm x 0.93 mm, and consumes as little as 0.1 µA in sleep mode, or up to 3.6 µA when sensing all three parameters.

Accelerate time to market with multi-sensor development kits

The [DA14585IOTMSENSOR](#) is a multi-sensor development kit from [Dialog Semiconductor](#) that uses environmental sensors from Bosch Sensortec and motion sensors from [TDK Invensense](#). This kit is important for designers because it is a good platform upon which to experiment with and develop drone sensing sensor fusion capabilities and accelerate time to market.

It has a [BME680](#) low-power gas, humidity, pressure, and temperature sensor, as well as an accelerometer, gyroscope, and magnetometer. The DA14585IOTMSENSOR's sensor fusion capabilities lets designers see how this feature can be used to both get better overall sensing performance, while also extending drone battery life.

Conclusion

Drones present an unusually difficult design challenge of requiring high functionality and long flight times. As with any design, the main tasks the device will be required to perform must be known in order to develop a plan to ensure an optimal architecture that meets the project requirements.

References

- [Drones...Up, Up, and Away](#)
- [Light-Weight Wireless Power Transfer for Mid-Air Charging of Drones](#) Samer Aldhafer, Paul D. Mitcheson, Juan M. Arteaga, George Kkelis, David C. Yates, IEEE 2017
- [Nonlinear Parity-Time-Symmetric Model for Constant Efficiency Wireless Power Transfer: Application to a Drone-in-Flight Wireless Charging Platform](#) Jiali Zhou, Bo Zhang, Wenxun Xiao, Dongyuan Qiu, Yanfeng Chen, IEEE 2018
- [DronAID: A Smart Human Detection Drone for Rescue](#) Rameesha Tariq, Maham Rahim, Nimra Aslam, Narmeen Bawany, Ummay Faseeha, IEEE 2018

An introduction to pressure sensors

By Ryan Smoot, Technical Support Engineer, CUI Devices



A pressure sensor is an electronic component that monitors or detects gas or liquid pressure (force) and transforms that information into an electrical signal that can be used to monitor or regulate that force. To further initiate a discussion on pressure sensors, however, it is worthwhile to start with some fundamental definitions. Pressure is the magnitude of force exerted by a gas or a liquid on a unit area of a surface. The relationship between pressure (P), force (F), and area (A) is given by the equation $P=F/A$. The traditional unit of pressure is the Pascal, defined as one Newton (N) per square meter. Pressure can also be described as the force needed to impede a fluid's expansion.

Pressure sensors come in a variety of technologies, which are discussed later in this article, and each technology will ultimately determine how a particular pressure sensor operates. Although many pressure sensors available today can be used with a broad range of fluids and gases, some fluids that are more viscous or thick (paper pulp, asphalt, crude oil, etc.) may require customized pressure sensors. Nevertheless, there is a pressure sensor type suitable for almost any scenario.

Addressing naming confusion

At a fundamental level, pressure sensors, pressure transducers, and pressure transmitters are

comparable in function, and hence, the terms are often used interchangeably. However, the main distinctions among them are in their output signals.

A pressure sensor senses the force of the pressure and generates an output signal that corresponds to the magnitude of the force being exerted. A pressure transducer transforms the detected force into a continuous voltage output (V), while a pressure transmitter converts the detected force into a current output (mA).

In common usage, pressure sensors may be referred to using a variety of terms, such as pressure transducers, pressure transmitters, pressure senders, pressure indicators, piezometers, and manometers. Regardless of the given nomenclature, these devices are implemented for the monitoring and regulation of pressure in numerous applications, and can also be used for measuring other variables, such as fluid/gas flow, altitude, and water level.

Pressure measurement types

In the realm of pressure measurement and pressure sensors, there are a variety of terms that must be understood to ensure optimal system performance and measurement accuracy. The specific type of pressure sensor

utilized in your application can significantly impact these factors, as pressure is typically measured in relation to a reference, such as atmospheric pressure at sea level.

One crucial term is Gauge Pressure, which is a measurement of pressure relative to the local ambient or atmospheric pressure. The indicated pressure is either higher or lower than the local atmospheric pressure.

Another significant term is Absolute Pressure, which is pressure measurement relative to a reference of zero pressure or a vacuum. The measurement obtained using an absolute pressure sensor remains the same irrespective of the location where it is measured.

Differential Pressure pertains to the difference in pressure between two distinct points in a system, which is frequently used to calculate the flow of liquids or gases within pipes.

Vacuum Pressure measures a negative pressure range as compared to ambient or local atmospheric pressure.

Lastly, Compound Pressure involves the measurement of both positive and negative pressure or vacuum, essentially combining Gauge Pressure and Vacuum Pressure.

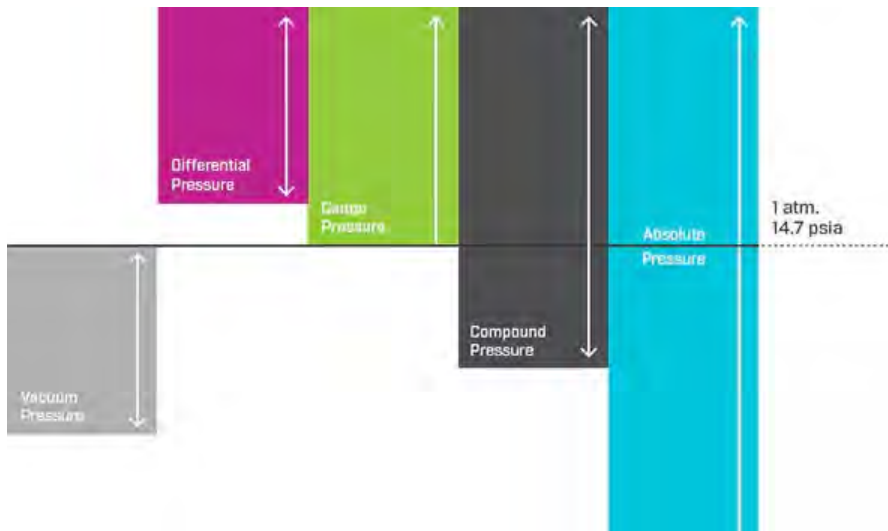


Figure 1: Visualizing the relationship between the variety of pressure measurements. (Image source: [CUI Devices](#))

Common pressure measurement technologies

The origins of pressure detection, comprehension, and measurement can be traced back to the pioneering work of Galileo in the late 1500s and Torricelli in the mid-1600s. The Bourdon Tube, the first pressure gauge, was invented in 1849, and it wasn't until 1930 that the first electrical output pressure transducers were introduced. With the rise of semiconductor technology, the number of different technologies utilized to detect this fundamental force has surged. Here is a brief overview of the primary pressure measurement technologies and their applications:

- **Capacitive:** detects alterations in electrical capacitance caused by pressure flexing a diaphragm

between the plates of a capacitor.

- **Inductive:** detects minute deflections of a diaphragm linked to a magnetic core that causes linear motion in the core. This motion varies the induced current and is transformed into an electrical signal.
- **Optical:** utilizes a light source that is gradually blocked by an increase in pressure and a sensor that produces a signal proportional to the change in the light. Fiber-optic sensors can also be used to measure changes in the path and phase of light caused by pressure.
- **Piezoelectric:** a quartz or ceramic material generates a variable electric charge proportional to the amount of compression applied to it by an external pressure.

Piezoresistive technology measures pressure by using the change in electrical resistance of a material when it is stretched.

- **Potentiometric:** utilizes a resistance device (potentiometer) and a sliding arm connected to a Bourdon tube. As the pressure changes, the arm moves, and a relative signal is produced by the potentiometer based on the force level.
- **Resonant:** force applied to a diaphragm with a vibrating wire alters the resonant frequency of the wire, which is converted into an electrical signal.
- **Strain Gauge:** transforms an applied force (pressure) into a change in electrical resistance that fluctuates with the applied force. This resistance can then be measured.

Pressure sensor types

To understand pressure sensors, it's also important to review the different types available for use in a design. Below are the basic types, presented in alphabetical order:

- **Diaphragm sensors:** incorporate thin, flexible, circular metal plates that deform under pressure.
- **Sealed sensors:** use atmospheric pressure at sea level as the reference pressure.
- **Solid-state sensors:** with no moving parts, these sensors use a semiconductor switching

element, such as a Field Effect transistor, to sense pressure.

- Strain gauge sensors: the resistance caused by a change in length due to an external force is measured and converted it into an electrical signal.
- Thin-film sensors: as the name implies, these sensors utilize a thin film containing resistive elements that alter resistance due to length and thickness changes induced by pressure.
- Vacuum sensors: designed to measure pressures that are below atmospheric levels. Typically, they utilize piezoelectric technology or measure the volume of gas in a particular space.
- Vented sensors: measure pressure relative to ambient barometric pressure.

Final design considerations

With the previous pressure sensor technologies, measurements, and types in mind, here are some final selection criteria to keep in mind when specifying a pressure sensor for a particular design. The first key parameter is the operating pressure range, which identifies the safe pressure range in which the device will perform as specified by the manufacturer. Operating temperature range, the maximum pressure that the sensor can tolerate before failure, and output type (analog/digital) are also important considerations. Output level, accuracy and drift, resolution, supply voltage, and environmental factors such as temperature, humidity, pressure, exposure to fluids, radiation, and physical

distance between the sensor and any receiving device should also be taken into account. By considering all these parameters, an appropriate pressure sensor can be selected for a specific application that meets the necessary operating conditions and performance requirements.

Conclusion

As an electrical engineer, it is important to understand that measuring pressure and utilizing that data for process control and monitoring is crucial in many industries, such as manufacturing and healthcare. Accurate and reliable pressure sensing is necessary to ensure product and service quality and safety. With advancements in technology, pressure sensors are now available in various types, technologies, sizes, outputs, and accuracies. Choosing the right pressure sensor for a specific application requires careful consideration of operating parameters, such as sensor type, pressure range, temperature range, maximum pressure, output type, accuracy, resolution, supply voltage, and environmental factors.

Fortunately, CUI Devices offers a line of [piezo-based pressure sensors](#) that can meet these requirements. Their sensors are available in multiple pressure types and operating ranges, allowing for flexible and accurate measurements.

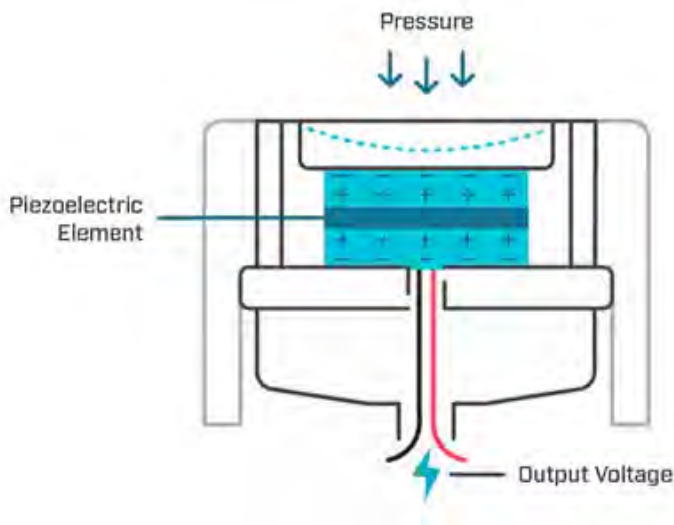
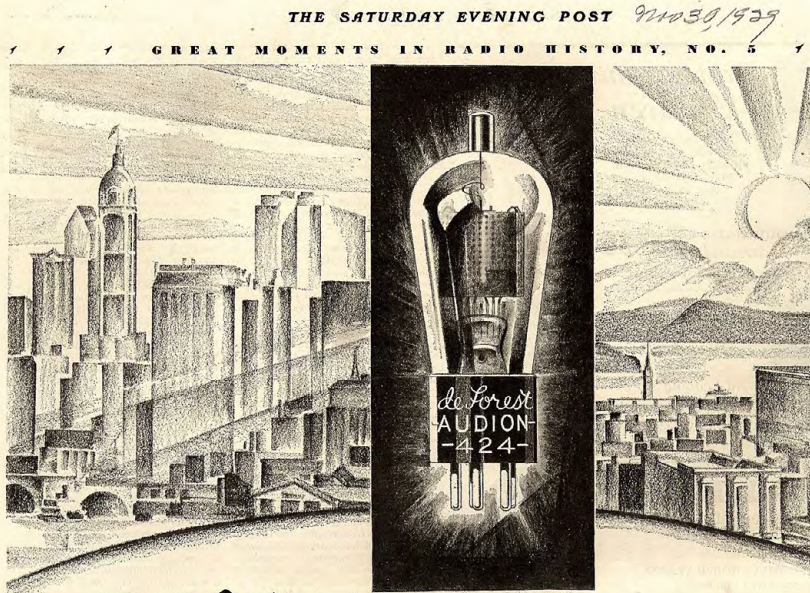


Figure 2: Example of a pressure sensor utilizing a piezoelectric diaphragm. (Image source: CUI Devices)



When NEW YORK said "Hello" to SAN FRANCISCO

Until Dr. Lee De Forest invented the amplifying tube which makes radio possible, telephone conversation was limited to a few hundred miles. Before a message spanned the continent, the human voice faded out until it was no longer audible. Dr. De Forest suggested that however faint the voice might become, his tubes would give it fresh energy at repeater points.



DR. LEE DE FOREST, THE "FATHER OF RADIO" AND THE INVENTOR OF THE FIRST RADIO TUBE, THE AUDION.

There would be no limit to telephoning. To test this, New York was connected with the Pacific Coast. "Hello!" said New York—and in San Francisco it sounded as though the speaker were in the next room. It was a great moment in radio history.

For twenty-three years, De Forest inventions have been the very basis of the radio industry. Every radio

tube, no matter what its name, is made by license agreement under patents owned by De Forest Radio Company, but only De Forest Audions bear the name of the inventor. They are acknowledged to be the world's standard.

Before you select any tubes for your radio, insist upon a tone-test comparison with De Forest Audions. It will speedily convince you of the superiority of these tubes. DR. FOREST RADIO CO., JERSEY CITY, N. J.

Branch Offices located in: BOSTON, NEW YORK, PHILADELPHIA, ATLANTA, PITTSBURGH, CHICAGO, MINNEAPOLIS, ST. LOUIS, KANSAS CITY, DENVER, LOS ANGELES, SEATTLE, DETROIT, DALLAS, CLEVELAND

1906

1929

de Forest AUDIONS

EVEREADY RAYTHEON TUBES



NO OTHER TUBE IS SO STRONGLY BUILT AS

EVEREADY RAYTHEON

Look at this exclusive 4-Pillar construction—with its eight points of support—cross-anchored top and bottom. No other tube can be built like this, for it is patented! No legal troubles with Eveready Raytheons. No "frozen" stocks. And you stand to profit by all worth-while tube patents.

TELEVISION TOO!

EVEREADY RAYTHEON is among the first to produce television tubes for sending and receiving, for talking movies and similar uses. The Eveready Raytheon line is complete—with standard receiving tubes, battery and A.C. operated, rectifying tubes, Photo-Cells and Kino-Lamps. In addition, we developed and make the original gaseous rectifying tube for "B" eliminators—the famous B-H tube—for which there is an enormous sale.

NATIONAL CARBON COMPANY, Inc.
General Offices: New York, N. Y.
Branches: Chicago Kansas City
New York San Francisco
Div. of Union Carbide and Carbon Corporation



The Eveready Raytheon Kino Lamp for television purposes is the first tube designed specifically to hold light waves with efficiency. The Eveready Raytheon B-H tube is a long life gaseous rectifying tube for television, used also for talking pictures.

4-PILLAR TUBES

IMAGE 1-02

IMAGE 1-01

The rise of designators: from DeForest to Western Electric

By David Ray
Cyber City Circuits

The before times

There once was a time before the age governed by part numbers and catalogs. The industry was young, and everything was chaos. Before the late 1920s, vacuum tubes were primarily used for R&D, purpose-built, and made in low volume. Consumer A.M. radios did exist at the time, but the variety of tubes available to consumers was so small that each could have its own model name or arbitrary identifier.

As quickly as a small vacuum tube and radio manufacturer sprung up, they were bought up by the competition, and everyone wanted to be unique and difficult in their way.

Each manufacturer would use their own sizes, form factors, pinouts, and part numbers. As a radio service person, you had to always keep a dozen different vacuum tube databooks with you, just so that you could find substitutions and that's only if you were lucky.

Then, could you believe it, multiple manufacturers would use the same part number for two completely different parts? After World War 2, many of the small brands had been swallowed up by the behemoths of their day, which made repairing and maintaining the existing equipment even harder. There needed to be

some sort of 'registered standard' for parts. Today, every tiny part inside of your favorite electronic devices has a part number. How did we get here?

This is the story of the naming convention used in the EIA RS-370: Designation System for Discrete Semiconductor Devices.

The government takeover of the American Marconi company

Marconi Wireless Telegraph Company of America

At the beginning of the twentieth century, the American DeForest Wireless Telegraph Company was the largest telegraph provider in the United States. The company owned and maintained many patents for aspects of wireless telegraphy but couldn't defend against patent infringement. [1] Many other individuals and small businesses sprung up around the country. They blatantly infringed on the patents, and the DeForest Company eventually ran out of money defending them. In 1904, the company was purchased by a group of investors through a leveraged buyout and reorganized as the United Wireless Telegraph Company.

Starting, the company was already drowning in debt. So, it did what many companies today would do: sell capital stock. Across the country, it placed advertisements in newspapers, selling shares for ten dollars each, and in 1910, they reported that the stock was worth upwards of forty-two dollars. [2]

They were keen to advertise all over the mid-west and sell as many shares as possible. As they created new shares, the value of any existing dilutable shares

United Wireless Telegraph Company
 Owing a controlling or dictating interest in American De Forest, Marconi, other and subsidiary companies, thus practically controlling the entire wireless field.

Capital Stock \$20,000,000
 of which \$10,000,000 is in preferred participating and \$10,000,000 is common stock.

Par Value of Share \$10, fully paid and non-assessable
 Gen. H. Parker, managing director for Pacific Coast and Alaska
 202-204 Arcade Bldg., Seattle, Wash.
 (office—189 Broadway, New York; 47 Broadway, New York)

OFFICERS
 Abraham White, President Gen. C. K. Wolfe, Treasurer
 C. G. Wilson, Vice-President J. Gordon English, Secretary

DIRECTORS
 Abraham White, N. Y.; James H. De Forest, Wireless Telegraph Co.
 H. B. McChesney, N. Y.; Andrew Magallon, N. Y.; Director
 Marconi Wireless Telegraph Co. of America
 Don Glavin, ex-President and Director of Western Union
 Gen. H. Parker, Seattle, Wash.
 C. C. Wilson, Denver, Colo.; Pres. International News and
 Reading Company

After years of experimenting and the expenditure of millions of dollars, wireless telegraphy has been placed on a successful operative basis on both land and sea and the world has begun to realize that it is the most useful and far reaching of man's inventions.

The Marconi and American De Forest systems are foremost in the field, and together embrace the fundamental principles of successful wireless telegraphy—made one for sea operation, the other in land service, while each can perform both kinds of work.

They have proved and demonstrated the practicability of wireless telegraphy, and put it into practical commercial operation. Capitalized accordingly, considering the wonderful value of the results that have been accomplished, and their irreplaceable position in the wireless field with its vast possibilities, they enjoy

intolerable advantages.

The United Wireless Telegraph Company has been formed by friends of both the Marconi and American De Forest Wireless Telegraph Companies to combine their interests and subordinate all the international wireless systems throughout the world and fully develop and operate this method of communication.

There is promised as soon as the possible extent of this company's service through the Wireless Telegraph Company is ascertained with that field service that can daily transmitting messages between each city and to all parts of sea, over electric landlines, wireless being now equipped with instruments. The land and sea service may be extended almost without limit.

Both the Marconi and American De Forest systems are now working \$100,000,000 and in the United States \$100,000,000 and in the world \$100,000,000 each, and the total of \$200,000,000 is being raised in the next few months.

We invite subscriptions at \$10.00 per share, in the preferred participating capital stock of United Wireless Telegraph Company, per value \$10.00, fully paid and non-assessable, carrying 7 per cent. annual dividends, and full participation in the profits of the company after a like amount of dividend is paid on the common stock.

Application must be made immediately to secure

THIS AD WILL POSITIVELY NOT APPEAR AGAIN

Investigation of Wireless Business.

The Federal Grand Jury has begun an investigation in New York City into the affairs of the United Wireless Telegraph Company, three of the officers of which were arrested and released on bail. They are charged with sending out literature designed to mislead the public in regard to the concern's stock and capitalization. The post office authorities assert that the officers conducted one of the "most gigantic schemes to defraud investors that has ever been unearthed in this country." It is alleged that the company was formed for the purpose of selling worthless stock; that its claim of possessing more than \$14,000,000 worth of assets is wholly false, and that the stock has steadily decreased in value because the business has been a losing one. Altogether there are about 28,000 stockholders, scattered principally through the West. According to the Post Office authorities, these stockholders stand to lose upward of \$20,000,000.

The president of the company claims that it has a fully paid-up capital of \$100,000, and for the last three years has carried an average daily balance of more than \$100,000. He states that "The company has equipped 310 ships plying the waters of the Atlantic and Pacific Oceans and the Great Lakes with its system of wireless telegraphy. These ships are in actual daily operation and communicate with the company's 100 land stations, which are also in daily operation."

IMAGE 2-01

dropped. Eventually, the company was accused of being formed only to sell worthless stock. [3] They had diluted their capital shares, causing early investors to lose much of their value. Soon, the United Wireless Telegraph Company came under federal investigation for postal fraud.

The company's name became synonymous with fraud, and it is recorded that the postal authorities claimed that it was one of the 'most gigantic schemes to defraud investors that has ever been unearthed in this country.' [3] Their "stockholders" lost up to twenty million dollars in this scam. This is equivalent to six hundred fifty million dollars today.

By 1912, the company's president was in prison for stock fraud, and the company fell into insolvency. The Marconi Company took the opportunity to pick up the

pieces and gain a larger footprint in the United States. It formed the Marconi Wireless Telegraph Company of America, more often known as the 'American Marconi Company,' a subsidiary of the British Marconi Company. Through these acquisitions and others, the Marconi Company had collected the world's largest catalog of wireless radio patents and controlled most of the wireless communication abilities worldwide.

General Electric and the 200 kW transmitters

Five years later, in 1917, the United States entered the First World War. President Woodrow Wilson knew the importance of a strong Navy and supported any and all

IMAGE 2-02

efforts to expand and strengthen it, including ensuring an effective and reliable communication infrastructure. The United States Navy wanted the American Marconi Company to replace its 50 kW transmitter stations with 200 kW transmitters, allowing the Navy to communicate with all ships at sea. The Marconi company reluctantly pushed back, not wanting to invest in the new equipment.

Rather than further negotiation, the Navy commandeered the transmitter stations and transferred control to General Electric for national security. It turns out General Electric was glad to pay for the cost of the new 200 kW transmitters.

Following the war's end, the American Marconi Company attempted to regain control of

these overpowered transmitting stations. The Navy argued that instead of allowing a foreign company exclusive control over global communication, the United States government should force the Marconi Company to divest from all American holdings and transfer control to General Electric. [1] Which they did.

IMAGE 2-04



IMAGE 2-05

Radio Corporation of America

In October 1919, General Electric merged all these assets together into the Radio Corporation of America, better known as RCA. The founding charter for the new company stated that *'no person shall be eligible for election as a director or officer of the corporation who is not at the time of such election a citizen of the United States'*, to keep the US Navy satisfied. [1]

RCA started out already owning a majority of wireless radio patents worldwide. With an army of lawyers on its payroll, RCA pursued any company using its patents without a license, swiftly suing them into bankruptcy. They often purchased the company after it crashed into the ground and picked it apart. Not above industrial espionage, they would do anything to ensure that other companies could not succeed.

Much later, RCA would face legal action in the Supreme Court for violating antitrust laws over the decades.

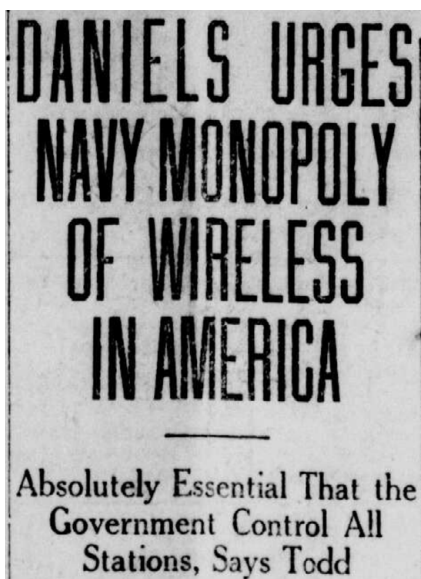


IMAGE 2-03



The first '2Nxx' transistors

Electrical manufacturers geared to war production

By the late 1930s, RCA's part numbering system had become a generally accepted standard in the United States. However, other companies, the military, and European companies stubbornly used their own proprietary systems.

During World War 2, the lack of a consistent standard numbering system across the industry became a mission-readiness problem.



IMAGE 3-01

Joint electron tube engineering council

In 1944, several major manufacturers and groups gathered to create the Joint Electron Tube Engineering Council, known today as JEDEC. [4] From 1944 to 1947, the group focused on standardizing all aspects of manufacturing, including plate thickness, materials, base and socket types, and part designations. As a result, the RCA numbering system was recommended to replace all other systems in the United States. Europe would continue using its existing systems.

In 1948, then chairman of JETEC, Virgil M. Graham said, 'As JETEC is a unique organization, deriving its authority and responsibility from two-parent associations whose views and methods of

MISCH METAL • NIGROSINE • PORCELAIN • PETROLEUM JELLY • ZINC
CALCIUM ALUMINUM FLUORIDE • RESIN (SYNTHETIC) • ETHYL ALCOHOL

MATERIALS USED IN RCA RADIO TUBES

LEAD ACETATE • MALACHITE GREEN • GLYCERINE • ZINC CHLORIDE • IRON
MARBLE DUST • WOOD FIBER • STRONTIUM NITRATE • LEAD OXIDE • ZINC OXIDE
LAVA • MICA • TIN • SODIUM CARBONATE • SODIUM NITRATE • SILVER OXIDE

BARIUM CARBONATE	CALCIUM CARBONATE
ARSENIC TRIOXIDE	AMMONIUM CHLORIDE
STRONTIUM CARBONATE	POTASSIUM CARBONATE

ISOLANTITE	BAKELITE
MOLYBDENUM	PHOSPHORUS
ALUMINA	SILICON
BORAX	SHELLAC
BARIUM	TUNGSTEN
COPPER	TITANIUM
CARBON	SILICA
CHROMIUM	GLASS
CALCIUM	MAGNESIA
CAESIUM	PLATINUM
COBALT	STRONTIUM
IRIDIUM	MAGNESIUM
MONEL	ROSIUM
MERCURY	NICKEL
CALCIUM OXIDE	COBALT OXIDE
BARIUM NITRATE	THORIUM NITRATE

Gases Used in Manufacture
NEON — HYDROGEN — CARBON DIOXIDE — ILLUMINATING GAS
HELIUM — ARGON — NATURAL GAS — NITROGEN — OXYGEN

Elements Entering into the Manufacture
ARGON — ALUMINUM — BORON — BARIUM — CAESIUM — CALCIUM — COPPER — CARBON — CHROMIUM — CHLORINE
COBALT — HYDROGEN — HELIUM — IRIUM — IRON — LEAD — MAGNESIUM — MERCURY — MOLYBDENUM
NICKEL — NEON — NITROGEN — OXYGEN — POTASSIUM — PHOSPHORUS — PLATINUM — SODIUM — SILVER
SILICON — STRONTIUM — TUNGSTEN — THORIUM — VANADIUM — TITANIUM — TIN — TUNG — TUNG — TUNG — TUNG — TUNG

IMAGE 3-02

operation are so widely divergent, I believe that it is an important tribute to those who conceived and organized JETEC that it has worked so well and accomplished so much for the industry in the few years of its operation.'

Bell Labs and Western Electric

In the early 1950s, there was a rush to make the first commercially viable transistor. Bell Labs developed the first point-contact transistor in 1947. Western Electric, the manufacturing subsidiary of AT&T, was positioned to work with the new technology earliest. Bell Telephone Laboratories and Western Electric were both subsidiaries of AT&T, enabling a quick transition from development to production.

The story goes that engineers at Western Electric needed a way to number their production designs and decided to use the existing JETEC standard for naming vacuum tubes as inspiration. An early example of this is the Western Electric 2N23 Germanium Bead Transistor. [5] According to the standards used for vacuum tubes at the time, the character 'N' was used for non-standard (other) type bases, but since vacuum tubes were well standardized by this point, there were very few needs for this character any longer.

Note from Writer: There is an information gap concerning the written standard used at AT&T and Western Electric during this time. If you or a loved one have a copy of the specific internal standard that AT&T used to designate vacuum tubes in the late 1940s to early 1950s, please get in touch with technical.content@digiqukey.com with the subject line 'Retro Electro' with information. Thank you.

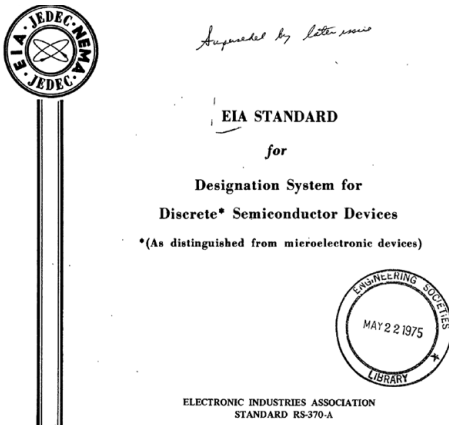


IMAGE 4-01

The designation system for discrete semiconductor devices EIA RS-370

By the 1970s, JEDEC (formally JETEC) was maintaining the registration of new designs. The naming convention used by Western Electric twenty years earlier became formalized in 1975 by the publication of the Electronic Industries Association Recommended Standard RS-370: Designation System for Discrete* Semiconductor Devices (* as distinguished from microelectronic devices). The RS-370 governs the part

numbers for diodes, transistors, and optoelectronic devices. It is important to know that this system was never intended for Integrated Circuit devices.

The current standard is available on the JEDEC website for [free download](#).

How does the EIA-370 work?

The reader knows part numbers like the 1N4001 and the 2N2222A. Notice that they consist of three or four sets of characters. The 2N2222A transistor is an excellent example of how the EIA-370 numbering system works.

Part numbers consist of four groups of characters.

The **first character** is the number of useful connections ('n') minus one. Since the 2N2222A is a transistor with three connections, the first character is '2'. For parts with more than five useful connections, the character '4' is used. This wasn't the case for vacuum tubes. Instead, this number would tell the user the voltage of the filament used or the power rating of the tube.

It is important to recognize that 1Nxxxx and 2Nxxxx part numbers are not related, meaning a 1N2222 and a 2N2222 have no inherent characteristics in common other than being discrete semiconductor devices.

The reader may ask, why is it 'n minus one' and why not just the number of pins? Consider that the ordinary farm-grown diode, which can be purchased from Digikey, has two connections: the anode and the cathode. There will never be a single-pin semiconductor device to start numbering with '1'.

The **second character** can be either a 'C' or an 'N'. Introduced in 1982 with the EIA-370B, the character 'C' is used for unencapsulated dies, while the character 'N' is used when a die is encapsulated in a registered package. So, the '2C2222' would describe the bare die that would otherwise be used inside a 2N2222 transistor.

Fun Fact: The EIA-370 is maintained and reviewed by the JEDEC Committee on Terms, Definitions, and Symbols. They are also responsible for other hits like the JESD88F Dictionary of Terms for Solid State Technology and the JESD100B.01 Terms, Definitions, and Letter Symbols for Microcomputers, Microprocessors, and Memory Integrated Circuits. Both are available as free downloads at JEDEC.org

The character 'N' was used for transistors because in the standard for naming vacuum tubes, the 'N' meant 'other' or 'none' and was used mainly for crystals.

The **third set of characters** is assigned consecutively, starting with the number 21. This means that up to 2,201 different registered transistors existed before the release of the 2N2222.

Finally, the **fourth character** is a suffix used to designate revisions to a part, where the part can be substituted for any previous version but not vice versa. The suffix can also be used for devices with special characteristics.

The suffix 'R' is used for diodes meant for reverse polarity but have packages identical to those of a forward-polarity device. Additional suffix characters 'S' and 'L' are sometimes used for super-fast-acting diodes.

Thoughts on the evolution of this standard

The rampant growth of wireless technology in the early twentieth century marks a milestone in civilization. Like most new

technology, a crisis precipitates the change needed to create new generalized standards. World War II brought the issue of unconventional part designators to the forefront.

The journey from the DeForest Telegraph Company to the government intervention that created the Radio Corporation of America and consolidated the vast array of patents was pivotal, shaping the industry for all electrical engineers and hobbyists. Consider what the world would be like if the United Wireless Telegraph Company became a successful venture instead of a textbook example of stock fraud during its time.

The writer would like to thank the members of the reference desk at the Linda Hall Library and Jack Ward at the Transistor Museum.

References

- [1] "The Founding of RCA and the Relationship Between RCA and Cunningham," [Online]. Available: <https://vacuumtubesinc.com/cunninghampage>. [Accessed 06 05 2024].
- [2] The Fargo Forum, "A Letter, and What It Means to Holders of United Wireless Telegraph Stock," The Fargo Forum, 11 05 1910.
- [3] Electrical World, "Investigation of Wireless Business," Electrical World, vol. LV, no. 25, p. 1634, 23 06 1910.

[4] A. C. Streamer, "Electical Manufacturers Geared to War Production," Electrical World, p. 18119, 20 01 1945.

[5] J. Ward, "Western Electric 2N23," Transistor Museum, [Online]. Available: http://semiconductormuseum.com/PhotoGallery/PhotoGallery_2N23.htm.

[6] JEDEC, "JEDEC History," [Online]. Available: <https://www.jedec.org/about-jedec/jedec-history>. [Accessed 29 04 2024].

[7] Microchip, Datasheet: ATtiny1614 / ATtiny1616 / ATtiny1617, 2017.

[8] Panasonic Industries, Chip Resistors Array - EXB Type, Panasonic, 2020.

[9] "Wireless Companies Merge," New York Times, p. 4, 10 01 1904.

Image Citations

- [1-01] DeForest Advertisement (The Saturday Evening Post | March 30, 1929)
- [1-02] Eveready Advertisement (Circa Early 1930s)
- [2-01] Advertisement for United Wireless Telegraph Company Stock
Citation: Investigation of Wireless Business (Electrical World | June 23, 1910)
Citation: Daniels Urges Navy Monopoly of Wireless in America (Santa Ana Register | Santa Ana, Ca | Dec 6, 1918)
- [2-04] American Radio to Absorb Marconi Co. (New York Sun | New York City, NY | March 23, 1919)
- [2-05] RCA Logo (Circa 1919)
- [3-01] Electrical Manufacturers Geared to War Production (Electrical World | Jan 20, 1945)
- [3-02] RCA Advertising (Circa 1933)
- [4-01] Cover page of the 1975 JEDEC classic Standard for Designation System for Discrete Semiconductor Devices

There is a gap in official information available on this topic from the 1940s through the 1960s. If you or a loved one have any information that may help with future articles, please email technical.content@digikey.com with the subject line 'RETRO ELECTRO' and details. Thank you.

1904

The American DeForest Wireless Telegraph Company is reorganized as the United Wireless Telegraph Company

1912

United Wireless is picked up by the American Marconi Company

1917

The US Navy assumes control of the American Marconi Company

1919

General Electric starts the Radio Corporation of America

1944

The Radio Manufacturers Association and the National Electrical Manufacturers Association join to establish the Joint Electron Tube Engineering Council (JETEC) [6]

1958

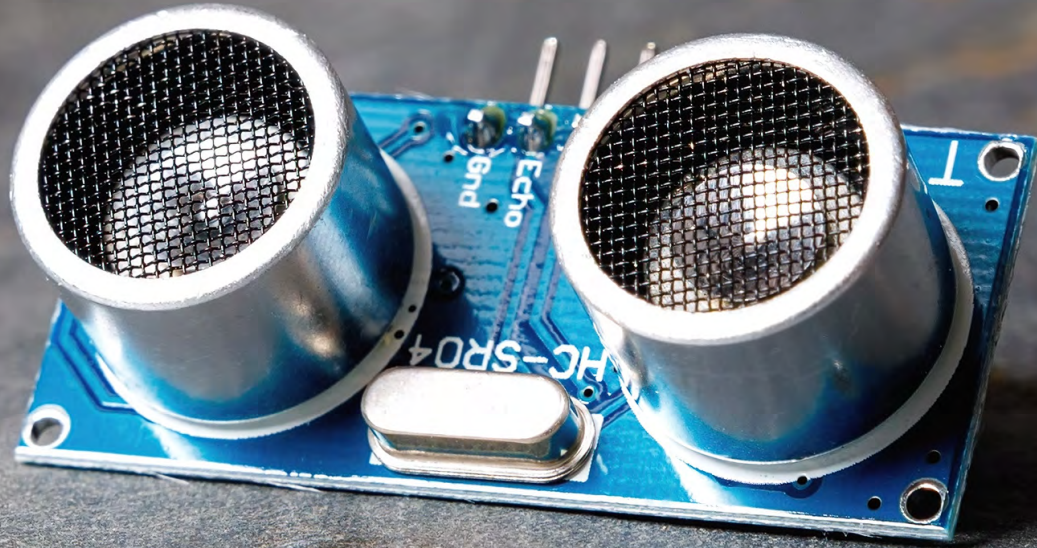
ETEC rebrands to Joint Electron Device Engineering Council (JEDEC) [6]

1975

EIA Standard for Designation System for Discrete Semiconductor Devices – RS-370-A is Published

1982

The EIA-370-B is published, formalizing the use of the letter symbol 'C'



The basics of applying ultrasonic transducers for sensing objects or fluid flow

By: Bill Schweber

Contributed By DigiKey's North American Editors



no regulatory restrictions, and avoids radio frequency (RF) spectrum allocation, as well as electromagnetic interference (EMI) and radio frequency interference (RFI) issues.

Though well established as a methodology, to fully realize the benefits of ultrasonic sensing, designers need a good understanding of its operating principles, available components, and associated circuit requirements. They must also consider architectural approaches, such as whether to use separate transmit and receive units—which allows for placement of each in different locations—or use a combined single-unit transceiver. Finally, they must provide a suitable electronics driver and receiver which can operate at the optimal

frequency for position sensing/detection and fluid flow sensing.

This article provides a basic introduction to ultrasonic transducers and their application in object detection and flow sensing. Real-world ultrasonic devices from [PUI Audio](#) are presented by way of example, and an appropriate driver IC and associated development kit are described to enable application development.

Simple principle, adopted from nature

Ultrasonic detection is a sophisticated version of the basic echolocation principle used by animals such as dolphins and bats (Figure 1).

The Internet of Things (IoT) and the expanding role of artificial intelligence (AI) at the network edge have raised interest in making applications more intelligent and ambient aware. As a result, designers need to consider appropriate sensing options, many of which can rely upon well-established technologies to avoid complexity. For example, ultrasonic energy is widely used to sense the presence of nearby objects and even determine their distance, as well as to measure fluid flow rates.

The advantages of ultrasound are that it is relatively easy to apply, is accurate, has minimal safety or risk factors, carries

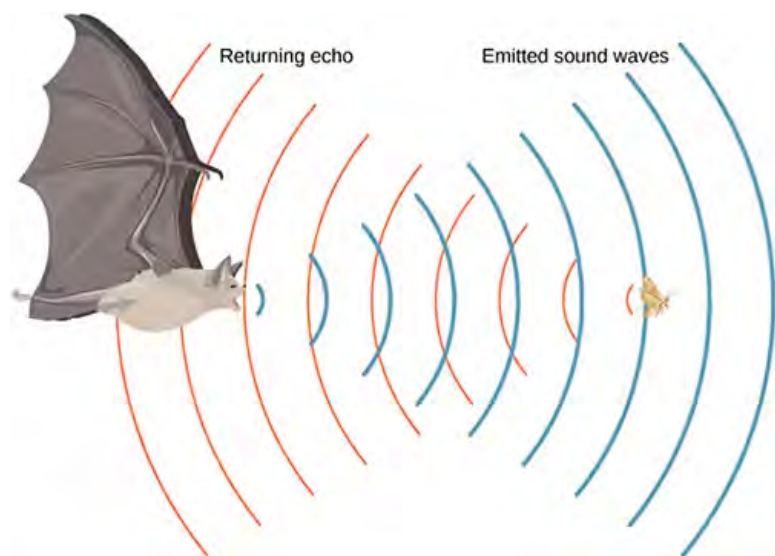


Figure 1: Electronic acoustic detection and position sensing has its origins in echolocation which is effectively used by living creatures such as bats. (Image source: Wikipedia)

In operation, a brief pulse of acoustic energy is generated by a transducer, which is usually a piezoelectric device. After the pulse ends, the system switches to receive mode and awaits the reflection (echo) of that pulse. When the transmitted acoustic energy encounters an impedance transition or discontinuity, such as between air and a solid object, some of that energy is reflected and can be detected, usually by a piezoelectric device.

Acoustic impedance is based on the density and acoustic velocity of a given material, and it is important to determine the amount of reflection that occurs at the boundary of two materials having different acoustic impedances.

The proportion of energy that is reflected is a function of the material type and its absorption coefficient, as well as the impedance differential at the boundary between materials. Hard materials such as stone, brick, or metal reflect more than soft materials such as fabric or cushions.

The acoustic impedance of air is four orders of magnitude less than that of most liquids or solids. As a result, the majority of ultrasonic energy is reflected to the transducer based on the large difference in reflection coefficients. The acoustic cross section is a metric analogous to radar cross

section and is determined by the target object's material and size.

This detection and distance sensing is similar to what happens when radar RF energy or lidar optical energy encounters an impedance discontinuity, and some of that energy is reflected back to the source. However, while the overall concept is the same, there is a big difference: ultrasound energy is not electromagnetic energy. Its use of the frequency spectrum is not regulated, and it has very few restrictions. One pertinent restriction is excessive sound pressure level (SPL), a consideration that is generally not relevant to sensing/detection applications, as most of these operate at fairly low power levels.

Propagation and media matter

There's one other big difference: ultrasound sensing/detection can only be used in a propagating medium such as air, other gases, or liquids. The attenuation and propagation characteristics of acoustic energy through various media are the opposite of RF and optical energy. Acoustic energy propagates well through liquids, while RF energy generally does not. Optical energy also has high attenuation in most liquids.

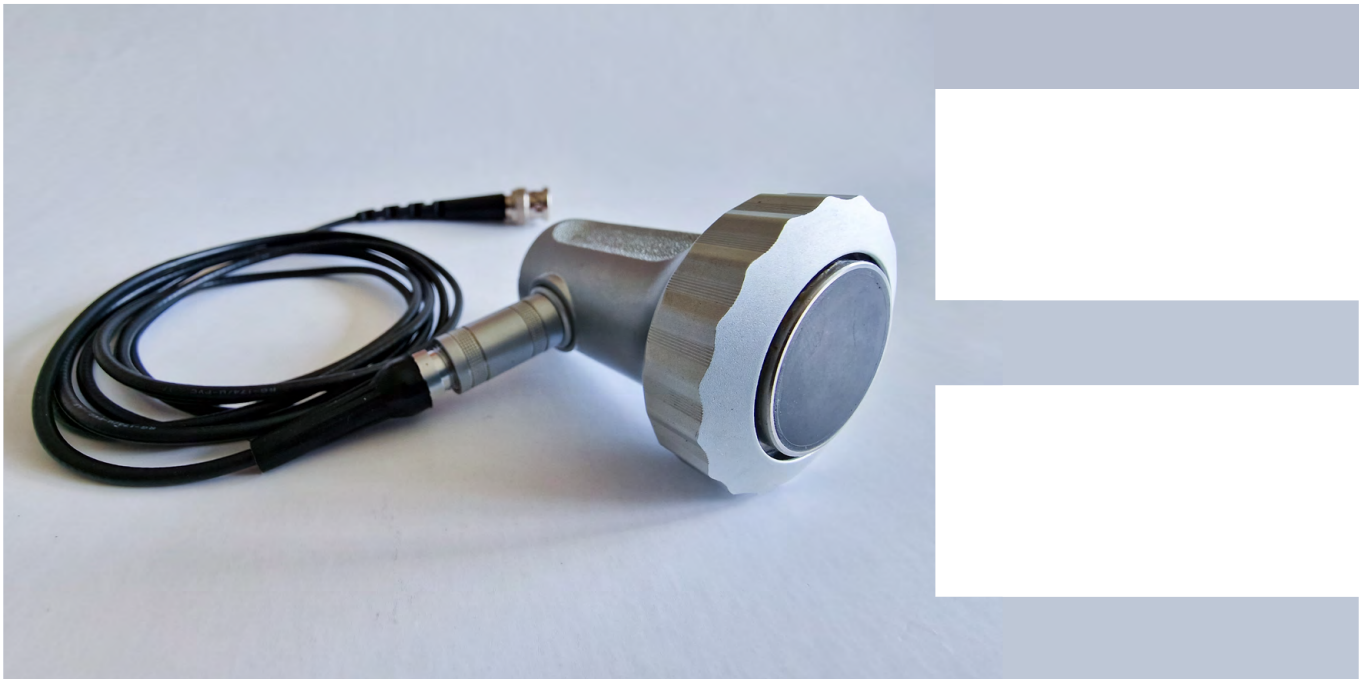
Further, unlike acoustic energy, both RF and optical have low attenuation in a vacuum.

In its simplest implementation, the ultrasonic system is used solely to detect the presence or absence of an object or person within an overall zone of interest by detecting a return signal of sufficient strength. By adding a timing measurement, the distance to the target can also be determined.

In more sophisticated systems where the distance to the object must also be calculated, a simple equation can be used: distance = $\frac{1}{2}$ (velocity \times time), using the round-trip time between the emitted pulse and received reflection, and the established speed of sound in air which is about 343 meters per second (m/s) at +20°C (+68°F). If the medium is a fluid or gas other than air, the appropriate propagation speed must be used.

Note that the speed of sound in air varies slightly with temperature and humidity. Therefore, ultraprecise distance sensing applications require that one or both of those factors must be known, and a correction factor added to the basic equation.

Interestingly, as an example of engineers turning a negative factor into a positive one, there



are advanced temperature sensing systems that exploit this shift in propagation speed versus temperature. These systems measure temperature by using precise timing of the reflected ultrasound pulse reflection over a known distance. They then do a “reverse correction” to determine what temperature would have caused that change in propagation speed.

Transducer parameters start the process

After determining the application requirements, designers must then select a suitable audio driver and associated receiver that

can operate at the appropriate frequency, typically at a relatively high 40 kilohertz (kHz) for position sensing/detection, and several hundred kilohertz for fluid flow sensing. The benefits of high-frequency transducers include increased resolution and focused directivity (forward-facing beam pattern), but the disadvantage is increased signal path attenuation.

The rate at which the ultrasonic energy scatters and is absorbed while propagating through the medium of air increases with frequency. This results in a decrease in the maximum detectable distance if other factors are held constant. The 40 kHz frequency is a compromise

between factors such as efficiency, attenuation, resolution, and physical size, all of which are related to wavelength.

To begin the selection process, it’s helpful to know that transducers used for ultrasonic sensing are characterized by several top-tier parameters. Among these are:

- Operating frequency, tolerance, and bandwidth: As noted, 40 kHz is common for many basic applications, with a typical tolerance and bandwidth of several kilohertz.
- Drive voltage level: This specifies the voltage level for which the transducer provides optimal performance. It can range from a few tens of volts to 100 volts, or more.

- **SPL:** This defines the magnitude of the audio output at the defined drive level; it can easily reach 100 decibels (dB) or more. Higher SPL offers coverage over greater distances (a typical ultrasound application has a range in the tens of feet).
- **Receiver sensitivity:** This characterizes the voltage output of the piezoelectric transducer at a given SPL. The higher this number, the easier it will be to overcome system noise and provide an accurate reading.
- **Directivity:** This defines the spread of the transmitted beam as well as the angular range over which the receiver is most sensitive. Typical values range from 60° to 80° at 40 kHz, usually measured to the angle at which response is 6 dB below the value at the 0° angle.

functions (called a monostatic arrangement) can simplify physical set-up while minimizing space requirements and transducer cost (Figure 2).

The PUI Audio [UTR-1440K-TT-R](#) (Figure 3), a 40 kHz ultrasonic transceiver, is a viable choice

for this configuration. It has a diameter of just 14.4 millimeters (mm) and a height of 9 mm. It is designed to operate from an AC drive voltage of 140 volts peak-to-peak (V_{p-p}) and presents a nominal load of 1800 picofarads (pF) to the driver. Its echo sensitivity is better than 200 millivolts (mV) and its directivity is 70° ±15°.

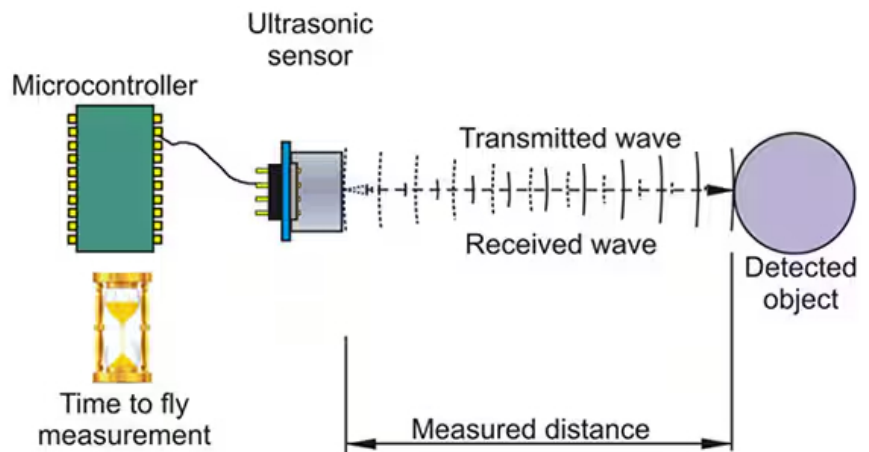


Figure 2: In a monostatic arrangement, a single transducer is used for both transmit and receive functions. (Image source: Science and Education Publishing Co.)

Positioning the transducers

One of the factors that determines the choice of a transducer is the relative position and orientation of the object being sensed. If the object is directly in front of the source and all or partially at a right angle to the incident energy, some of that impinging energy will be reflected directly back to the source.

In this situation, the use of a single transducer for both transmit and receive

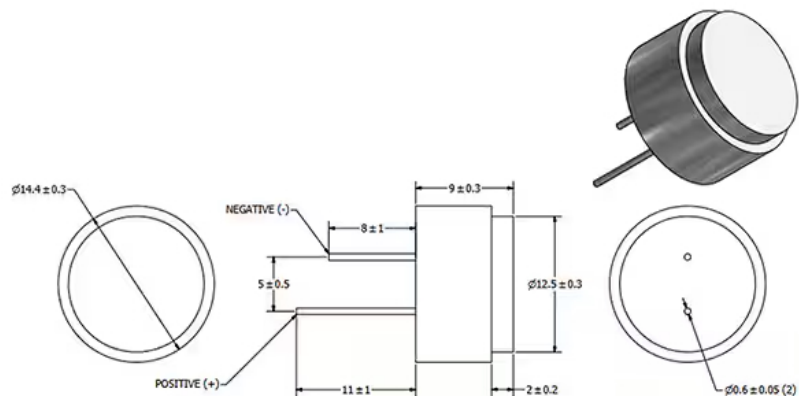


Figure 3: The UTR-1440K-TT-R is a basic 40 kHz ultrasonic transceiver that combines a transmitter and a receiver in a single housing. (Image source: PUI Audio)

In some cases, the source and receiver transducers are separate devices but are located next to each other in what is called a collocated arrangement (Figure 4).

Another option is to have them separated by a substantial distance and also have different orientations if the object being sensed is at an angle. This is called a bistatic configuration. In this case, the object deflects the impinging energy rather than reflecting it back to the source. Separate devices also allow for flexibility in their selection to match the application. It also allows for flexibility in the power of the transmitter's drive circuit as it's no longer proximal to the sensitive analog circuitry of the receiver.

For these situations, a pairing such as the [40 kHz UT-1640K-TT-2-R](#) ultrasonic transmitter and [UR-1640K-TT-2-R](#) ultrasonic receiver may be a good choice. The transmitter measures 12 mm high and has a diameter of 16 mm. It requires just 20 VRMS drive, and it produces an SPL of 115 dB while presenting a nominal capacitance of 2100 pF and 80° beamwidth directivity. The complementary receiver has the same appearance, dimensions, directivity, and capacitance as the transmitter (Figure 5).

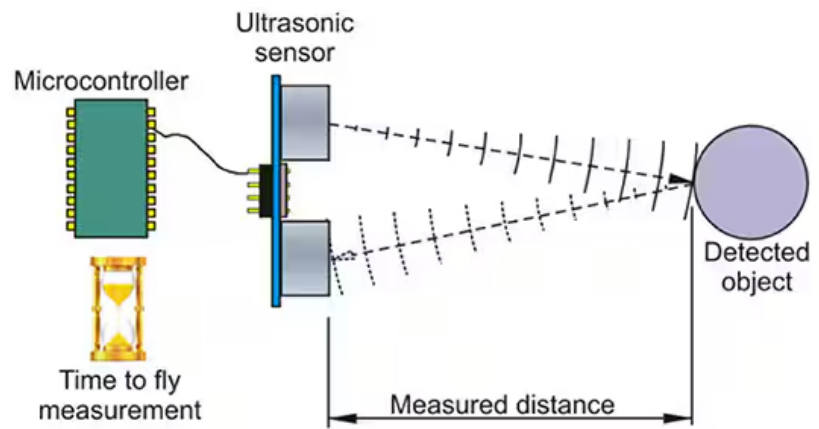


Figure 4: In a collocated arrangement, the ultrasonic source and receiver are located adjacent to each other. (Image source: Science and Education Publishing Co.)

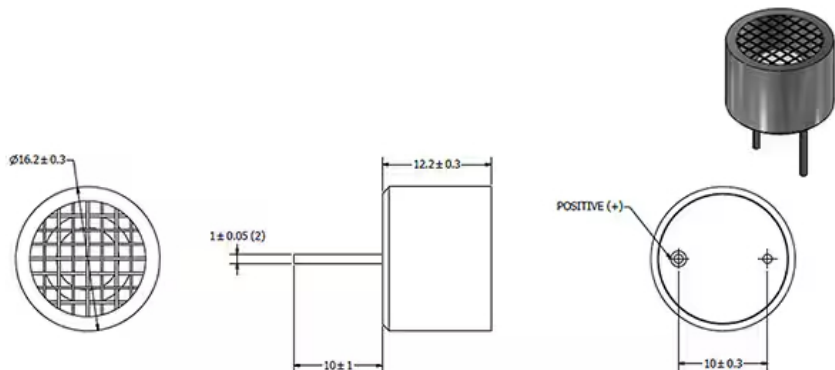


Figure 5: The UT-1640K-TT-2-R ultrasonic transmitter and the UR-1640K-TT-2-R ultrasonic receiver provide different, complementary functions, but have the same form factor and dimensions. (Image source: PUI Audio)

Sensing fluid flow

Beyond basic object detection, ultrasonic transducers are used for non-invasive, non-contact measurement of liquid and gas

flow rates. For these applications, the transducers operate at higher frequencies, typically above 200 kHz, to provide the needed measurement resolution.

In a typical flow application, two sensors are placed a known distance apart. The flow rate can then be calculated given the distance and the transit time that it takes for sound to travel between the two transducers in both directions, as the moving fluid carries the ultrasonic energy at different speeds in each direction.

This time difference is directly proportional to the velocity of the liquid or gas in the pipe. Determination of the flowing velocity (V_f) begins with the equation: $V_f = K \times \Delta t / T_L$, where K is a calibration factor for the volume and time units used, Δt is the time differential between upstream and downstream transit times, and T_L is the zero-flow transit time.

Various compensation and correction factors are added to this basic equation to account for fluid temperature, and the angle between the transducers and the pipe, among other considerations. In practice, an ultrasonic flow meter requires real-world “hardware” and fittings (Figure 6).

Transit-time flow meters work well with viscous liquids, provided that the Reynolds number at minimum flow is either less than 4,000 (laminar flow) or above 10,000 (turbulent flow), but has significant non-linearities in the transition region between the two. They are used to

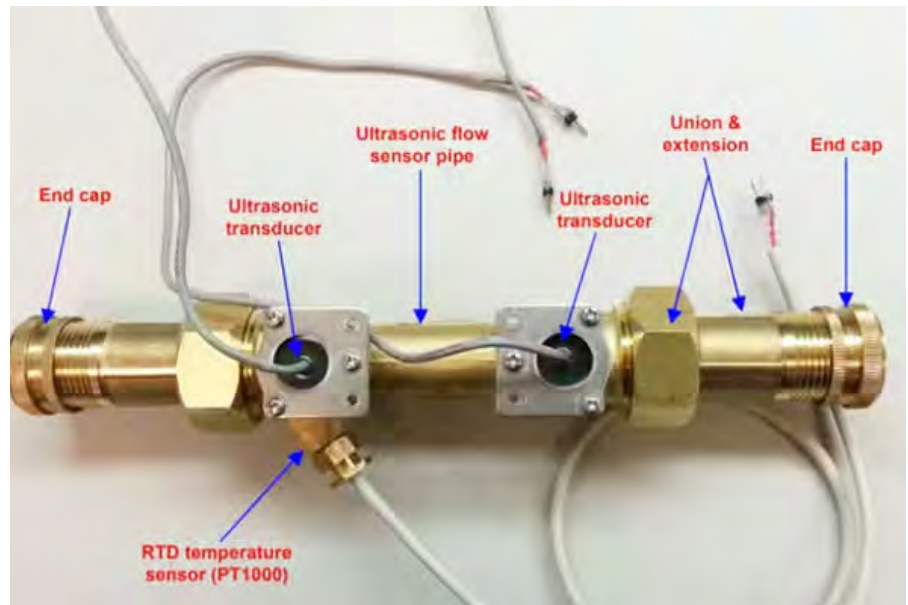


Figure 6: An actual transit-time ultrasonic flowmeter requires various fittings and connections; note the dual ultrasonic transducers. (Image source: Circuit Digest)

measure the flow of crude oils in the petroleum industry, and are also widely used for measuring cryogenic liquids down to -300°C , as well as for molten metal flow metering – two temperature extremes.

PUI offers ultrasonic transducers that are specifically designed for transit-time fluid flow applications. The [UTR-18225K-TT](#) operates at 225 ± 15 kHz and has the narrow beam angle needed for this application of just $\pm 15^{\circ}$. This transmit/receive transducer has a diameter of 18 mm and a height of 9 mm with 2200 pF of capacitance. It can be driven with a $12 V_{p-p}$ train of square waves and up to $100 V_{p-p}$ at a low duty cycle.

It also takes drive and signal conditioning circuitry

An ultrasonic detection system comprises more than just the piezoelectric transducers. Appropriate and very different circuitry is needed to meet the drive requirements of the transducer in transmit mode and for low-level analog front-end (AFE) signal conditioning in receive mode. While some users build their own circuitry, ICs are available that can conveniently provide the basic drive and AFE functions along with additional features.

For example, the [Texas Instruments PGA460](#) is a 5.00 mm × 4.40 mm, 16-lead IC designed for use with transducers such as the PUI Audio UTR-1440K-TT-R 40 kHz ultrasonic transceiver. This highly integrated system-level IC provides an on-chip ultrasonic transducer driver and signal conditioner and includes an advanced digital signal processor (DSP) core (Figure 7).

The PGA460 features a complimentary low-side driver pair that can drive a transducer either in a transformer-based topology for higher drive voltages by using a step-up transformer, or in a direct-drive topology using external high-side FETs for lower drive voltages. The AFE consists of a low-noise amplifier (LNA) followed by a programmable time-varying gain stage feeding into an analog-to-digital converter (ADC).

The digitized signal is processed in the DSP core for both near-field and far-field object detection using time-varying thresholds.

The time-varying gain offered by the PGA460 is a feature often used with ultrasonic transducers, whether for basic object detection or advanced medical imaging systems. It helps to overcome the unavoidable yet known-in-advance attenuation factor of the acoustic signal energy as it propagates through the medium.

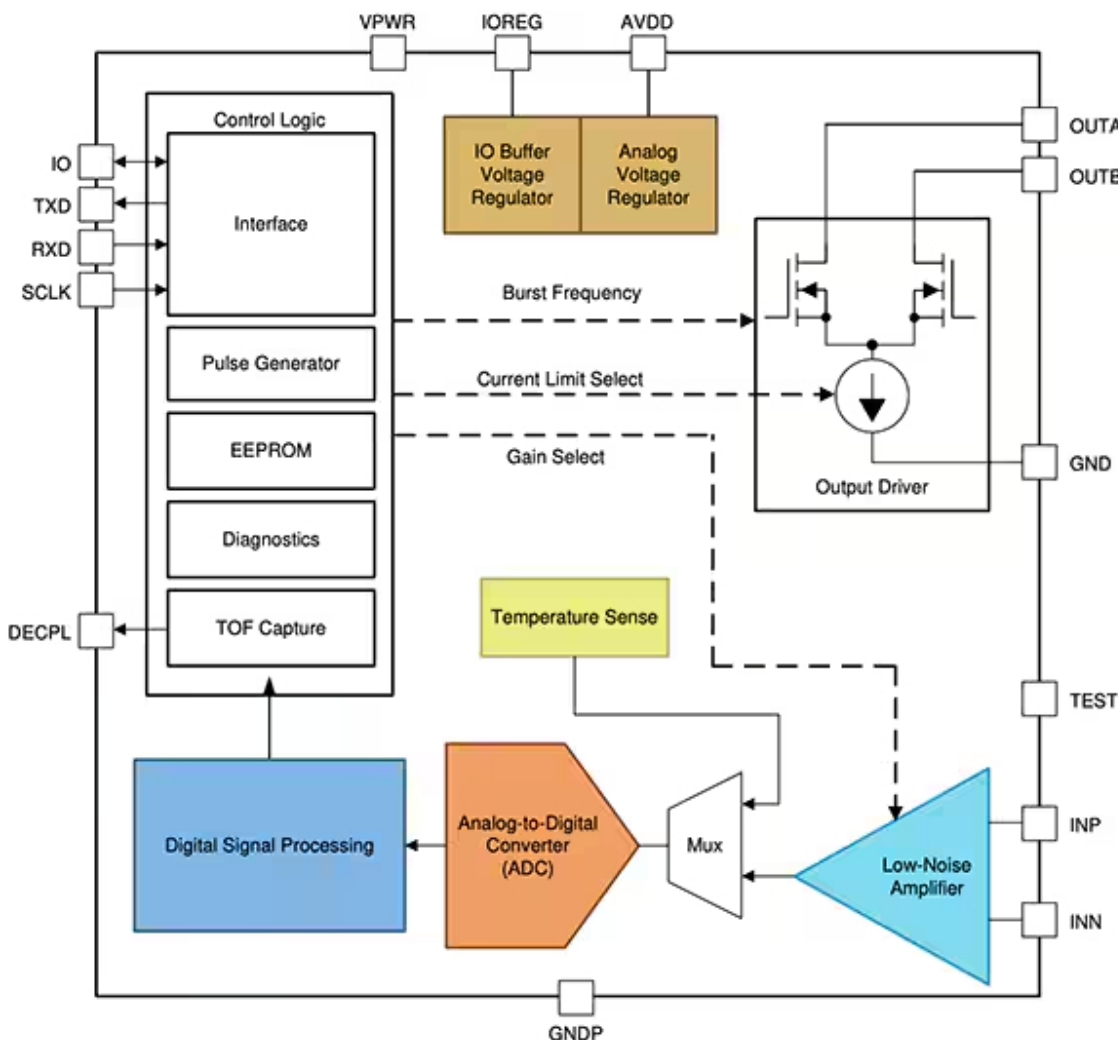


Figure 7: The PGA460 is a complete interface for both transmit and receive functions of an ultrasonic transducer. It includes power drive circuitry, an AFE, and a DSP core to run related algorithms. (Image source: [Texas Instruments](#))



Since this attenuation and the propagation speed are both known, it is possible to compensate for the unavoidable loss by “ramping up” the AFE gain versus time, effectively cancelling the attenuation versus distance effect. The result is that the system signal-to-noise ratio (SNR) is maximized regardless of the sensing distance, and the system can handle a wider dynamic range of received signals.

To further explore the use of these transducers, Texas Instruments offers the [PGA460PSM-EVM](#) evaluation module, which works with PUI Audio’s UTR-1440K-TT-R 40 kHz ultrasonic transceiver (Figure 8).



Figure 8: The PGA460PSM-EVM evaluation module is based on the PGA460 and simplifies the exploration of ultrasonic system operation using the PUI Audio UTR-1440K-TT-R 40 kHz ultrasonic transceiver. (Image source: [Texas Instruments](#))

This module requires only a few external components plus a power supply for operation (Figure 9). It is controlled by commands received from a PC-based graphical user interface (GUI), to which it returns data for display and further analysis. In addition to basic functionality and setting of operational parameters, it allows users to display the ultrasonic echo profile and measurement results.

Conclusion

Piezoelectric ultrasonic transducers provide a convenient and effective way to sense nearby objects and even measure their distance. They are reliable, easy to apply, and help



designers avoid RF spectrum or EMI/RFI regulatory issues. They can also be used for non-contact measurement of fluid flow rates. Interface ICs for both their transmit

and receive functions, supported by an evaluation kit, simplify their integration into a system while providing flexibility in the setting of their operating parameters.

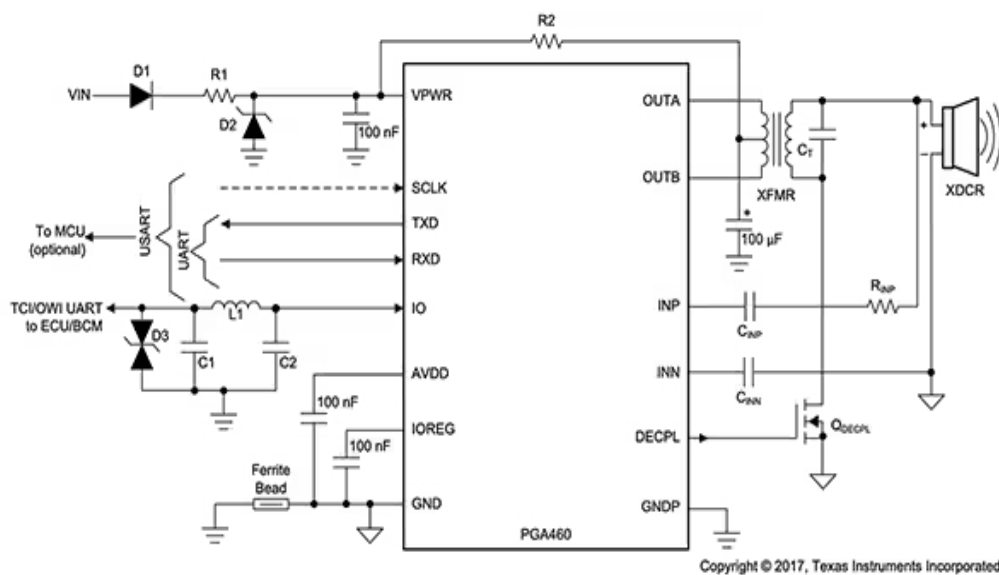


Figure 9: The PGA460PSM-EVM evaluation module connects to a PC with a GUI that allows users to operate and control the transducer and see critical waveforms, among other functions. (Image source: Texas Instruments)

How to choose and use angle sensors for power steering, motors and robotics

By Majeed Ahmad
Contributed By DigiKey's North American Editors





As factories and vehicles become more automated, accurate and low-latency sensing of motor shaft speed and position is critical for process control, system reliability, and safety. To address these needs, designers require angular rotation sensors that are fast and precise, with the flexibility to address magnetic field variations and axial misalignment.

Complicating the issue for designers are ever-present cost and time pressures, as well as the nature of the operating environments for industrial and automotive applications, which can be challenging in terms of chemicals and oils, as well as temperatures and EMI. Other considerations include wear and tear and ever-changing configurations, which require a degree of flexibility within the sensing device.

This article describes the role of angle sensors and shows how position sensing features such as speed and low latency can be customized using specific combinations of magnetic input and sensor element. Sample sensor solutions from [AKM Semiconductor](#), [Infineon Technologies](#), and [Monolithic Power Systems](#) are then introduced, and their implementation discussed.

The role of angle sensors

Angle sensors are used to sense motor shaft position and speed variations for steering angle sensing for automobiles and high-precision control in robotic systems. They determine the absolute angular position of a diametrically magnetized cylinder on a rotating shaft by detecting the orientation of an applied magnetic field and measuring its sine and cosine components. As the shaft may be rotating at high speed, it's critical that the data from the sensor be acquired and processed quickly, with minimal latency.

One of four magnetic technologies are typically used: Hall effect, anisotropic magnetoresistance (AMR), giant magnetoresistance (GMR), and tunnel magnetoresistance (TMR) (Figure 1). When using any of these technologies, designers must first determine a suitable distance from the magnet surface to the sensor based on specific parameters such as magnetic properties, sensor specification, and assembly tolerances.

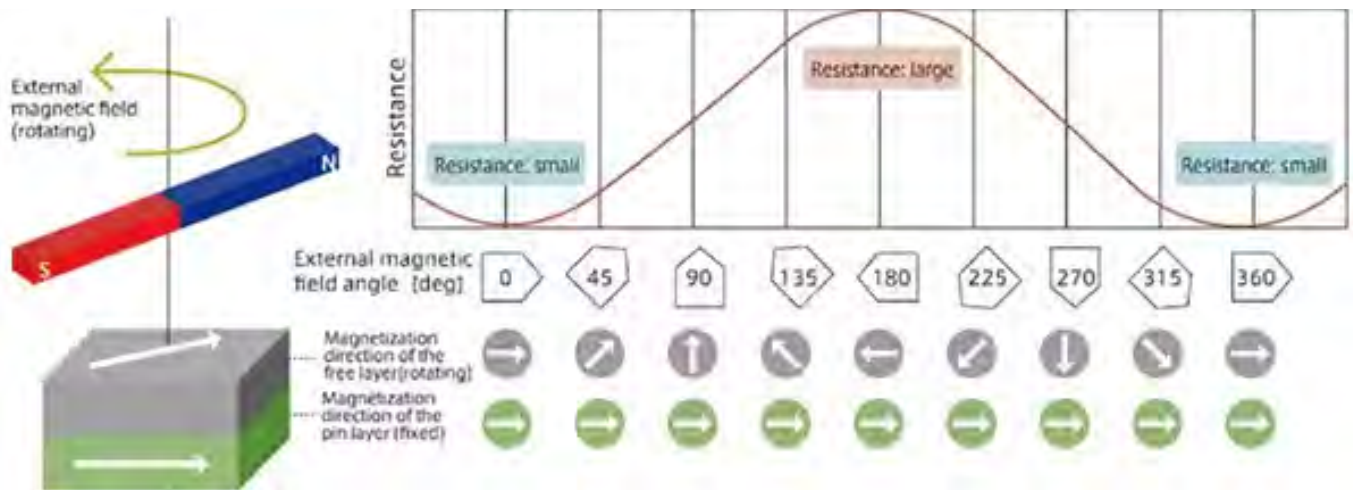


Figure 1: When a magnet is rotated on a TMR sensor, the resistance of the sensing element changes with the rotation angle. (Image source: DigiKey)

This air gap must be consistent with parameters such as magnet size and remanence, also known as residual magnetization. Designers must also ensure that air gap variations don't result in magnetic fields that are either too low or too high. This requires careful consideration of the appropriate magnet for the application's air gap (Figure 2).

That said, angle sensors can support a wide range of spatial configurations and magnetic field strengths, including both off-axis or side-shaft mounting and end-of-shaft configurations. To help accommodate variations, on-chip non-volatile memory is used to store configuration parameters such as reference zero angle position, ABZ encoder settings, and phase information for the motor windings.

Next, the device's ability to detect various magnetic field strengths allows developers to customize the angle sensor for specific functions like diagnostics and axial movement sensing. The availability of programmable magnetic field strength thresholds also facilitates the implementation of a push or pull button function outputted as two logic signals.

However, while features like speed, low latency and resolution depend on application requirements, safety is at the heart of angle sensor designs. The compliance to functional safety standards further affirms the commitment for accuracy and reliability-conscious automotive and industrial design environments.

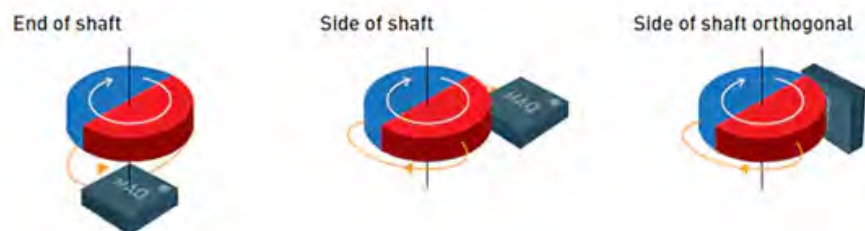


Figure 2: Designers can choose a magnet-to-sensor position based on design considerations such as the required level of immunity to external field disturbance and air gap tolerance. (Image source: Monolithic Power Systems)



Meeting functional safety requirements

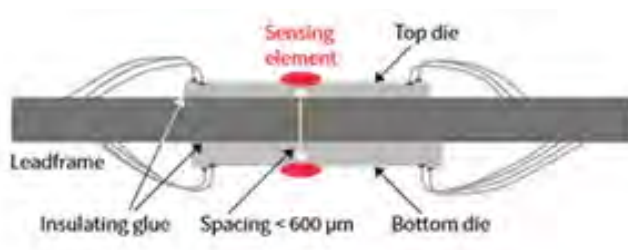
The angle sensors used in automotive applications require a high degree of precision, down to 0.1° , to help ensure compliance with the ISO 26262 functional safety standard in the face of a highly demanding operating environment. The applications for these sensors include position measurement in brushless DC (BLDC) motors for pumps, wipers, brakes, valves, flaps, pedals, and steering angle.

The accuracy of 0.1° applies across the entire temperature range and product lifecycle. Moreover, at low magnetic flux densities, between 10 millitesla (mT) and 20 mT, where the angle error significantly increases, angle sensors serving automotive and industrial designs must still achieve angle errors as low as 0.2° .

Additionally, angle sensors should be easily integrated into safety-critical designs such as electric power steering (EPS) systems, which are crucial for autonomous features like automated parking and lane keeping.

To address ease of use, Infineon's XENSIV [TLE5109](#) and [TLE5014](#) angle sensors are available in both single and dual die versions, and integrate both the sensing and logic elements on a single chip (Figure 3). Dual die versions are more suitable for ASIL-D safety applications.

Figure 3: The side view (left) of a dual die angle sensor (right) for safety-critical applications that uses top-bottom placement to shrink space and save on cost by using an inexpensive ferrite magnet. (Image source: Infineon Technologies)



The TLE5109A16E2210XUMA1 is part of a line that comprises high-precision AMR fast analog angle sensors with an error angle of 0.1° . Though AMR-based angle sensors are designed for 180° angle measurement, they are also applicable for 360° measurement in motors with an even number of pole pairs because the AMR sensing element actually measures the double angle, sine and cosine (Figure 4). Their small angle error also makes them suitable for a broad array of magnetic fields, with flux densities ranging from 10 mT to more than 500 mT.

The TLE5109 angle sensors operate from 3.3 volt or 5 volt supplies. Other features include a short start-up time of between 40 microseconds (μs) and $70 \mu\text{s}$ to ensure minimal latency and support for speeds of more than 30,000 revolutions per minute.

The TLE5014C16XUMA1 is one of a line of GMR sensors that can be programmed to accommodate a wide range of applications by storing the required configuration in on-board EEPROM (Figure 5). These sensors boost flexibility and ease of use by also offering a choice of interfaces that includes PWM, SENT, SPC, and SPI.

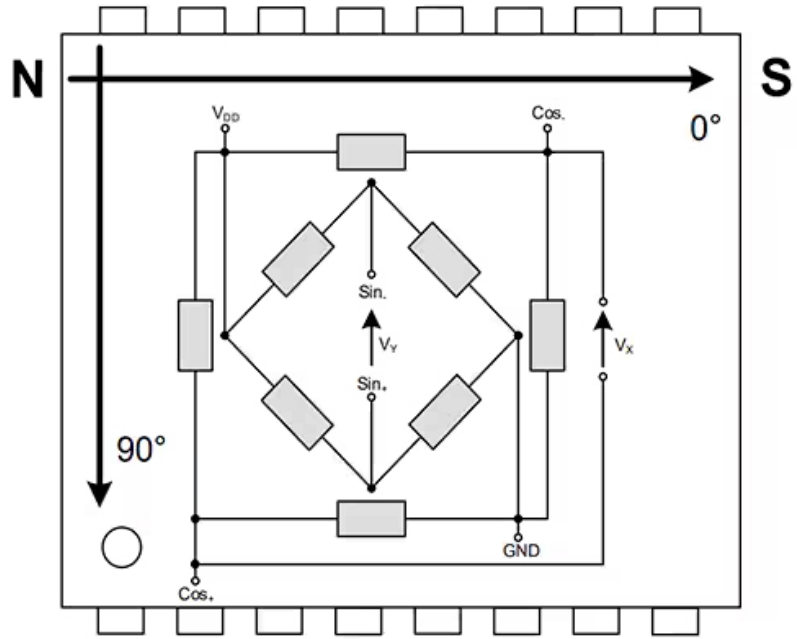


Figure 4: The AMR-based angle sensor is designed for 180° angle measurement, but it can be used to measure through the full 360° because it measures both sine and cosine angles. (Image source: Infineon Technologies)

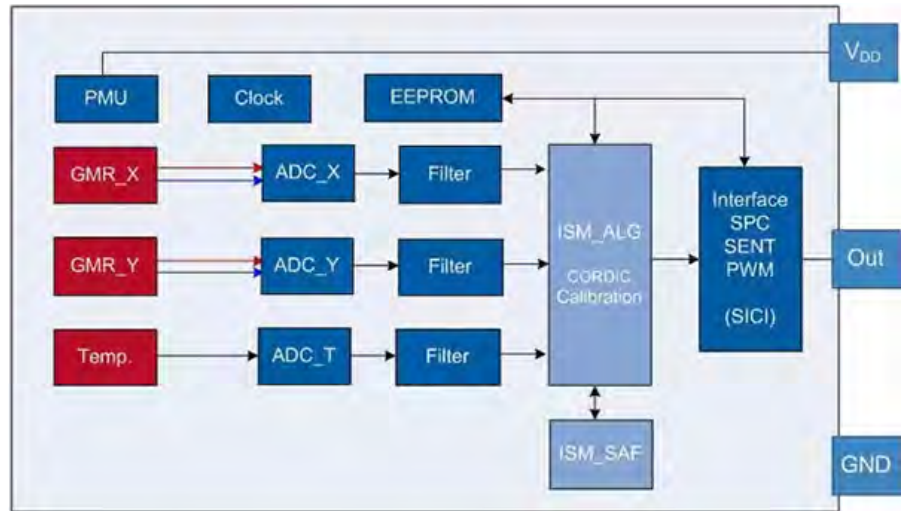


Figure 5: The pre-configured and pre-calibrated TLE5014 angle sensors have the flexibility to be programmed to adapt to any application using the on-board EEPROM. (Image source: Infineon Technologies)

The TLE5014 angle sensors typically draw 25 milliamps (mA) from supply voltages of up to 26 volts (absolute maximum) and meet ISO 26262 ASIL-C for the single die and ISO 26262 ASIL-D for the dual die versions.

Key performance parameters

To fully realize the ability of angle sensors to reduce audible noise and optimize motor smoothness and torque, designers should carefully consider the key parameters: accuracy, speed, latency, axial misalignment, and magnet drift.

For example, high-accuracy readouts are crucial for automotive and industrial environments, despite harsh environmental conditions. That makes factors like thermal stability and air gap tolerance vital in an angle sensor's ability to meet accuracy objectives without adding cost and complexity to the system design.

To meet such requirements at minimal cost, Monolithic Power Systems' MagAlpha magnetic position sensors—[MA302GQ-P](#), [MA702GQ-P/Z](#), and [MA730GQ-Z](#)—can be mounted on the edge of the board for both end-of-shaft and side-shaft (off-axis) configurations.

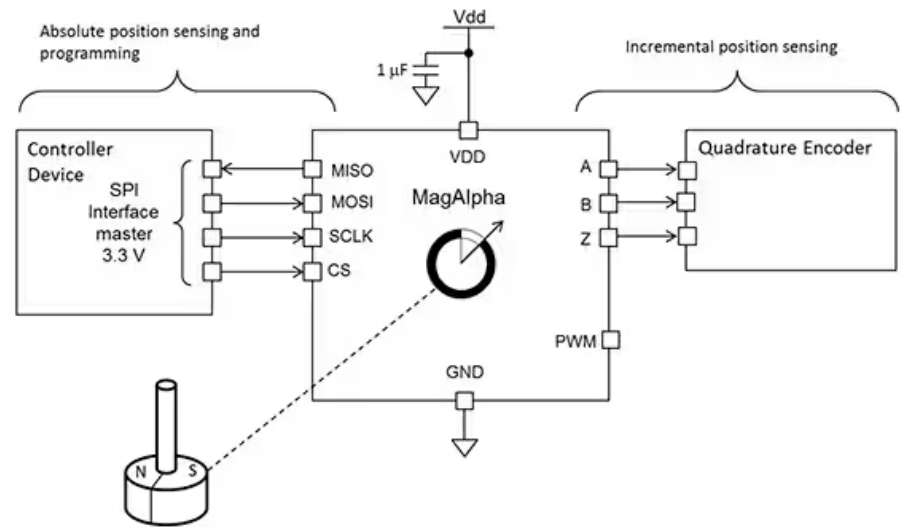


Figure 6: The contactless MagAlpha MA730GQ-Z features 14-bit resolution and provides digital readouts over the SPI link. (Image source: Monolithic Power Systems)

For speed, the contactless sensing and 12-bit resolution absolute angle encoder allow MA302 sensors to provide accurate angle measurement from 0 rpm to 60,000 rpm. The MagAlpha MA730GQ-Z features 14-bit resolution and provides digital readouts over the SPI link (Figure 6).

However, for slow operations like human-machine interface (HMI) or manual controls where the rotating speed remains below 200 rpm, the company offers the MagAlpha [MA800](#), a digital magnetic sensor designed to replace analog potentiometers or rotary switches. It's used with a

diametrically magnetized cylinder of 2 millimeters (mm) to 8 mm, and its magnet configurations and shapes are flexible.

The MA800 has lower resolution (8 bits) but does feature on-chip non-volatile memory and programmable magnetic field strength thresholds. These make it suitable for applications that require the implementation of push-button readouts via register bits as well as output signals.

Zero latency angle sensors

The **AK7451** is a 12-bit angle sensor that detects rotation speed and angles by measuring the intensity of a magnetic field. It features a combination of magnets operating parallel to the IC surface while offering tracking speeds of up to 20,000 rpm. After detecting the magnetic field vector parallel to the IC surface, it outputs the absolute angular position of the magnet, and subsequently, the relative angular position.

The AK7451 employs the tracking servo system architecture to ensure zero latency rotation angle sensing. The zero-latency angle sensor can output up to eight-pole UVW winding phases (Figure 7), which significantly improves its versatility, allowing it to serve a broad array of motor drive and encoder applications.

Also, the expansion of the ABZ phase output resolution setting from four types to 16 types enhances motor control usability. It also allows AK7451 angle sensors to facilitate rotor position detection in DC

brushless motor-driven operation without Hall IC installation.

Here, it's worth mentioning that for some position sensing applications, latency is not a critical issue. In electric power steering (EPS) hand wheel angle sensing, for example, a new angle value is requested every millisecond (ms). Also, it's important to distinguish between errors caused by sensor IC and magnetic input, allowing the angle sensor IC to be used to compensate for the errors related to magnetic input.

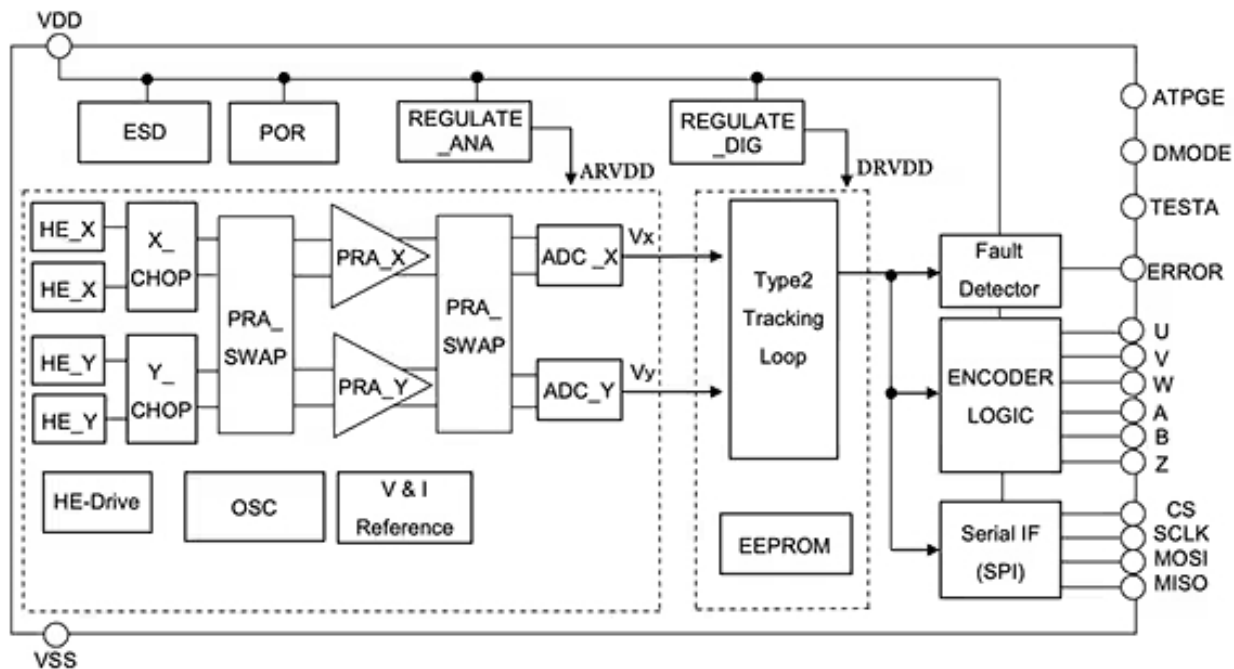


Figure 7: AK7451 enables designers to program 16 ABZ output resolution settings and eight UVW output pulse number settings via EEPROM. (Image source: AKM Semiconductor)



Conclusion

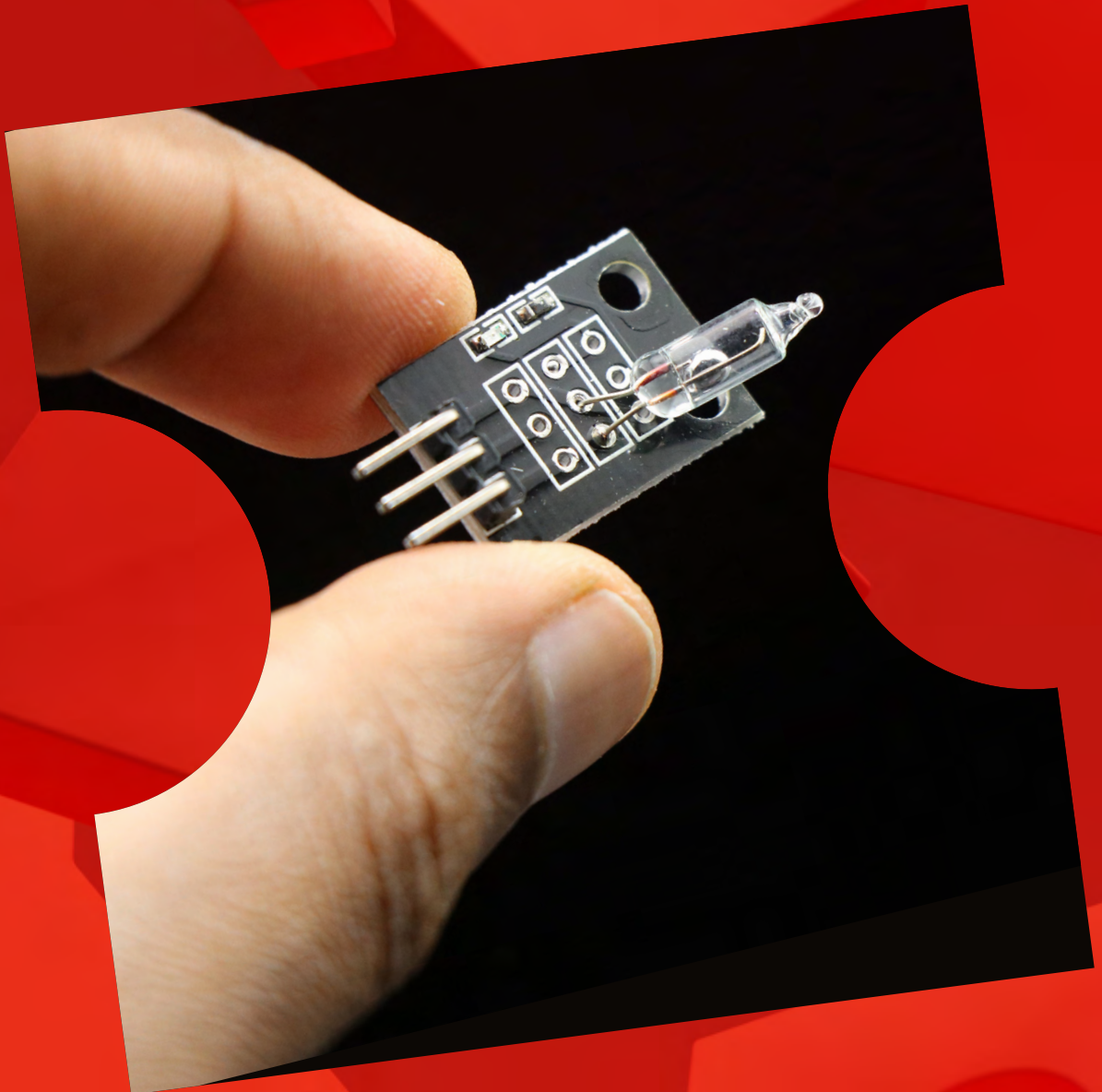
While greater accuracy and smaller form factors largely drive the feature set in angle sensors for automotive and industrial applications, compliance with functional safety standards sums up the overall value proposition of these high-precision devices. However, to fully leverage their capabilities, designers need to carefully consider specific application requirements to

get clarity on performance parameters such as appropriate air gap, magnetic field strength, rotation speed, and angle error.

As shown, once these requirements are established, there is a wide variety of contactless sensors available that provide the necessary accuracy, speed, and programmable flexibility to meet them.

Using a MEMS sensor for vibration monitoring

By Jay Esfandyari, Tom Bocchino, STMicroelectronics



Vibration Monitoring (VM) has been around for quite a long time and has been used to monitor the health of a machine, equipment, or a structure. The vibration data collected via dedicated sensors during the operation of a machine is monitored and analyzed in real-time.

The main goal of vibration monitoring is to reduce the risk of fatal damages and potential line-down situations which leads to final operational cost control and reduction.

The vibration data from a [vibration sensor](#) can be used as a stand-alone input or be combined with other sensor data depending on the operational requirements. For example, in a factory automation application, the vibration data can be combined with:

- [Temperature](#)
- Smoke
- [Humidity](#)
- [Pressure](#)
- [Sound](#)

This combination generates a complete system that will provide a more robust and reliable solution.

In some other use cases such as structural monitoring, the vibration data can be combined with the tilt position data that is collected via an inclinometer to determine the health of the structure.

The collected data are fed into dedicated algorithms, including the emerging artificial intelligence (AI) algorithms, to develop a model that can predict potential future failure. The model prediction information can then be used to build knowledge for making decisions on whether any immediate actions need to be taken to avoid productivity loss.

A new trend in factory automation is the emergence of AI algorithms which can be trained based on sensor data to predict which tasks should be performed. This lessens the burden on individual operators who previously had to make critically difficult and time-consuming decisions. An autonomously automated factory takes away the responsibility of individual operators and reacts automatically to any changing operating conditions.

Vibration sensor

A key component in a vibration monitoring application is a vibration sensor. The latest vibration sensors are based on MEMS technology using the same concept of acceleration detection in an accelerometer. The main difference is in the bandwidth of the sensor. A MEMS accelerometer has a typical bandwidth of 3 kHz, however, a vibration sensor is capable of detecting the vibration at significantly higher bandwidth.

The capability of a vibration sensor to capture high-frequency signals enables more accurate frequency analysis of the vibration. The latest MEMS vibration sensor offers a bandwidth of over 6 kHz which will be discussed later.

A MEMS-based vibration sensor has many use cases and Figure 1 provides a list of some major applications. Motor vibration monitoring is an essential building block of successful factory automation. Vibration monitoring in railways can help avoid catastrophic train accidents. Home appliances such as washing machines have been equipped with vibration monitoring since the inception of MEMS sensors in industrial applications. The structural monitoring application has gained momentum since the emergence of MEMS sensors at an affordable cost. For example, municipalities bear the responsibility to monitor bridge vibration to ensure that structures are in good health and sound condition. The bridge vibration data, particularly during peak traffic hours, can provide valuable information on any abnormality that may cause the collapse of the bridge.

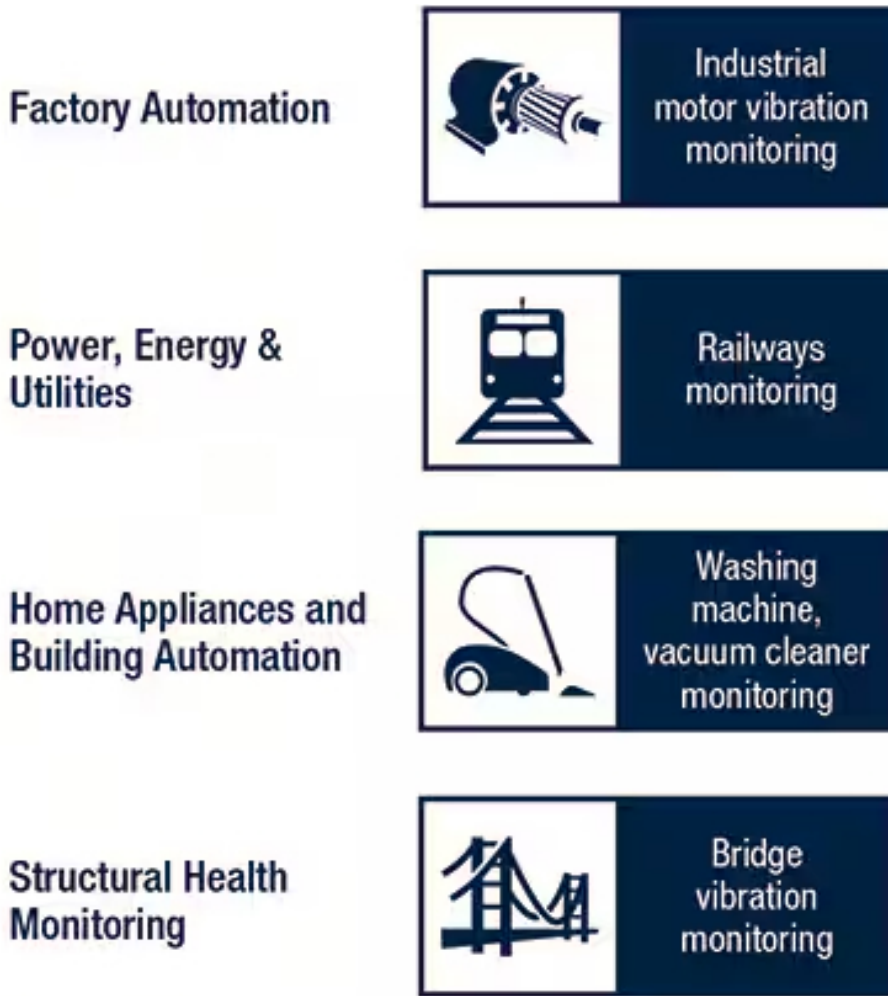


Figure 1: Some MEMS sensor vibration sensor applications. (Image source: STMicroelectronics)

The technical specifications of a vibration sensor need to be carefully analyzed to ensure that the sensor can meet the requirements of the target application. Table 1 depicts the major parameters of one of the latest vibration sensors offered by STMicroelectronics. This device can capture the vibration

in the 3-dimensional space (x, y, z). The three degrees of freedom offered by this device provide the flexibility to position the device in mounting orientation.

The full-scale range of up to 16 g of acceleration per axis is sufficient to cover the vibration amplitude range that is typically required to monitor the health of a machine.

This device offers an ultra-wide bandwidth, flat frequency response up to 6.3 kHz, and embedded filtering which eliminates frequency aliasing.

Another major characteristic of this device is the very low spectral noise density. This is a very important advantage when low-frequency vibration needs to be captured.

PARAMETER	VALUE
N. of axes	3-axis
Full Scale [g]	±2/±4/±8/±16
Output i/f	Digital: SPI
Bandwidth (-3 dB) [kHz]	5
ODR (kHz)	26.7
Noise Density [$\mu\text{g}/\sqrt{\text{Hz}}$]	90 (65 in single axis)
Current Consumption [mA]	1.1
Features	FIFO (3 kbyte) Programmable HP filter Interrupts Temp. sensor Embedded self-test
Operating Temperature	-40°C to +105°C
Operating Voltage [V]	2.1 + 3.6
Package (mm)	LGA 2.5x3x0.83 14-lead

Table 1: The major parameters of the latest vibration sensors offered by STMicroelectronics.

Compared to the existing vibration sensor, the operating temperature range is extended to +105°C to meet the requirement of a demanding operating environment.

The device can be operated either in a 3-axis mode or a single-axis mode which can be selected through dedicated registers. In the 3-axis mode, all three axes (x, y, z) are simultaneously active. In the single-axis mode only one axis is active. In single-axis mode, the resolution (noise density) of the active axis significantly improves.

Vibration monitoring applications

Vibration monitoring usually refers to the analysis of the vibration of a machine, equipment, or an appliance as part of a comprehensive application that is known as Condition Monitoring (CM) or Condition-based Monitoring (CbM). The vibration analysis plays a significant role in monitoring the health of the machine over time. However, in addition to the vibration data collection, a complete condition monitoring solution incorporates multiple sensors to collect vital equipment parameters including temperature, noise, pressure, smoke, and humidity.

Each of these sensors provides valuable information on a specific condition of the machine. These sensor data are fused, processed, and analyzed to build knowledge of the overall condition of the machine to make critical decisions on machine maintenance.

Figure 2 illustrates some of the major applications of vibration monitoring in various markets. The breakdown in this figure highlights the importance of vibration data collection and analysis as part of a comprehensive solution for CM. Additional sensors can be used to collect data that will be fused together for a reliable and effective outcome. In the latest solutions offered in the industry,



Figure 2: Various applications of Vibration Monitoring. (Image source: STMicroelectronics)

intelligent algorithms using sensor data bring the capabilities and effectiveness of such solutions to a new level. These innovative and powerful solutions can help significantly reduce the cost and inefficiencies associated with equipment line-down situations that would otherwise be inevitable.

Cloud computing has become one of the critical parts of an extensive solution involving sensor data collected from multiple locations of an enterprise to ensure that there is no interruption at any

level at any location. The central processing unit in the cloud is used to combine and analyze all the data and monitor the involved machines and equipment in real-time to ensure a smooth and uninterrupted operation.

Figure 3 provides a list of the essential building blocks of a vibration monitoring system. Depending on the needs and requirements of the system, a variety of sensors can be mounted on the equipment that must be monitored. The list of

sensors includes:

- Vibration
- Inertial sensor module
- Temperature
- Humidity
- Pressure
- Ambient light sensor
- Inclinometer

A processing unit is required to analyze the collected data. Depending on the amount of the data, privacy, data security, latency, and power requirements, the analyses may be performed at the local processing unit or

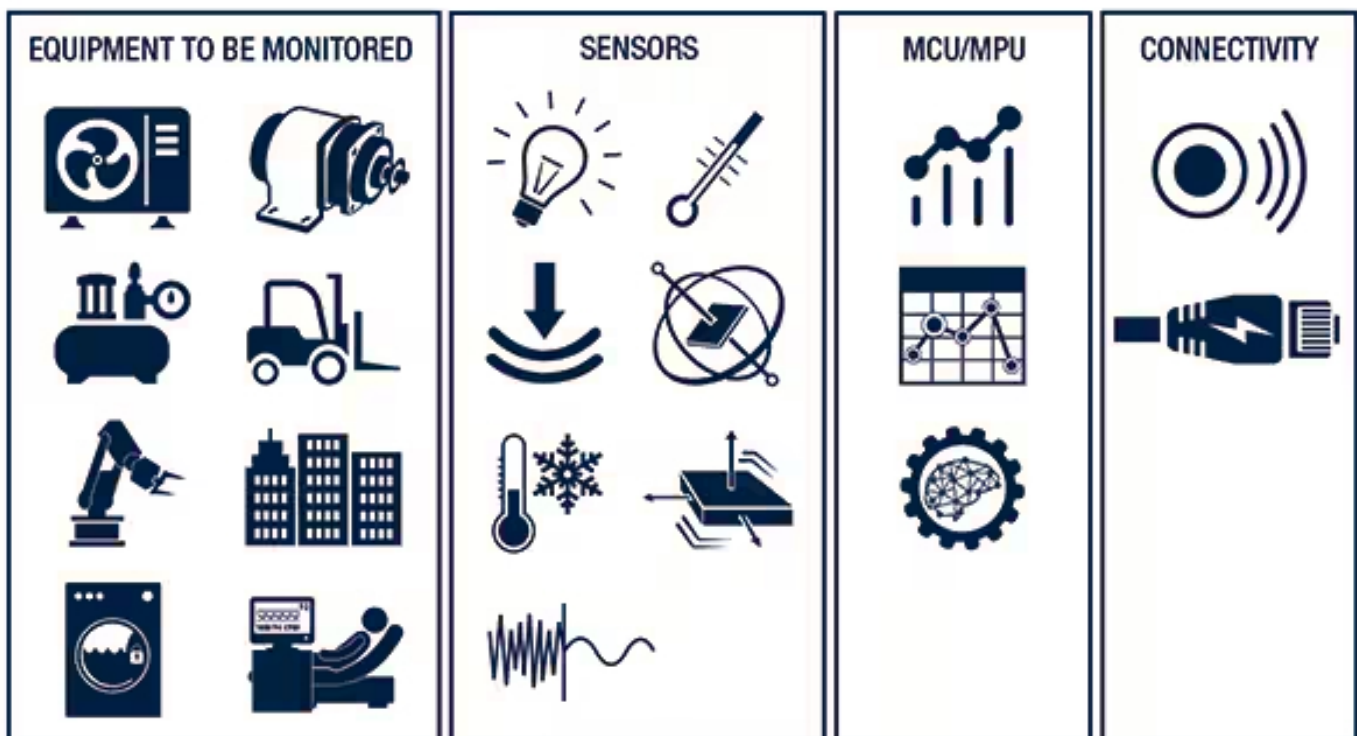


Figure 3: Building blocks of a vibration monitoring system. (Image source: STMicroelectronics)

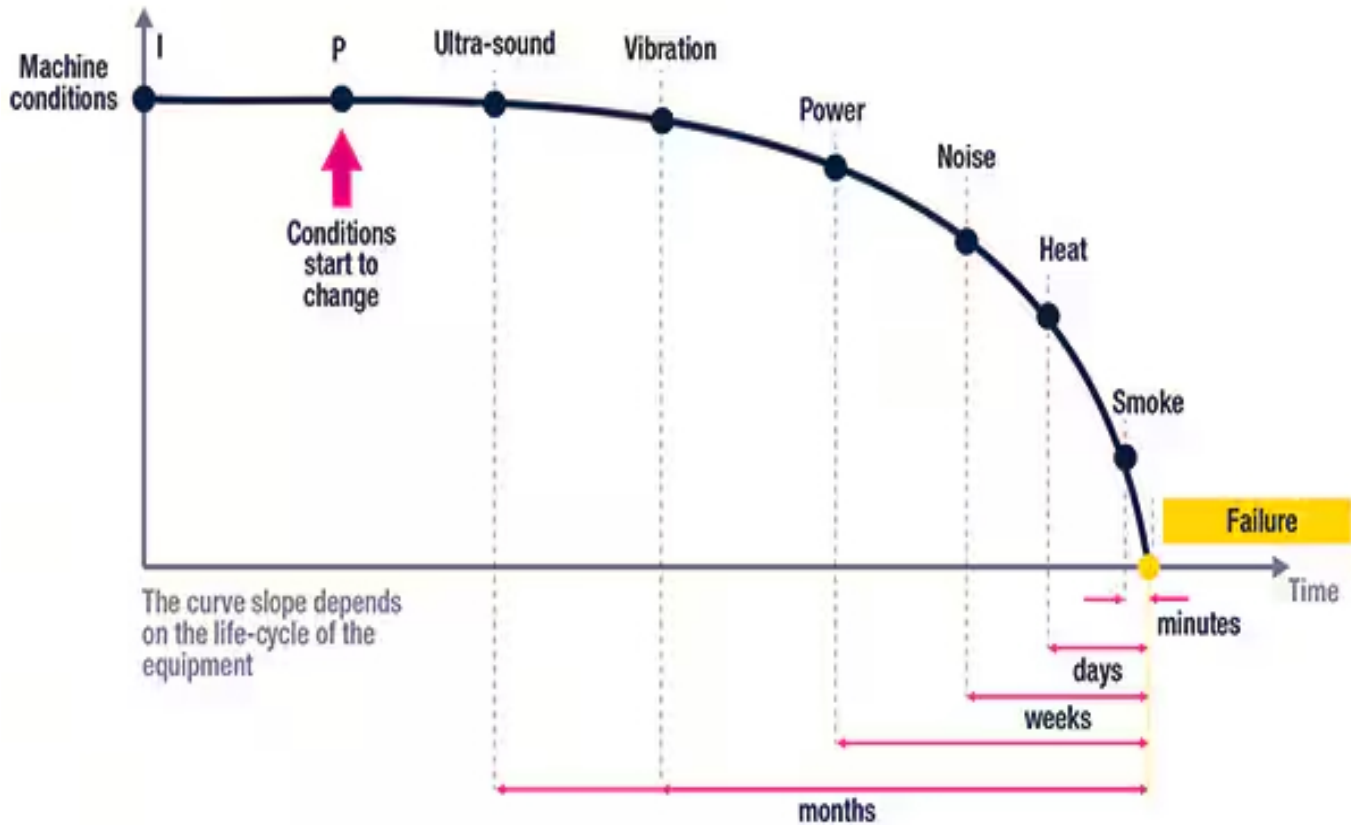


Figure 4: IPF-Curve. (Image source: STMicroelectronics)

transmitted to a cloud processing center where all the data from multiple pieces of equipment is collected and analyzed.

At some point after the installation and during the operation of the machine, the condition of the machine starts to change. It is critical to have all the required sensors installed to collect data on ultrasound and audible noise,

vibration, power consumption, temperature, and any potential smoke. As time passes, the necessity of collecting machine parameters and sensor data becomes critical to monitor the health of the machine.

Figure 4 depicts the typical Installation and Point of Failure (IPF) curve of a machine that is being monitored. The time from

the machine condition change to the final failure may take months or even years before it starts to show symptoms of failure. Early analysis of the sensor data can give an indication of the machine health and trained AI algorithms using sensor data as input can predict a failure and initiate the process of taking the necessary actions.

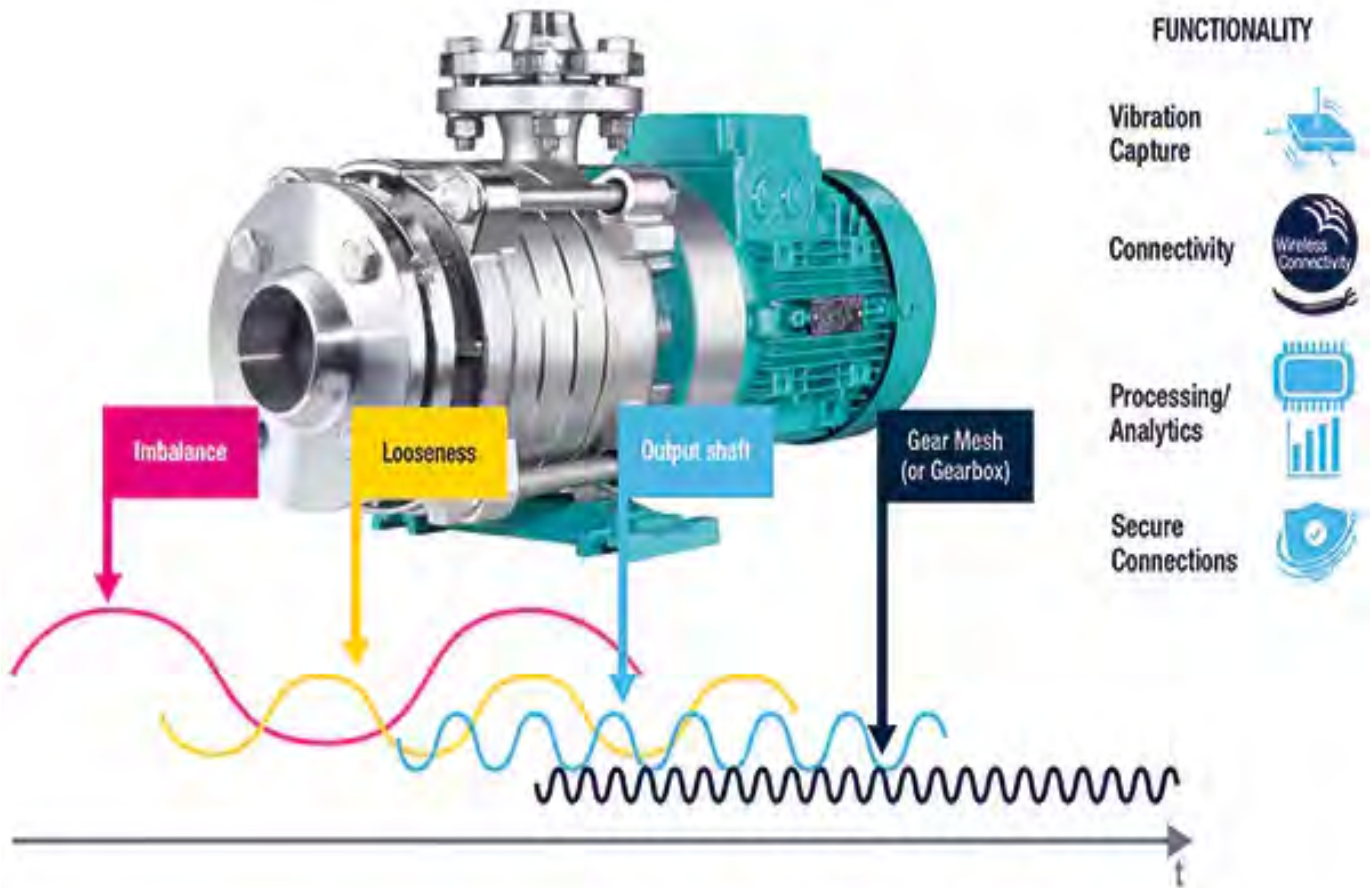


Figure 5: Vibration monitoring of an electric pump in various conditions. (Image source: STMicroelectronics)

Figure 5 provides an example for vibration monitoring of an electric pump. Different conditions, such as imbalance, looseness, output shaft, and the gearbox of the pump can be monitored using a vibration sensor. The vibration sensor data is then transmitted for further extensive analysis including a Fast Fourier Transfer (FFT) of the vibration data that can determine the individual frequency signature of these conditions.

A condition monitoring system for an electric motor can have several components in addition to the electric motor. The solution can have multiple sensors including the ones for vibration, temperature, pressure and other sensors depending on the requirements of the operating environment. The connectivity option between the pump and the processing unit can be a wired or wireless one with dedicated communication

protocols. The processing and analysis unit can provide pump diagnostics and visualization tools to help the operator proactively identify and tackle issues such as pump irregularities that could result in operational downtime and disruptions. This proactive engagement can increase a company's profit by lowering operating and maintenance costs for the factory.

Conclusion

Many sensors are being deployed to implement a comprehensive solution for predictive maintenance. The latest MEMS-based vibration sensors have enabled efficient and cost-effective vibration monitoring solutions in factory automation, power utilities, home appliances, and structural health surveillance and supervision. Vibration monitoring can be deployed as a stand-alone solution or as part of condition-based monitoring which has been emerged as an integrated part of a comprehensive solution to monitor various machines by collecting and analyzing the data in real-time. This solution has empowered the factories of the 21st century to proactively monitor and address issues arising from machine productivity disruptions and line-downs. Vibration monitoring is a critical building block of a comprehensive solution in any factory automation.

References

Ultra-wide bandwidth, low-noise, 3-axis digital vibration sensor: <https://www.st.com/en/mems-and-sensors/iis3dwb.html>

Analog bottom port microphone with frequency response up to 80 kHz for Ultrasound analysis and Predictive Maintenance applications. <https://www.st.com/en/mems-and-sensors/imp23absu.html>

Low-voltage, ultra-low-power, 0.5 °C accuracy I²C/SMBus 3.0 temperature sensor. <https://www.st.com/en/mems-and-sensors/stts22h.html>

<https://www.st.com/en/applications/factory-automation/condition-monitoring-predictive-maintenance.html#overview>

<https://www.st.com/en/applications/factory-automation.html>



Use IMUs for precise location data when GPS won't suffice



The ability to locate the position of any suitably enabled system anywhere on Earth using the Global Navigation Satellite Systems (GNSS) is useful, but there are a few problems associated with using only GNSS receivers for positioning. These problems can be overcome by using inertial measurement units (IMUs) to complement GNSS.

This article discusses the embedded use of IMUs, which employ gyroscopes, accelerometers, and magnetometers to measure location based on an initial starting point. It then introduces suitable example solutions and how to use them.

How IMUs complement GNSS

The problems with GNSS are fourfold. Firstly, GNSS signals are very directional and so can be blocked by buildings. Secondly, receivers have warm and cold startup times measured in the tens of seconds and stretching to one minute or more. This startup time is needed for the receiver to acquire and lock onto the multiple satellite signals required for a position fix.

Thirdly, the GNSS position update rate is limited to once per second. That's fine for tracking large, slow moving objects, but the startup time is far too long and the update rate is far too slow for many embedded applications. Fourthly, GNSS accuracy is measured in meters, which is too coarse for use in most embedded applications. These applications are as diverse as robotics and virtual reality, which do not involve ground transportation.

IMUs provide the finer positioning resolution and faster update rates that are required by many embedded applications. Also, IMUs provide relative position data from a known starting point as opposed to the absolute positioning information from a GNSS receiver, so the two types of position sensors are complementary.

Modern electronic IMUs available as board mountable components are based on microelectromechanical systems (MEMS) technology, making them small, light, and relatively rugged. They come with varying capabilities in terms of degrees of freedom (DOF), and unlike GNSS receivers, IMUs do not depend upon radio signals. They also

consume very little power, and they're available from a variety of sources with a wide range of resolution and accuracy.

With these characteristics IMUs can be used to augment positioning information from GNSS receivers. (See "[Design Location Tracking Systems Quickly Using GNSS Modules.](#)")

Anatomy of an IMU

Motion sensors react to and detect physical motion, including parameters such as acceleration, movement rate, or distance. Inertial sensors are a special class of motion sensor. IMUs integrate a number of motion sensors into one device and can provide high accuracy positioning information. They react to the motion of the sensor itself.

IMUs incorporate one or more of the following motion sensor types:

- **Gyroscope sensors** measure angular position changes, usually expressed in degrees per second. Integrating angular rate over time results in a measured angle of travel which can be used to track changes in orientation. Gyroscope sensors are available with one, two, or three axes corresponding to pitch, roll, and yaw angles.

Gyroscopes track relative movement independently from gravity, so errors from sensor bias or integration result in a position error called "drift."

- **Accelerometer sensors** measure linear acceleration, including acceleration components caused by device motion and acceleration due to gravity. The acceleration is measured in Gs, which are multiples of the earth's gravitational force (1 G = 9.8 meters/second²). Accelerometers are available with one, two, or three axes, which define an X, Y, Z coordinate system. Accelerometer data can be used to measure static device orientation by computing the measured angle of the device and compensating for gravitational force. Periods of complex motion can complicate the orientation calculation.
- **Magnetic sensors** measure magnetic field strength, typically in units of microTeslas (μT) or Gauss (100 μT = 1 Gauss). The most common magnetic sensor used for mobile electronics is a three-axis Hall-effect magnetometer. The magnitude of the Earth's magnetic field varies between 25 and 65 μT , and in angle of inclination depending on geographic location. For the continental United States, the

intensity varies between 45 and 55 μT , at an angle between 50 and 80 degrees. By computing the angle of the detected earth's magnetic field, and comparing that measured angle to gravity as measured by an accelerometer, it is possible to measure a device's heading with respect to magnetic north with high accuracy. An adjustment based on the current latitude and longitude is needed to get a true north heading.

- **Pressure sensors** measure differential or absolute pressure with units typically in hectopascal (hPa) or milliBar (mbar), which are equivalent. Standard atmospheric pressure at sea level is defined as 1013.25 hPa. Changes in altitude cause corresponding changes in detected ambient air pressure and can be used to track vertical motion.

Motion tracking using IMUs employs sensor fusion to derive a single, high accuracy estimate of relative device orientation and position from a known starting point and orientation. Sensor fusion involves combining the IMU's various motion sensor outputs using complex mathematical algorithms developed either by the IMU manufacturer or the application developer. Position calculations

using sensor fusion can produce the following measurements:

- **Gravity** – specifically the earth’s gravity and excludes the acceleration caused by the motion being experienced by the device. An accelerometer measures the gravity vector when the IMU is stationary. When the IMU is in motion, the gravity measurement requires fusing data from an accelerometer and a gyroscope and subtracting out the acceleration caused by motion. Applications that require orientation detection with respect to the earth can use gravity measurements.
- **Linear acceleration** – equivalent to the acceleration of the device as measured by the accelerometer, but with the gravity vector subtracted. IMU linear acceleration can be used to measure movement in three-dimensional space. The accuracy of this value depends on the tracking accuracy of the gravity vector.
- **Orientation (attitude)** – the set of Euler angles including yaw (azimuth), pitch, and roll, as measured in units of degrees.
- **Rotation vector** – derived from a combination of data from accelerometer, gyroscope, and magnetometer sensors. The rotation vector represents a rotation angle around a specified axis.

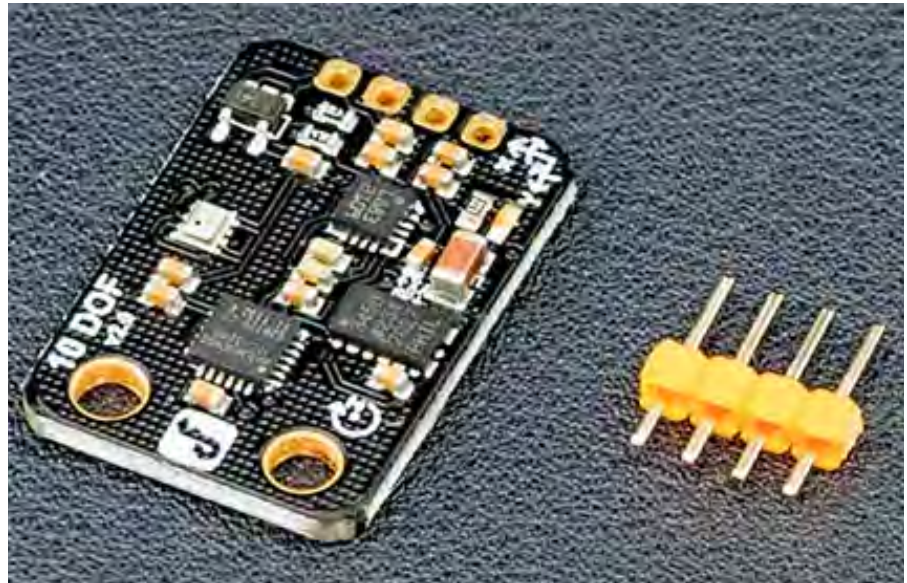


Figure 1: DFRobot’s SEN0140 10 DOF MEMS IMU sensor board integrates an accelerometer, a magnetometer, a gyroscope, and a barometric pressure sensor. (Image source: DFRobot)

IMUs can be used for a variety of applications including consumer (mobile phones), medical (imaging), industrial (robotics), and military (head tracking). The required IMU accuracy depends on the application requirements.

Six degrees of freedom

DOF refers to the possible movements of a rigid body within three-dimensional space. There are only six DOF in 3D space: three DOF for linear translation (forward/back, up/down, left/right) and three DOF for rotations (pitch, yaw, and roll). No matter how complex the motion, any

possible movement of a rigid body in space can be expressed as a combination of the six basic DOF.

However, in the world of IMUs, there are numerous references to 9 DOF and even 10 DOF sensors. This nomenclature can be rather confusing given that there are only six total DOFs used to describe movement. The nine DOF number comes from adding up the DOF for each type of sensor contained inside the IMU. So, if an IMU has a 3 DOF accelerometer, a 3 DOF gyroscope, and a 3 DOF magnetometer, then it’s called a 9 DOF IMU. Adding an atmospheric pressure sensor to the mix for measuring altitude creates a 10 DOF IMU.

Use IMUs for precise location data when GPS won't suffice

```
#include <Wire.h>
#include <FreeSixIMU.h>
#include <FIMU_ADXL345.h>
#include <FIMU_ITG3200.h>
#include <HMC5883L.h>

float angles[3]; // yaw pitch roll
float heading;

short temperature;

long pressure;

// Set the FreeSixIMU object
FreeSixIMU sixDOF = FreeSixIMU();
HMC5883L compass;

// Record any errors that may occur in the compass.
int error = 0;

void setup(){
  Serial.begin(9600);
  Wire.begin();
  delay(5);
  sixDOF.init(); //init the Acc and Gyro
  delay(5);
  compass = HMC5883L(); // init HMC5883
  error = compass.SetScale(1.3); // Set the scale of the compass.
  error = compass.SetMeasurementMode(Measurement_Continuous); // Set the measurement mode to Con
  if(error != 0) // If there is an error, print it out.
    Serial.println(compass.GetErrorText(error));
  bmp085Calibration(); // init barometric pressure sensor
}

void loop(){
  sixDOF.getEuler(angles);
  temperature = bmp085GetTemperature(bmp085ReadUT());
  pressure = bmp085GetPressure(bmp085ReadUP());
  getHeading();
  PrintData();
  delay(300);
}

void getHeading(){
  // Retrieve the raw values from the compass (not scaled).
  MagnetometerRaw raw = compass.ReadRawAxis();

  // Retrieved the scaled values from the compass (scaled to the configured scale).
  MagnetometerScaled scaled = compass.ReadScaledAxis();

  // Values are accessed like so:
  int MilliGauss_OnThe_XAxis = scaled.XAxis; // (or YAxis, or ZAxis)

  // Calculate heading when the magnetometer is level, then correct for signs of axis.
  heading = atan2(scaled.YAxis, scaled.XAxis);
  float declinationAngle = 0.0457;
  heading += declinationAngle;

  // Correct for when signs are reversed.
  if(heading < 0)
    heading += 2*PI;

  // Check for wrap due to addition of declination.
  if(heading > 2*PI)
    heading -= 2*PI;

  // Convert radians to degrees for readability.
  heading = heading * 180/M_PI;
}

void PrintData(){
  Serial.print("Euler Angle: ");
  Serial.print(angles[0]);
  Serial.print(" ");
  Serial.print(angles[1]);
  Serial.print(" ");
  Serial.print(angles[2]);
  Serial.print(" ");
  Serial.print("Heading: ");
  Serial.print(heading);
  Serial.print(" ");
  Serial.print("Pressure: ");
  Serial.print(pressure, DEC);
  Serial.println(" Pa");
}
```

Listing 1: This sample Arduino code extracts the sensor data from DFRobot's SEN0140 10DOF board. (Code source: DFRobot)

IMUs are available in a wide range of prices and capabilities. For example, [DFRobot's SEN0140](#) 10 DOF MEMS IMU sensor board is a compact IMU board that integrates an Analog Devices [ADXL345](#) accelerometer, a magnetometer from [Honeywell Microelectronics & Precision Sensors](#), a [TDK Invensense](#) gyroscope, and a [Bosch Sensortec](#) barometric pressure sensor.

The measurement specifications for the main SEN0140 sensors are:

ADXL345 accelerometer: 13-bit resolution at ± 16 g (maintaining 4 mg/LSB scale factor in all g ranges)

Honeywell Microelectronics & Precision Sensors magnetometer: ± 8 gauss magnetic full scale

TDK Invensense gyroscope: full-scale range of $\pm 2000^\circ/\text{second}$

Bosch Sensortec barometric pressure sensor: 4.35 PSI to 15.95 PSI (30 kPa to 110 kPa)

All four of these sensors are wired to the board's single SPI serial port, which means that the embedded processor must address and query each sensor separately. DFRobot's SEN0140 also incorporates a low noise LDO

for supplying regulated power to the sensors from a 3 to 8 volt supply.

DFRobot's 10 DOF IMU is directly compatible with Arduino development boards using an existing Arduino library. It can also be used with any microprocessor or microcontroller system that has an SPI port.

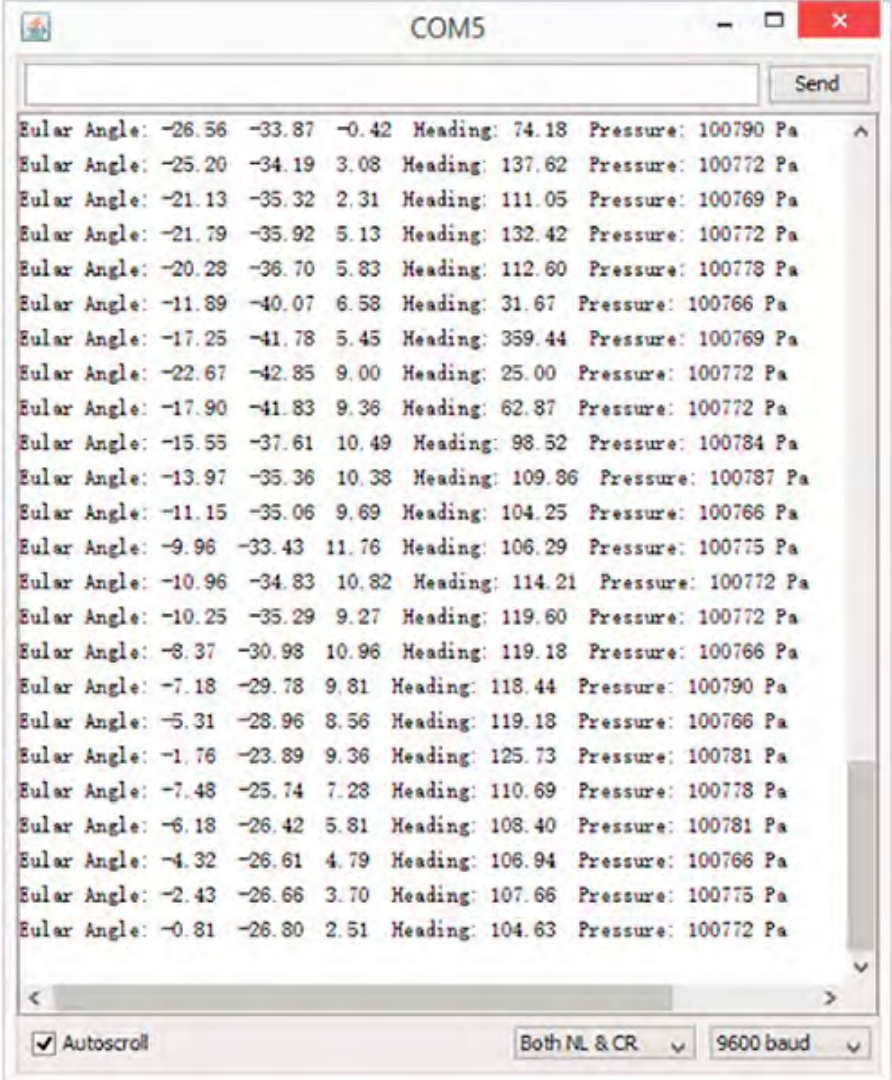
The following is sample Arduino code to extract the sensor data from DFRobot's SEN0140 10 DOF board (Listing 1):

This [Arduino](#) code produces the output shown in Figure 2.

[Digilent's 410-326](#) 9-axis IMU/barometer is based on an [STMicroelectronics' LSM9DS1](#) iNEMU IMU which incorporates a 3D accelerometer, a 3D gyroscope, and a 3D magnetometer with the following specifications:

- $\pm 2/\pm 4/\pm 8/\pm 16$ g linear acceleration full scale (3D accelerometer)
- $\pm 245/\pm 500/\pm 2000^\circ$ /second angular rate full scale (3D gyroscope)
- $\pm 4/\pm 8/\pm 12/\pm 16$ gauss magnetic full scale (3D magnetometer)

All three motion sensor types—accelerometer, gyroscope, and magnetometer—are integrated into one small package and connected through the LSM9DS1's I²C interface.



```
COM5
Send
Eular Angle: -26.56 -33.87 -0.42 Heading: 74.18 Pressure: 100790 Pa
Eular Angle: -25.20 -34.19 3.08 Heading: 137.62 Pressure: 100772 Pa
Eular Angle: -21.13 -35.32 2.31 Heading: 111.05 Pressure: 100769 Pa
Eular Angle: -21.79 -35.92 5.13 Heading: 132.42 Pressure: 100772 Pa
Eular Angle: -20.28 -36.70 5.83 Heading: 112.60 Pressure: 100778 Pa
Eular Angle: -11.89 -40.07 6.58 Heading: 31.67 Pressure: 100766 Pa
Eular Angle: -17.25 -41.78 5.45 Heading: 359.44 Pressure: 100769 Pa
Eular Angle: -22.67 -42.85 9.00 Heading: 25.00 Pressure: 100772 Pa
Eular Angle: -17.90 -41.83 9.36 Heading: 62.87 Pressure: 100772 Pa
Eular Angle: -15.55 -37.61 10.49 Heading: 98.52 Pressure: 100784 Pa
Eular Angle: -13.97 -35.36 10.38 Heading: 109.86 Pressure: 100787 Pa
Eular Angle: -11.15 -35.06 9.69 Heading: 104.25 Pressure: 100766 Pa
Eular Angle: -9.96 -33.43 11.76 Heading: 106.29 Pressure: 100775 Pa
Eular Angle: -10.96 -34.83 10.82 Heading: 114.21 Pressure: 100772 Pa
Eular Angle: -10.25 -35.29 9.27 Heading: 119.60 Pressure: 100772 Pa
Eular Angle: -8.37 -30.98 10.96 Heading: 119.18 Pressure: 100766 Pa
Eular Angle: -7.18 -29.78 9.81 Heading: 118.44 Pressure: 100790 Pa
Eular Angle: -5.31 -28.96 8.56 Heading: 119.18 Pressure: 100766 Pa
Eular Angle: -1.76 -23.89 9.36 Heading: 125.73 Pressure: 100781 Pa
Eular Angle: -7.48 -25.74 7.28 Heading: 110.69 Pressure: 100778 Pa
Eular Angle: -6.18 -26.42 5.81 Heading: 108.40 Pressure: 100781 Pa
Eular Angle: -4.32 -26.61 4.79 Heading: 106.94 Pressure: 100766 Pa
Eular Angle: -2.43 -26.66 3.70 Heading: 107.66 Pressure: 100775 Pa
Eular Angle: -0.81 -26.80 2.51 Heading: 104.63 Pressure: 100772 Pa
Autoscroll Both NL & CR 9600 baud
```

Figure 2: The Arduino code listed above produces this output, showing the status of the SEN0140 sensors. (Image source: DFRobot)



Figure 3: Digilent's 410-326 9-axis IMU/barometer uses an STMicroelectronics' LSM9DS1 iNEMU IMU that combines a 3D accelerometer, a 3D gyroscope, and a 3D magnetometer into one package. (Image source: Digilent)

[Thales Visionix's NavChip Precision 6-axis MEMS IMU](#) is derived from military technology, performing positional data acquisition and processing at a 1 kHz rate. It then processes and integrates the data down to a 200 Hz (or lower) user selectable rate. It also performs compensation using factory calibration and embedded temperature sensors to correct the other sensors' biases, scale factors, and misalignments. The specifications for its accelerometer and magnetometer are:

- Accelerometer: Full-scale angular rate of 2000°/s
- Magnetometer: Full-scale acceleration of $\pm 16g$

The NavChip module has both a TTL UART and an SPI port, and it has a 1 pulse/second input for synchronization with a GPS module. It's available in the [V14447-03-02](#) RS-422 evaluation kit for easier prototyping. The module has built-in test (BIT) modes for testing on command, along with continuous diagnostic monitoring. It is factory calibrated and temperature compensated over an operating temperature range of -40°C to $+85^{\circ}\text{C}$.

The factory calibration and temperature compensation allows Thales to add a series of stability specifications to the NavChip

module's data sheet that are not to be found on most other commercial IMU data sheets:

- Gyro bias in-run stability: $5^{\circ}/\text{hour}$
- Angular random walk: $0.18^{\circ}/\sqrt{\text{hour}}$
- Velocity random walk: $0.03 \text{ meters/second}/\sqrt{\text{hour}}$

The software angle

With all of the IMUs listed in this article, the software that extracts the raw sensor data is not difficult to write as demonstrated by the Arduino code listing above. However, the integration of these sensor

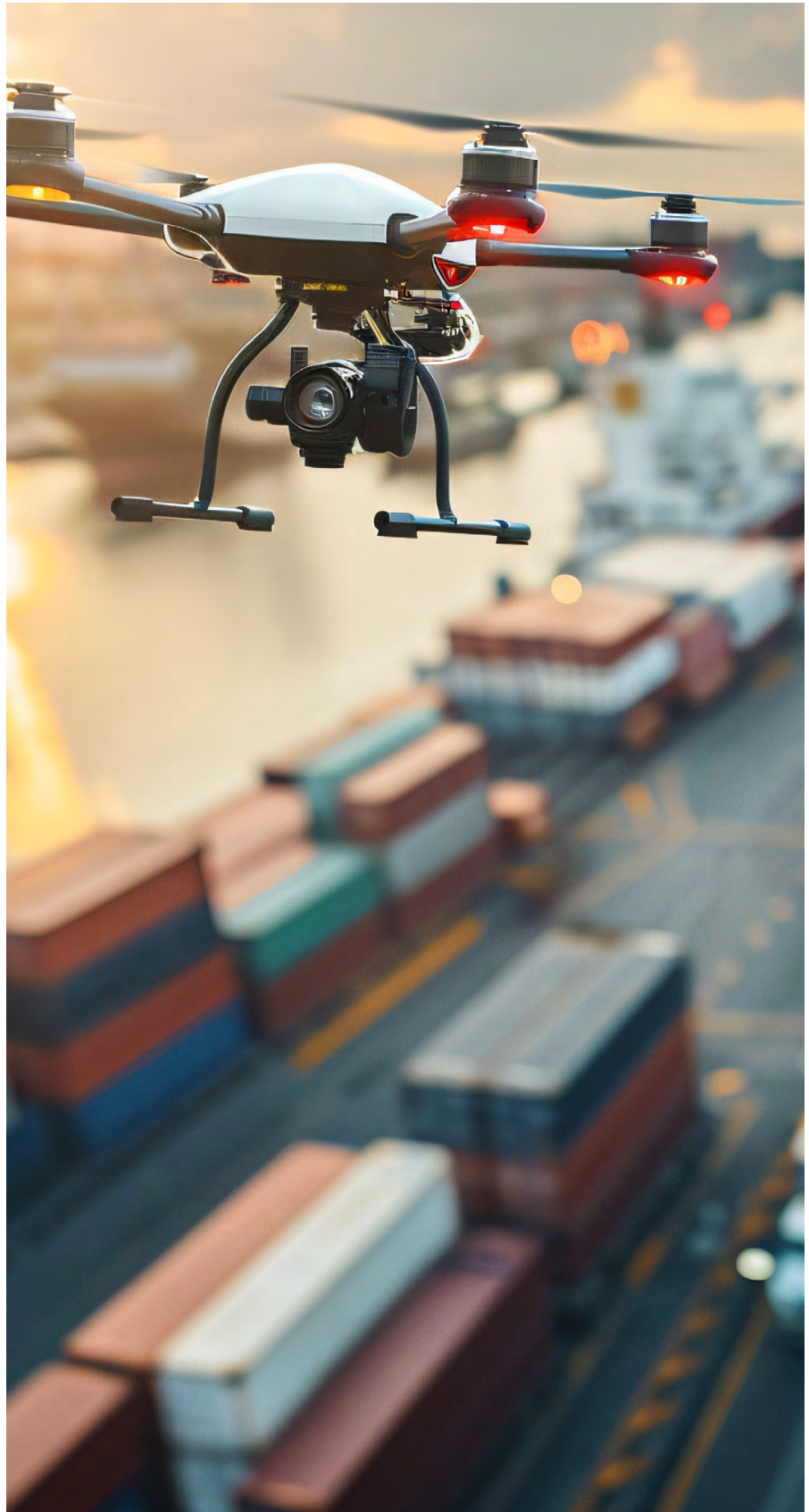
readings into usable navigation data is a more complex task. There are some open source packages specifically designed to incorporate IMU data into an application.

ArduPilot Mega (APM) is one such program specifically developed for autonomous drones. It supports both piloted and unpiloted (fully autonomous) flight and includes hundreds of GPS waypoints, camera control, and autonomous takeoff and landing. Because it's open source, the IMU code is open for inspection and can be repurposed for other types of applications.

The Robot Operating System (ROS) from the Open Source Robotics Foundation, is a flexible framework for writing robotics software. It is a collection of tools, libraries, and conventions that aim to simplify the task of creating complex and robust robot behavior across a wide variety of robotic platforms. ROS contains interface code for several IMUs to inform its navigation modules.

Conclusion

Many embedded applications require the ability to locate the system's position anywhere on earth. GNSS receivers alone are not sufficient, but when complemented by IMUs, finer positioning accuracy and faster update rates are attainable.



Use a PCR module to rapidly develop accurate, low-power radar-based sensors

By Stephen Evanczuk

Contributed By DigiKey's North American Editors





High resolution 3D sensor technology has emerged as a critical capability in applications ranging from gesture-based user interfaces to automotive driver assistance systems (ADAS). Among 3D sensor alternatives, radar technology offers features and performance characteristics unavailable with more conventional approaches. Still, developers find it challenging to maintain high accuracy and low power consumption, and there is a steep learning curve for deploying radar sensor systems.

Using an advanced technology called pulsed coherent radar (PCR), [Acconeer](#) has developed an integrated radar sensor that provides the combination of high accuracy and low power consumption required for smart products and other emerging applications.

This article describes Acconeer's PCR approach before introducing a radar module and associated development platform based on its technology. It then demonstrates how to use the platform to start designing sophisticated radar sensor technology into a wide range of systems including battery-powered smart products.

Why radar?

Able to provide millimeter scale resolution at high update frequencies, radar-based sensing technology can deliver highly accurate distance and motion data needed by applications for precision object detection, range measurement, position tracking, and more. By incorporating radar technology into smart product designs, however, developers are typically forced to choose between low power or high accuracy. As developers look to apply this technology in designs with limited power budgets, application requirements drive a growing need to maintain accuracy even at reduced power levels.

Advanced radar technology

An alternative approach to conventional radar designs offers a solution that combines the accuracy of sophisticated coherent radar methods with the reduced power requirements of pulsed radar systems. Pulsed radar designs shut down the transmitter between pulses, achieving lower power consumption but with lower accuracy. In contrast, coherent radar systems transmit a continuous train of pulses, using precise phase measurements of return signals to provide high accuracy measurements but at the cost of high power consumption.

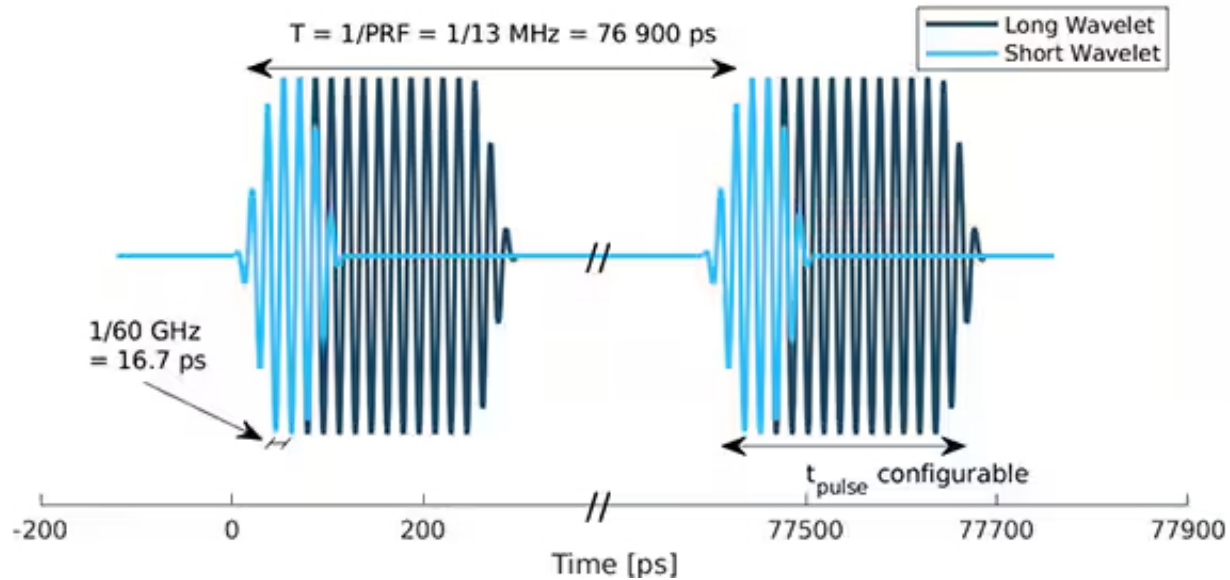


Figure 1: The Acconeer A111 pulsed coherent radar device achieves high accuracy at low power by transmitting long or short wavelets with carefully controlled pulse repetition frequency (PRF), center frequency (f_{RF}), and pulse duration (t_{pulse}). (Image source: Acconeer)

Acconeer combines these techniques in the PCR technology used in its [A111](#) radar sensor. Like pulsed radar, PCR technology keeps the radio turned off between transmissions, but as in coherent systems, the transmissions are bursts of pulses, or sweeps, with a known starting phase (Figure 1).

By tuning parameters such as pulse duration (t_{pulse}), developers can optimize signals for different applications. For example, developers can reduce t_{pulse} to generate the shorter wavelets needed to resolve small movements of individual

fingers in a gesture-controlled user interface application. Conversely, they can increase t_{pulse} to generate the high energy long wavelets needed to resolve obstructions in an automotive self-parking application.

Despite the attraction of PCR's technical advantages, few developers without significant expertise in radar technology could afford the time required to implement this technology on their own. Besides the challenges of designing an efficient millimeter wave (mmWave) front-end stage, developers would face

the considerable challenge of converting the acquired amplitude and phase data of reflected radar signals into useful measurements of distance and motion.

Designed to address these challenges, the Acconeer PCR-based A111 radar device and associated software development kit (SDK) abstract the low-level details of radar signal processing, delivering data in forms that can be more easily consumed by applications.

Integrated PCR front-end simplifies development

Simplifying the hardware aspects of PCR technology implementation, the Acconeer A111 provides a complete radar sensor that integrates a mmWave radar front-end with an antenna-in-package (AIP) in a 5.2 x 5.5 x 0.88 millimeter (mm) flip chip chip-scale package (fcCSP) (Figure 2).

Along with its mmWave radio frequency (RF) subsystem, the A111 includes a digital subsystem with dedicated memory areas for program and data for managing the mmWave radio subsystem. Separate subsystems provide phase-locked loop (PLL) timing and power management features including power-on reset (PoR) and separate low dropout (LDO) regulators for the device's multiple power domains.

With its picosecond scale time resolution, the device is typically capable of measuring distance with millimeter accuracy over a range of up to two meters. At the same time, its low power consumption allows developers to use it in battery-powered devices. Because of the A111 sensor's high level of integration, developers need only a few additional components besides a host microcontroller to implement radar sensing in their designs (Figure 3). Because the A111 can

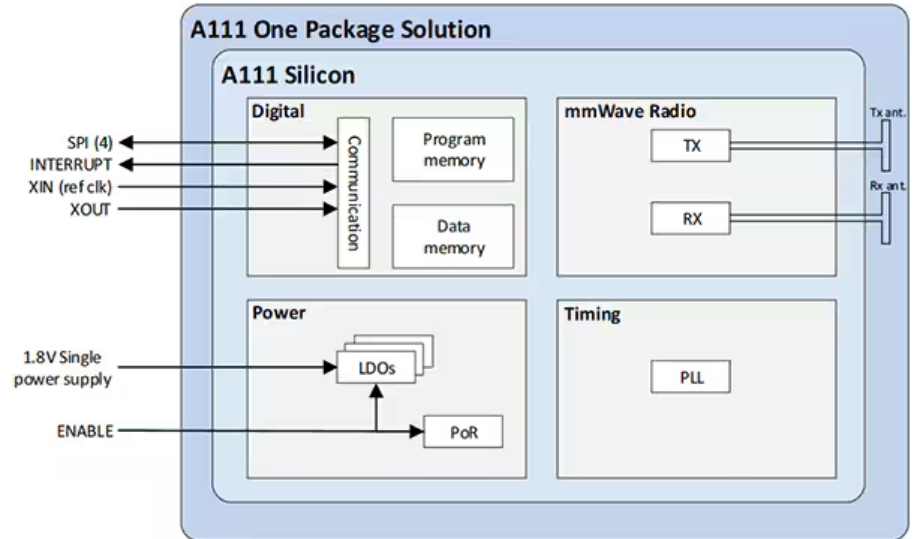


Figure 2: The Arduino code listed above produces this output, showing the status of the SEN0140 sensors. (Image source: DFRobot)

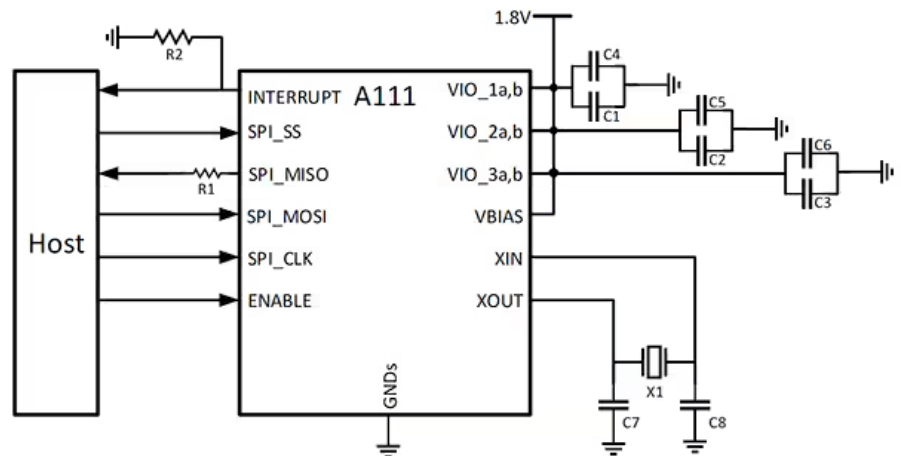


Figure 3: Because it integrates all the radio frequency and digital subsystems required for a radar front-end, the A111 enables developers to implement radar sensing with only a few additional components beyond the host microcontroller. (Image source: Acconeer)

operate without an aperture for its radar signals, developers can incorporate it in smart products without compromising existing ingress protection requirements.

The A111 functions as a conventional serial peripheral interface (SPI) device with serial data input (MOSI), serial output (MISO), clock (SPI_CLK),

and slave select signal (SS) ports. The A111's ENABLE pin allows developers to use the microcontroller to power up or power down the device, while the INTERRUPT pin allows developers to use the A111 to notify the microcontroller when measurements are ready.

By using ENABLE to turn off the A111 between pulse sweep transmissions, developers can reduce A111 power consumption to 66 μ A (typical). Conversely, while the A111 performs a series of sweeps and measurements, developers can place the host microcontroller in a low-power sleep state using the wait-for-interrupt (WFI) instruction available in [Arm®](#) Cortex®-M-based processors to wake the microcontroller when the A111 completes its operations and issues an interrupt.

Designers can add their own precision clock source, or rely on the device's internal clock circuit which only requires an external crystal oscillator such as [EPSON's TSX-3225](#). The device works with a single 1.8 volt supply for RF (VIO_1 and VIO_2) and digital (VIO_3). Alternatively, developers can use separate supply sources for more power intensive applications. The VIO_Na and VIO_Nb pins shown in Figure 3 are connected within the

device and Acconeer recommends that they be connected externally on the pc board as well.

Intended purely as a radar front-end device, A111 itself stores no firmware permanently, relying instead upon the host microcontroller to upload all sensor software as well as handle A111 sensor initiation, configuration, sweep acquisition and signal processing. Consequently, the choice of companion microcontroller is an important design decision. Acconeer notes that an Arm Cortex-M4-based microcontroller such as [STMicroelectronics' STM32L476](#) or [Nordic Semiconductor's NRF52840](#) is typically sufficient for handling relatively static operations such as distance measurement or basic motion detection. For more dynamic applications such as breathing motion detection or object tracking, Acconeer recommends an Arm Cortex-M7-based microcontroller such as [Microchip Technology's ATSAME70](#). As such, Acconeer pairs the A111 PCR device with an ATSAME70 in its [XM112](#) radar module.

The Acconeer XM112 module combines the A111 radar sensor with a Microchip Technology ATSAME70 microcontroller

to provide a complete radar subsystem. Developers can use the XM112 together with the [XB112](#) breakout board to immediately begin evaluating the A111 and building PCR-based software applications. Alternatively, developers can simply plug the 30-pin 24 mm x 16 mm module into their own PCBs to add a self-contained PCR subsystem to their custom designs. To perform radar sensing, developers can control the XM112 module through a serial connection with their development systems or execute software directly on the XM112 host ATSAME70 microcontroller.

Software interface

Regardless of hardware systems configuration, radar measurements are programmatically controlled using the Acconeer radar system software (RSS) application programming interface (API). The RSS API serves as the sole software interface for working with the A111. Acconeer does not support access to A111 registers through typical SPI transactions due to the complexity of the design, calibration, and processing requirements. Instead, all operations work through the RSS which provides A111 detector functionality. These detectors in turn build on lower level services through APIs for accessing different

types of preprocessed data from the A111. These services include:

- Envelope service which provides information about the amplitude of sensor data
- Power Bin service which provides amplitude information in predefined range intervals (bins)
- IQ service which provides IQ modulated data, allowing use phase and amplitude measurements to generate more accurate measurements than possible with amplitude only Envelope and Power Bin services

Within these services, developers can take advantage of special features for power management, range enhancement, and self-calibration, among others.

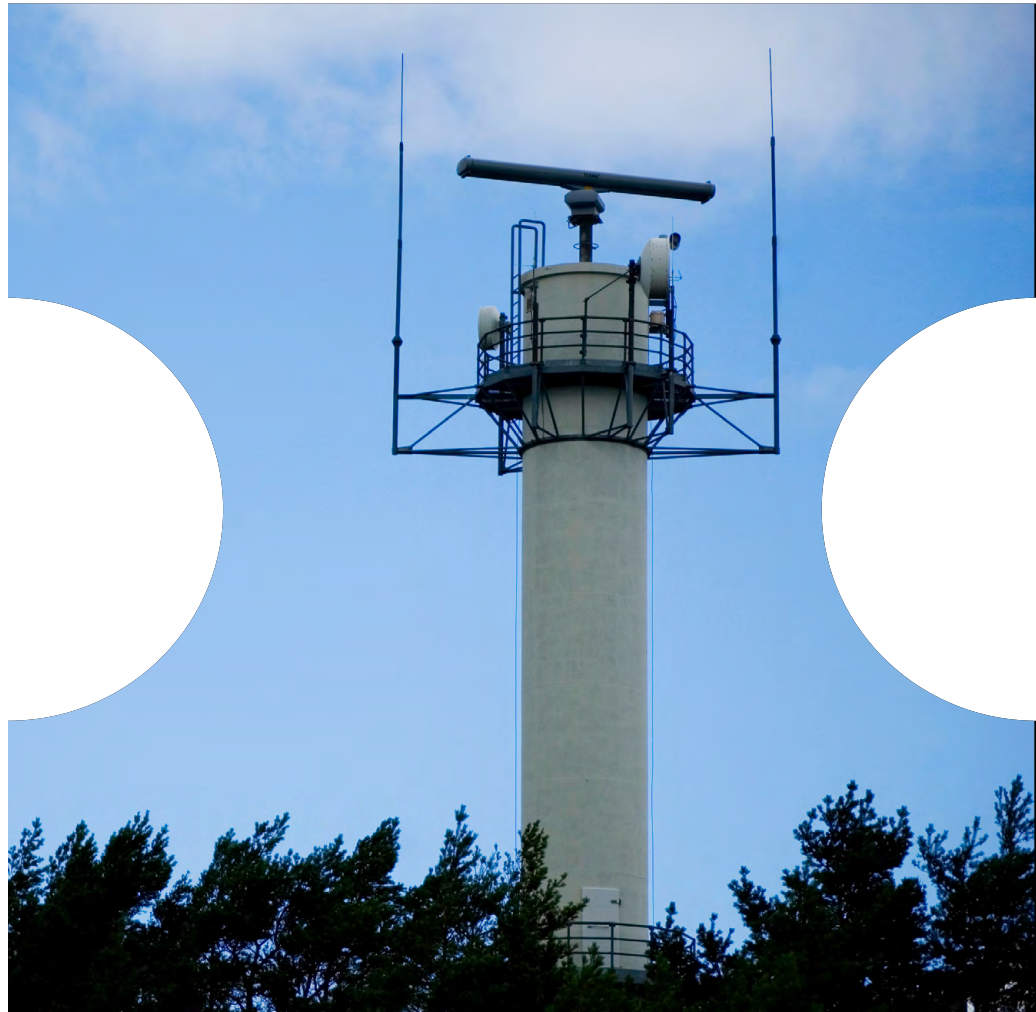
For power management, developers can place the device in one of four power modes that reduce power consumption by reducing the sensor update rate. The range enhancement feature allows developers to perform long sweeps that extend the measurement range up to 7 meters (m) under some conditions. Finally, the self-calibration feature allows developers to reduce power consumption associated with the calibration cycle that occurs whenever the device starts up. In battery-powered designs for the IoT, for example, devices may routinely be put in sleep mode or even turned off during extended periods of inactivity.

In many cases, performing self-calibration at the beginning of each wake cycle is unnecessary and simply wastes power. Instead, developers can store values from an initial calibration cycle in non-volatile memory and use those values to perform measurements reliably during later waking periods.

For production code development, engineers can download the full [software distribution package](#) which provides sample application

source code along with the Acconeer SDK. The SDK includes header files along with precompiled RSS libraries for Arm Cortex-M4 and Arm Cortex-M7 microcontrollers in separate microcontroller-specific distributions.

The SDK's C-language code samples illustrate the basic design pattern for using the RSS API to perform radar measurements in production applications. For any type of



measurement, this design pattern begins by initializing the system and RSS, calling three routines in sequence:

- `acc_driver_hal_init()`, which initializes the board and GPIOs
- `acc_driver_hal_get_implementation()`, which instantiates a C structure, `acc_hal_t`, that holds sensor and board properties as well as pointers to runtime handlers for memory allocation, semaphores, and others.
- `acc_rss_activate_with_hal()`, which activates the Radar System Services (RSS) utility itself

From this point, a typical measurement involves creating an object called a configuration that contains parameters associated with the sensor and the particular measurement. That configuration is then used to call an RSS API function to create the desired detector or service. The sample code illustrates the application of this design pattern in a module, `example_detector_distance_peak.c`, for creating and working with a distance peak detector. In that module, the `main()` routine (Listing 1) first performs initialization and RSS activation before creating a configuration (`acc_detector_distance_peak_configuration_create()`) and using that configuration to create a peak detector (`distance_peak_detect_with_blocking_calls()`).

```
int main(void)
{
    acc_detector_distance_peak_status_t detector_status;

    printf("Acconeer software version %s\n", ACC_VERSION);
    printf("Acconeer RSS version %s\n", acc_rss_version());

    if (!acc_driver_hal_init())
    {
        return EXIT_FAILURE;
    }

    acc_hal_t hal = acc_driver_hal_get_implementation();

    if (!acc_rss_activate_with_hal(&hal))
    {
        return EXIT_FAILURE;
    }

    //Create the detector configuration
    acc_detector_distance_peak_configuration_t distance_configuration = acc_detector_distance_peak_

    if (distance_configuration == NULL)
    {
        fprintf(stderr, "\nacc_service_distance_configuration_create() failed");
        return EXIT_FAILURE;
    }

    //Run distance peak detection in blocking mode
    detector_status = distance_peak_detect_with_blocking_calls(distance_configuration);
    if (detector_status != ACC_DETECTOR_DISTANCE_PEAK_STATUS_SUCCESS)
    {
        fprintf(stderr, "Running distance peak detector in blocking mode failed");
        acc_detector_distance_peak_configuration_destroy(&distance_configuration);
        acc_rss_deactivate();
        return EXIT_FAILURE;
    }

    detector_status = distance_peak_detect_with_blocking_calls_with_estimated_threshold(distance_c
    if (detector_status != ACC_DETECTOR_DISTANCE_PEAK_STATUS_SUCCESS)
    {
        fprintf(stderr, "Running distance peak detector in blocking mode with estimated threshold fa
        acc_detector_distance_peak_configuration_destroy(&distance_configuration);
        acc_rss_deactivate();
        return EXIT_FAILURE;
    }

    acc_detector_distance_peak_configuration_destroy(&distance_configuration);

    acc_rss_deactivate();

    return EXIT_SUCCESS;
}
```

Listing 1: This snippet from a sample application in the Analog Devices 3D ToF SDK distribution demonstrates the few steps required to acquire depth and IR images and classify them with an inference model. (Code source: Analog Devices)

In this sample application, the actual distance peak measurements are performed in the routine `distance_peak_detect_with_blocking_calls()`. This routine in turn uses the RSS API function `acc_detector_distance_peak_get_next()` to retrieve the actual measurement data from the A111 device (Listing 2). In

this case, the code places the `acc_detector_distance_peak_get_next()` measurement routine in a loop, decrementing a counter, `detection_runs`, until it performs 100 measurements.

Developers can implement their own detectors, using service calls in a similar design pattern

```

detector_status = acc_detector_distance_peak_activate(handle);
if (detector_status == ACC_DETECTOR_DISTANCE_PEAK_STATUS_SUCCESS)
{
    uint_fast8_t detection_runs = 100;

    while (detection_runs > 0)
    {
        reflection_count = 10;

        detector_status = acc_detector_distance_peak_get_next(handle,
                                                             reflections,
                                                             &reflection_count,
                                                             &result_info);

        if (detector_status == ACC_DETECTOR_DISTANCE_PEAK_STATUS_SUCCESS)
        {
            printf("Distance detector: Reflections: %u. Seq. nr: %u. (%u-%u mm): %s\n",
                  (unsigned int)reflection_count,
                  (unsigned int)result_info.sequence_number,
                  (unsigned int)(start_m * 1000.0f),
                  (unsigned int)(end_m * 1000.0f),
                  format_distances(reflection_count, reflections, metadata.free_space_absolute_o
            )
        }
        else
        {
            fprintf(stderr, "reflection data not properly retrieved\n");
        }

        detection_runs--;
    }
}

```

Listing 1: This snippet from a sample application in the Analog Devices 3D ToF SDK distribution demonstrates the few steps required to acquire depth and IR images and classify them with an inference model. (Code source: Analog Devices)

for initialization, RSS activation, configuration creation, and service instantiation. For example, to use the Envelope Service, developers would call `acc_service_envelope_configuration_create()` to create the necessary configuration and use that configuration as a parameter in calling `acc_service_create()` to instantiate a service object.

By exploring the C-language sample code, developers can quickly gain experience using the RSS API to build specialized radar applications with custom detectors. To help developers more rapidly gain familiarity with radar-based sensing in general and RSS services in particular,

Acconeer also provides sample code in its Python Exploration Kit software repository.

Designed to work with the Acconeer SDK and evaluation kits such as the XM112, the Python Exploration Kit helps developers take advantage of Python's productivity advantages for working with RSS services and detectors. Along with basic examples, the kit provides sample code for implementing very sophisticated measurement applications including detecting breathing patterns in sleeping subjects, using phase information to track relative movements, detecting approaching obstacles, and more.

Conclusion

Radar sensing technology can provide highly accurate measurements for distance and motion applications. However, it can consume a lot of power to achieve accuracy, and it typically involves a complex design process. By implementing PCR, the Acconeer A111 integrated radar sensor provides the combination of high accuracy and low power consumption required for smart products and other emerging applications. The companion software development kit (SDK) abstracts the complexity of radar signal processing, providing the kind of higher level data required at the application level.

Using the SDK with an A111-based development board, engineers can rapidly gain experience in radar sensing technology and quickly implement sophisticated applications able to discern objects and track movement with millimeter resolution.

Automate your future with DigiKey

If you're an

- MRO
- OEM
- Integrator
- or
- New to Automation

We can help with all things Automation.

Explore and connect today.

[digikey.com/automation](https://www.digikey.com/automation)

DigiKey

